

AD-A105 500

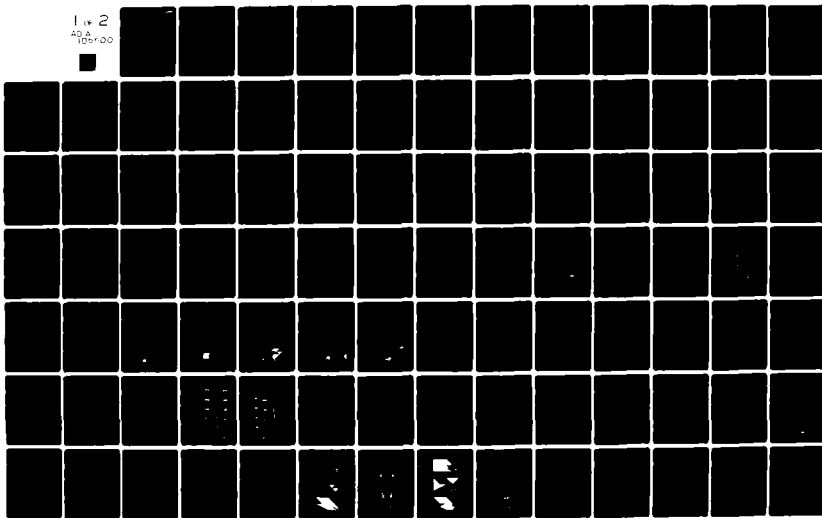
AIR FORCE INST OF TECH WRIGHT-PATTERSON AFB OH
FRACTURE PREDICTION IN PLANE ELASTO-PLASTIC PROBLEMS BY THE FIN--ETC(U)
1978 R G BELIE
AFIT-CI-79-261D

F/G 20/11

UNCLASSIFIED

NL

1 of 2
AD-A
105-500



AD A105500

DTIC FILE COPY

THE UNIVERSITY OF OKLAHOMA
GRADUATE COLLEGE

LEVEL II

①

FRACTURE PREDICTION IN PLANE ELASTO-
PLASTIC PROBLEMS BY THE FINITE
ELEMENT METHOD

A DISSERTATION

SUBMITTED TO THE GRADUATE FACULTY
in partial fulfillment of the requirements for the
degree of
DOCTOR OF PHILOSOPHY

DTIC
OCT 09 1981

BY

ROBERT GARY/BELIE

Norman, Oklahoma

1978

This document has been approved
for public release and sale; its
distribution is unlimited

81 10 6 213

UNCLASS

SECURITY CLASSIFICATION OF THIS PAGE (When Data Entered)

| REPORT DOCUMENTATION PAGE | | READ INSTRUCTIONS BEFORE COMPLETING FORM |
|---|--|--|
| 1. REPORT NUMBER 79-261D | 2. GOVT ACCESSION NO. <i>AD-A105500</i> | 3. RECIPIENT'S CATALOG NUMBER |
| 4. TITLE (and Subtitle) Fracture Prediction in Plane Elasto-Plastic Problems by the Finite Element Method | | 5. TYPE OF REPORT & PERIOD COVERED <i>Thesis/DISSERTATION</i> |
| | | 6. PERFORMING ORG. REPORT NUMBER |
| 7. AUTHOR(s) Robert Gary Belie | | 8. CONTRACT OR GRANT NUMBER(s) |
| 9. PERFORMING ORGANIZATION NAME AND ADDRESS AFIT STUDENT AT: The University of Oklahoma | | 10. PROGRAM ELEMENT, PROJECT, TASK AREA & WORK UNIT NUMBERS |
| 11. CONTROLLING OFFICE NAME AND ADDRESS AFIT/NR WPAFB OH 45433 | | 12. REPORT DATE 1978 |
| | | 13. NUMBER OF PAGES 85 |
| 14. MONITORING AGENCY NAME & ADDRESS (if different from Controlling Office) | | 15. SECURITY CLASS. (of this report) UNCLASS |
| | | 15a. DECLASSIFICATION/DOWNGRADING SCHEDULE |
| 16. DISTRIBUTION STATEMENT (of this Report) APPROVED FOR PUBLIC RELEASE, DISTRIBUTION UNLIMITED | | |
| 17. DISTRIBUTION STATEMENT (of the abstract entered in Block 20, if different from Report) | | |
| 18. SUPPLEMENTARY NOTES APPROVED FOR PUBLIC RELEASE: IAW AFR 190-17 | | <div style="text-align: right;"> <i>30 SEP 1981</i> <i>Fredric C. Lynch</i> FREDRIC C. LYNCH, Major, USAF Director of Public Affairs Air Force Institute of Technology (ATC) Wright-Patterson AFB, OH 45433 </div> |
| 19. KEY WORDS (Continue on reverse side if necessary and identify by block number) | | |
| 20. ABSTRACT (Continue on reverse side if necessary and identify by block number) ATTACHED | | |

FRACTURE PREDICTION IN PLANE ELASTO-
PLASTIC PROBLEMS BY THE FINITE
ELEMENT METHOD

| | |
|--------------|--|
| Approved For | |
| X | |
| Date | |
| By | |
| Title | |
| Institution | |
| Address | |
| City | |
| State | |
| Zip | |
| Dist | |
| Special | |
| A | |

APPROVED BY

J. Nakasimha Reddy

Franklin J. Apple

Charles W. Bert

Dennis M. Egle

James A. Payne

DISSERTATION COMMITTEE

ACKNOWLEDGMENTS

I wish to thank my wife, Nanette, and our boys, Scott and Michael, for their patience, understanding, and sacrifice which greatly contributed to the successful completion of this effort.

I am indebted to Dr. J. N. Reddy, my advisor, and Dr. C. Bert and Dr. D. Egle for their guidance and discussion, and Dr. F. J. Appl whose encouragement many years ago has culminated in this work. Most of all, I wish to thank these men for assisting me develop an appreciation for freedom of thought and logical problem solution.

I would also like to acknowledge the support of the School of Aerospace, Mechanical, and Nuclear Engineering at the University of Oklahoma during the test phase of this research, and thank the Merrick Computing Center at the University of Oklahoma for providing the computational time.

Finally, assignment by the United States Air Force to the University of Oklahoma for the completion of this study is gratefully acknowledged.

ABSTRACT

A finite element program based on the plane stress assumption is developed and applied to elasto-plastic fracture problems involving monotonically increasing loads. The program directly predicts the initiation and propagation of fracture in the structure. That is, the concept of stress intensity factor is not utilized in the present approach. The approach uses a piecewise linear approximation of the actual stress-strain curve for the material, and the maximum strain criteria to predict both the yield and fracture. An incremental loading technique is employed to load the structure, and a "zero modulus-unload reload" scheme is developed to handle the response of the structure at fracture. Comparisons with published data on a cracked panel, and the experimental data obtained during this study on tensile and cracked specimens show that the finite element program developed herein can accurately predict load and deflection at fracture, load-deflection curves, fracture initiation locations, and stable or unstable crack propagation. This approach is shown to be highly dependent on the mesh density in areas of high strain gradients.

TABLE OF CONTENTS

| | Page |
|--|------|
| LIST OF TABLES | vii |
| LIST OF ILLUSTRATIONS. | viii |
| Chapter | |
| I. INTRODUCTION | |
| I.1 Historical Background | 1 |
| I.2 Fracture Mechanics. | 3 |
| I.3 The Finite Element Method | 4 |
| I.4 Brief Review of Pertinent Literature. | 6 |
| I.5 Objectives of the Present Study . | 7 |
| II. THEORETICAL CONSIDERATIONS | |
| II.1 Governing Equations | 8 |
| II.2 The Finite Element Approach . . . | 13 |
| III. FINITE ELEMENT FRACTURE PROGRAMS | |
| III.1 Introduction. | 17 |
| III.2 Formulation | 18 |
| III.3 Description of the Computer Programs. | 29 |
| IV. CRACKED PANEL ANALYSIS | |
| IV.1 Introduction. | 35 |
| IV.2 Finite Element Analysis | 36 |
| IV.3 Cracked Panel Summary | 49 |
| V. TENSILE SPECIMEN ANALYSIS | |
| V.1 Introduction. | 50 |
| V.2 Experimental Study. | 51 |
| V.3 Finite Element Analysis | 54 |
| V.4 Tensile Test Analysis Summary . . | 63 |

| Chapter | Page |
|--|------|
| VI. CRACKED SPECIMEN ANALYSIS | |
| VI.1 Introduction | 66 |
| VI.2 Experimental Tests | 67 |
| VI.3 Finite Element Analysis. | 67 |
| VI.4 Cracked Specimen Analysis Summary. | 80 |
| VII. CONCLUSIONS AND RECOMMENDATIONS | 81 |
| BIBLIOGRAPHY. | 83 |
| APPENDIX I, THE FINITE ELEMENT PROGRAM, FRACTURE. | 85 |

LIST OF TABLES

| TABLE | | Page |
|-------|---|------|
| 3.1 | Example of Tabulated Material Properties | 21 |
| 5.1 | Comparison of Experimental and FEM Loads and Deflection at Fracture | 65 |

LIST OF ILLUSTRATIONS

| FIGURE | Page |
|--|------|
| 2.1 Elasto-Plastic Stress-Strain Curve. . . | 12 |
| 2.2 Maximum Strain and von Mises Yield Criteria | 14 |
| 2.3 The Constant Strain Triangular Element | 14 |
| 3.1 Linear Approximation of a Stress- Strain Curve. | 19 |
| 3.2 Typical Element Response, "Zero Modulus-Unload Reload" Method | 24 |
| 3.3 Stress-Strain Curve with Zero Modulus Section | 27 |
| 3.4 Flow Chart for the Program FRACTURE . . | 30 |
| 4.1 Cracked Panel Dimensions and FEM Models. | 37 |
| 4.2 Numerical Convergence, Cracked Panel Study | 40 |
| 4.3 Effect of Mesh Refinement Along the Crack Path. | 41 |
| 4.4 FEM Crack Growth Prediction | 42 |
| 4.5 Effects of Element Orientation. | 42 |
| 4.6 Plastic Regions | |
| (a) Load = 10,000 LB. | 44 |
| (b) Load = 20,000 LB. | 44 |
| (c) Load = 25,000 LB. | 45 |
| (d) Load = 30,000 LB. | 46 |
| (e) Load = 34,000 LB. | 47 |
| (f) Load = 36,087 LB. | 48 |
| 5.1 Tensile Test Specimen Dimensions. . . . | 52 |
| 5.2 Tensile Test Load Deflection Curves . . | 53 |
| 5.3 Linearized Stress-Strain Curve. | 53 |

| FIGURE | | Page |
|--------|--|------|
| 5.4 | Tensile Test FEM Models | 55 |
| 5.5 | FEM Load Deflection Predictions for Tensile Test Specimens. | 57 |
| 5.6 | Yield Regions for Tensile Test Specimen. | 59 |
| 5.7 | Crack Locations, FEM Predictions and Experimental Results for Tensile Test Specimen. | 64 |
| 6.1 | FEM Models of Cracked Specimens | 69 |
| 6.2 | Numerical Convergence, Cracked Specimen Analysis | 71 |
| 6.3 | Effect of Load Increment and Element Size for the Cracked Specimen Analysis | 72 |
| 6.4 | Load Deflection Curves for Cracked Specimen Analysis | 73 |
| 6.5 | Yield Region for Specimen with a 0.023" Crack | |
| | (a) Load = 1806 LB. | 74 |
| | (b) Load = 3020 LB. | 74 |
| | (c) Load = 4000 LB. | 75 |
| | (d) Load = 4500 LB. | 75 |
| | (e) Load = 5000 LB. | 75 |
| | (f) Load = 5000 LB, Overall Results . | 76 |
| | (g) Load = 5200 LB. | 77 |
| | (h) Load = 5325 LB. | 77 |
| | (i) Load = 5433 LB. | 77 |
| | (j) Load = 5433 LB, Overall Results . | 79 |

NOMENCLATURE

| | |
|------------|---|
| A_0 | Initial area |
| D_g | Gage deflection |
| D_{pp} | Pin-to-pin deflection |
| DEPR | Incremental element principal strain |
| D_r | Pin-to-gage boundary deflection per unit load |
| E | Elastic modulus |
| E_e | Elastic modulus |
| E_i | Incremental tangent modulus |
| E_s | Secant modulus |
| E_{si} | Incremental secant modulus |
| ECH | Array of strains for next element property changes |
| EPRI | Total element principal strains |
| I | Potential energy |
| L | Load |
| LI | Incremental load |
| S_{ij} | Compliance coefficient |
| T | Temperature change |
| u, v | Displacement in the x and y directions, respectively |
| u_i, v_i | Nodal displacements in the x and y directions, respectively |
| v | Volume |
| W | Width of tensile specimen neck |
| α_i | Coefficients of thermal expansion |

α_i, β_i , Interpolation coefficients
 γ_i
 Δ Element area
 ϵ_i Strain components
 $\epsilon_x, \epsilon_y, \epsilon_z$, Strains in the x, y and z directions
 ϵ_{xy} Tensor shear strain relative to x and y axes
 ϵ_{yp} Yield strain
 ϵ_1, ϵ_2 Principal strains
 μ Poisson's ratio
 μ_e Elastic Poisson's ratio
 μ_i Incremental Poisson's ratio
 σ_j Stress components
 $\sigma_x, \sigma_y, \sigma_z$, Normal stresses in the x, y and z directions
 $\sigma_{xy}, \sigma_{yz}, \sigma_{zx}$ Shear stresses relative to xy, yz, and zx axes
 σ_{yp} Yield stress
 σ_1, σ_2 Principal stresses
 ψ_i Interpolation functions
 $\{F\}$ Force vector
 $\{u\}$ Displacement vector
 $[B]$ Strain displacement coefficient matrix
 $[E]$ Stress-strain coefficient matrix
 $[K]$ Stiffness matrix

IT WOULD BE HARD TO IMAGINE A TIME WHEN
SOMEONE, SOMEWHERE, DID NOT LOOK DOWN ON
SOME BROKEN SOMETHING AND WONDER WHY.

FRACTURE PREDICTION IN PLANE ELASTO-
PLASTIC PROBLEMS BY THE FINITE
ELEMENT METHOD

CHAPTER I

INTRODUCTION

I.1 Historical Background

On the 10th of January 1954, a B.O.A.C. Comet, the first pressurized commercial jet airliner, fell into the sea near Rome, killing 29 passengers and its crew of 6. The Comet fleet was immediately grounded and carefully inspected and modified. Comet service resumed on the 23rd of March, and 16 days later, a second Comet was lost. Subsequent investigations determined that the Comet had met airworthiness requirements effective at the time; however, these requirements, based on static analysis and testing, were insufficient to predict the type of cyclic failure experienced by the Comets.

As a result of these accidents, fatigue analysis and testing became an integral part of aircraft design. Fatigue

analysis frequently took the form of a damage accumulation theory such as Miner's rule. With Miner's rule, the number of cycles at each stress level is divided by the number of cycles to failure at that level. These fractions are then summed with failure indicated by a total accumulation of one. Fracture testing was accomplished by subjecting an airframe to "blocks" of loading which would simulate those anticipated in actual service. The inaccuracies in this type of fatigue approach required considerable conservatism (along with the associated high cost) to insure the integrity of the structure. Typically, airframes were required to withstand one and a half times the maximum static load and four times the number of cyclic loads expected to be encountered in service. Additionally, most fatigue philosophies dictated that any cracking was to be considered a failure.

The loss of a U.S. Air Force F-111 in 1969 initiated a rethinking of airframe design and analysis concepts.¹ Failure in this aircraft was traced to a small manufacturing flaw in a wing pivot fitting, not to a design induced fatigue. In a fashion reminiscent of the Comet incidents, it became apparent that static and fatigue concepts alone would not predict the type of failure incurred by this aircraft. It also became clear that a more efficient approach would be to design a structure to be crack tolerant, and that some analytic method would be necessary to accomplish

this goal.

I.2 Fracture Mechanics

Fracture mechanics theory which had been successfully applied to crack instability research was adapted to this new design role. A popular form of the fracture mechanics "law" is

$$da/dN = C f(K)$$

where da/dN is the crack growth rate (a being the crack length, N the number of cycles), C is a material constant, and K is the stress intensity factor which relates the stress conditions with the crack length.² When coupled with a damage tolerance approach to design, an initial flaw size (usually the minimum crack size which can be repeatedly detected by nondestructive inspection) is assumed. The crack is then grown according to the appropriate fracture mechanics "law" until it reaches a critical crack length. This information is then used to establish inspection intervals for the structure. During the course of the design, any area found to have unacceptably rapid crack growth (i.e., inspection intervals are too close) must be redesigned. The advantage of such a procedure is that accurate analysis and inspection can safely extend the structure to its full useful life. However, due to the randomness of possible initiation sites, each area of the structure must be analyzed.

Unfortunately, the application of a fracture mechanics "law" to all areas of a large structure is a difficult, if not impossible, bookkeeping task. The stress intensity factors must be determined for each area of the structure for each type of loading, a time consuming effort even for simple geometries and loadings. Then these factors must be combined in the proper manner to establish the crack growth rates. Additionally, Boyd³ pointed out that the assumptions associated with fracture mechanics "laws" are more restrictive than is generally realized. The most significant defect in the application of these fracture mechanics approaches to practical aircraft structures lies in their elastic formulation. Structural metals, however, exhibit a large degree of plastic deformation ahead of the crack tip which significantly affects their response. Some attempts have been made to provide correction factors for this effect, but they only further the gap between the physical phenomenon and the analytical technique.

I.3 The Finite Element Method

If the finite element method, which has enjoyed enormous success in the application to structural mechanics problems over the last three decades, could be employed successfully to directly predict fracture in structures, the shortcomings of present methods could be overcome. The method has already been used in fracture mechanics to cal-

culate stress intensity factors. However, a direct procedure of predicting fracture would eliminate the laborious task of calculating stress intensity factors for all regions of a structure and using them to predict fracture. Additionally, the fracture mechanics approach based on the stress intensity factor does not take into account the plastic deformation associated with the fracture phenomena in non-brittle materials. Since the finite element method can also be used to analyze structural problems involving material nonlinearities, it seems obvious to employ the method to directly predict fracture in elasto-plastic materials using a realistic stress-strain law.

In the finite element method (FEM), a given structure is divided into substructures, called finite elements. These elements can be of different shapes and sizes (a physical continuum can be viewed as a collection of smaller elements). A typical element is isolated from the collection and its physical properties, such as the stiffness coefficients, are developed using piecewise approximation of the variables. Then the discrete set of equations governing the complete structure are obtained by putting the element equations together. Generally, the accuracy of the predicted structural response improves with the number of elements (i.e., with the decrease of element size), and the order of approximation which is used to represent the solution. With respect to fracture studies, the FEM offers a

unique opportunity to include the effects of the material nonlinearities. The inherent flexibility and ease of application of the FEM suggests that it is a valuable design tool for direct prediction of fracture as well as the response of structures in the presence of cracks.

I.4 Brief Review of Pertinent Literature

The finite element method has already been used in many studies⁴⁻¹¹ to investigate fracture processes. Most of these investigations have centered on examining the localized effects of fracture and the effects of cracks on structures, rather than on predicting actual catastrophic failure loads and deflections. Newman¹⁰ studied the effects of various parameters such as the mesh size, strain hardening, and critical strain on finite element fracture prediction; however, no experimental results were used for comparison. On the other hand, Miller et al.¹¹ presented a finite element solution and experimental results for a cracked panel under monotonically increasing stress. Unfortunately, the finite element predictions did not show close agreement with experimental data. These predictions also varied significantly with the method of load redistribution at fracture. Furthermore, the nodal uncoupling method used by Newman, Miller and others is restricted to fracture prediction along lines of symmetry.

I.5 Objectives of the Present Study

The present investigation is concerned with the development of a finite element program to directly predict fracture in non-brittle materials under monotonically increasing loads. The procedure involves the use of a piecewise linearized stress-strain curve, with an incremental loading. This study also involved experimental investigation of fracture to determine the accuracy of the numerical predictions. Thus, the goal of this research was to determine if the finite element method could provide an accurate and useable design tool for the analysis of fracture and crack growth in practical structures. To accomplish this goal, simple, non-trivial two dimensional (plane stress) structures under uniaxial loading were considered. This study further defines the factors affecting accurate prediction of fracture by the finite element method, and determines if the results obtained by Miller represent typical errors to be expected by such a method. Accuracy of the method is demonstrated by comparison with experimental data.

CHAPTER II

THEORETICAL CONSIDERATIONS

II.1 Governing Equations

In a continuum, application of loads results in stresses. At any point in the structure, there are nine stress components; however, only six of them, three normal stresses (σ_x , σ_y , σ_z) and three shearing stresses (σ_{xy} , σ_{yz} , σ_{zx}), are independent. The stresses induce strains in the material. For a three dimensional linear elastic anisotropic material, the six strains (ϵ_i) are related to these stresses as follows:

$$\epsilon_i = S_{ij} \sigma_j + \alpha_i T \quad (2.1)$$

where S_{ij} 's are the compliance coefficients, α_i 's are the coefficients of thermal expansion, and T is the temperature change. There are 36 compliance coefficients, but due to symmetry of S_{ij} only 21 are independent. For isotropic materials the number of independent coefficients is two.

Here it is assumed that the material is isotropic and the temperature changes are negligible. Since only thin sections are to be modeled, a state of plane stress (with

respect to the xy-plane) is assumed to exist in the body. That is, $\sigma_{zz} = \sigma_{zx} = \sigma_{zy} = 0$. In view of these assumptions, Eq. (2.1) becomes

$$\begin{aligned}\epsilon_x &= \frac{1}{E} (\sigma_x - \mu \sigma_y) \\ \epsilon_y &= \frac{1}{E} (\sigma_y - \mu \sigma_x) \\ \epsilon_z &= -\frac{\mu}{E} (\sigma_x + \sigma_y) \\ \epsilon_{xy} &= \left(\frac{1+\mu}{E}\right) \sigma_{xy}\end{aligned}\tag{2.2}$$

where E is the modulus of elasticity, and μ is Poisson's ratio. These equations can be inverted to express the stresses in terms of the strains:

$$\begin{aligned}\sigma_x &= \frac{E}{1-\mu^2} (\epsilon_x + \mu \epsilon_y) \\ \sigma_y &= \frac{E}{1-\mu^2} (\epsilon_y + \mu \epsilon_x) \\ \sigma_{xy} &= \frac{E}{1+\mu} \epsilon_{xy}\end{aligned}\tag{2.3}$$

Note that equations (2.2) and (2.3) are valid only in the linear elastic portion of the stress-strain curve.

The kinematic analysis of the body, under the assumption of small displacements, gives the following strain-displacement equations:

$$\epsilon_x = \frac{\partial u}{\partial x}, \quad \epsilon_y = \frac{\partial v}{\partial y}, \quad \epsilon_{xy} = \frac{1}{2} \left(\frac{\partial u}{\partial y} + \frac{\partial v}{\partial x} \right)\tag{2.4}$$

where u and v denote the displacements along x and y -directions, respectively.

Finally, to complete the description of the equations, the equations of equilibrium must be added,

$$\frac{\partial \sigma_x}{\partial x} + \frac{\partial \sigma_{xy}}{\partial y} = 0, \quad \frac{\partial \sigma_{xy}}{\partial x} + \frac{\partial \sigma_y}{\partial y} = 0 \quad (2.5)$$

wherein the body forces are assumed to be zero. Equations (2.3) - (2.5) must be appended with appropriate boundary conditions of the problem.

Since this study involves loading of the body through the linear elastic, nonlinear elastic and plastic regions of the stress-strain curve, we must have a relationship between the stresses and strains in these regions. In the present study, where aluminum (2024-T3) was used, it is assumed that the nonlinear elastic portion is negligibly small.

These two remaining regions are shown in Figure 2.1 for a uniaxial stress state. In the initial linear region, the material response is elastic and structures whose loads result in stresses in this region will return to their original shape when the loads are removed. Structures loaded into the plastic zone, however, take on a permanent set on unloading (dashed line of Figure 2.1).

In order to analyze the nonlinearity introduced by the plastic response, the curve in Figure 2.1a is divided into a series of linear portions as shown in Figure 2.1b, with the tangent modulus and incremental Poisson's ratio replacing the elastic constants previously mentioned.

Next, the choice of failure criteria to determine yield and fracture should be considered. The commonly

used failure criterion is that of von Mises, which shows the best agreement with experimental yield data for metals. For the case of plane stress, von Mises criterion takes the form

$$\sigma_1^2 - \sigma_1\sigma_2 + \sigma_2^2 = \sigma_{yp}^2 \quad (2.6)$$

where σ_1 and σ_2 are the principal stresses, and σ_{yp} is the yield stress. If the left hand side is less than σ_{yp}^2 , yield does not occur. The surface described by Eq. (2.6) is shown in Figure 2.2. Problems arise in extending von Mises' criterion into the plastic range with the incremental approach used in this study (this will be discussed in detail in Chapter III); therefore, the maximum strain criterion was used. In this theory, yield occurs when the maximum strain exceeds the strain at yield. That is

$$\begin{aligned} \epsilon_1 &= \pm \epsilon_{yp} \\ \text{or } \epsilon_2 &= \pm \epsilon_{yp} \\ \text{or } \epsilon_3 &= \pm \epsilon_{yp} \end{aligned} \quad (2.7)$$

where ϵ_1 , ϵ_2 , and ϵ_3 are the principal strains. Conversion of these equations to equivalent principal stresses is also shown in Figure 2.2. As can be seen, when $\sigma_1 \gg \sigma_2$ or $\sigma_2 \gg \sigma_1$, both theories give approximately the same results. Since the stress fields in the parts to be analyzed meet this requirement, the use of the maximum strain criterion is justified for this study.

The maximum strain criterion can also be extended along the stress-strain curve to predict subsequent changes

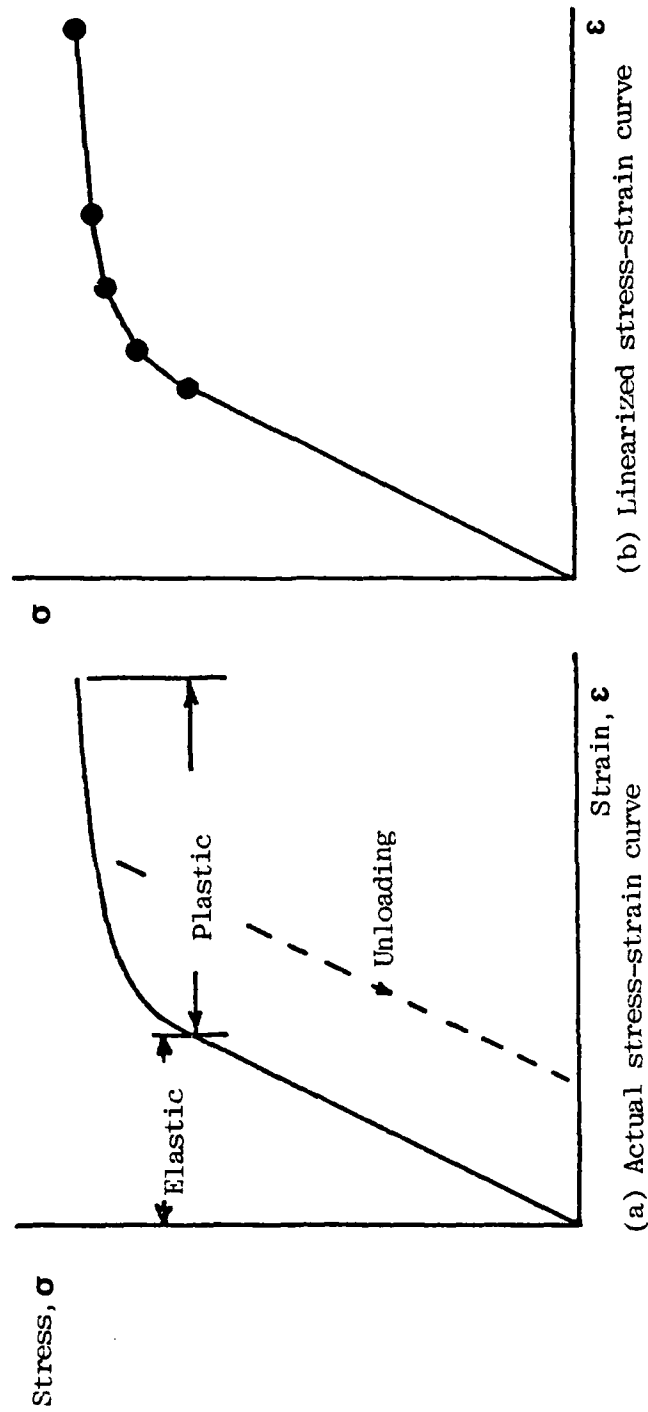


Figure 2.1. Elastoplastic Stress-Strain Curve

in modulus and finally the fracture.

The principal strains used in Eq. 2.7 can be obtained from the following equation:

$$\epsilon_{1,2} = \frac{\epsilon_x + \epsilon_y}{2} \pm \sqrt{\left(\frac{\epsilon_x - \epsilon_y}{2}\right)^2 + (\epsilon_{xy})^2} \quad (2.8)$$

A similar equation may be used to obtain principal stresses.

With the basic continuum equations developed here, a suitable procedure must be employed to obtain a solution.

II.2 The Finite Element Approach

The finite element method (FEM) is employed to solve the elasticity equations for each increment of load. Only a brief discussion of the method will be presented here; however, for a more thorough presentation, see Ref. 12.

The basic element used in this study is the standard constant strain triangle (CST) shown in Figure 2.3. The element has a total of six displacement degrees of freedom, one in each direction at each of three nodes. The displacement field is approximated by the linear relation of the form

$$u = \sum u_i \psi_i(x, y), \quad v = \sum v_i \psi_i(x, y) \quad (2.9)$$

where u_i , v_i are the nodal values of the deflections (at node i), and the ψ_i 's are element interpolation functions, given by

$$\psi_i = \frac{1}{2\Delta}(\alpha_i + \beta_i x + \gamma_i y) \quad (2.10)$$

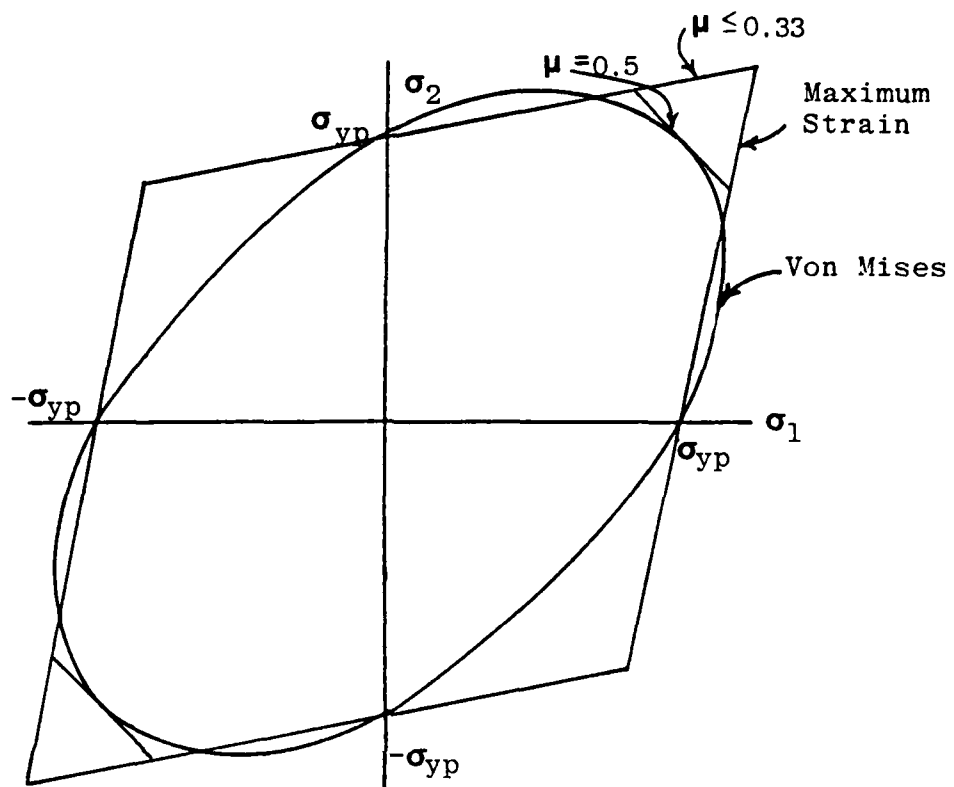


Figure 2.2. Yield Criteria

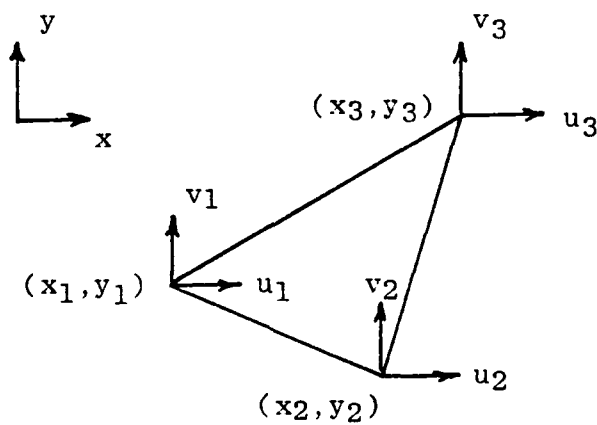


Figure 2.2. Maximum Strain and Von Mises Yield Criteria.

where Δ = area of the triangle,

$\alpha_i = x_j y_k - x_k y_j$, $\beta_i = y_j - y_k$, $\gamma_i = x_k - x_j$, and (x_i, y_i) are the coordinates of node i .

Combining Eqs. (2.4) and (2.9) gives:

$$\begin{aligned}\epsilon_x &= \frac{\partial u}{\partial x} = \sum_{i=1}^3 u_i \frac{\partial \psi_i}{\partial x} \\ \epsilon_y &= \frac{\partial v}{\partial y} = \sum_{i=1}^3 v_i \frac{\partial \psi_i}{\partial y}\end{aligned}\quad (2.12)$$

$$\epsilon_{xy} = \frac{1}{2} \left(\frac{\partial u}{\partial y} + \frac{\partial v}{\partial x} \right) = \frac{1}{2} \left(\sum_{i=1}^3 u_i \frac{\partial \psi_i}{\partial y} + \sum_{i=1}^3 v_i \frac{\partial \psi_i}{\partial x} \right)$$

In matrix form

$$\begin{aligned}\begin{Bmatrix} \epsilon_{xx} \\ \epsilon_{yy} \\ 2\epsilon_{xy} \end{Bmatrix} &= \begin{bmatrix} \frac{\partial \psi_1}{\partial x} & 0 & \frac{\partial \psi_2}{\partial x} & 0 & \frac{\partial \psi_3}{\partial x} & 0 \\ 0 & \frac{\partial \psi_1}{\partial y} & 0 & \frac{\partial \psi_2}{\partial y} & 0 & \frac{\partial \psi_3}{\partial y} \\ \frac{\partial \psi_1}{\partial y} & \frac{\partial \psi_1}{\partial x} & \frac{\partial \psi_2}{\partial y} & \frac{\partial \psi_2}{\partial x} & \frac{\partial \psi_3}{\partial y} & \frac{\partial \psi_3}{\partial x} \end{bmatrix} \begin{Bmatrix} u_1 \\ v_1 \\ u_2 \\ v_2 \\ u_3 \\ v_3 \end{Bmatrix} \\ &= [B] \{u\}\end{aligned}\quad (2.13)$$

The governing equations for this element are derived from a minimization of potential energy (I) for the system.

$$I = \frac{1}{2} \int_{vol} \{\epsilon\}^T \{\sigma\} dv + \text{Force Terms} \quad (2.14)$$

since from Eq. (2.3) (in matrix form)

$$\{\sigma\} = [E] \{\epsilon\} \quad (2.15)$$

$$I = \frac{1}{2} \int_{vol} \{\epsilon\}^T [E] \{\epsilon\} dv + \text{Force Terms} \quad (2.16)$$

and substituting from Eq. 2.13,

$$I = \frac{1}{2} \int_{vol} \{u\}^T [B]^T [E] [B] \{u\} dv + \text{Force Terms} \quad (2.17)$$

Applying variational methods to this equation to minimize I ($\delta I = 0$) results in the governing equation for this system.

$$\{F\} = [K] \{u\} \quad (2.18)$$

where $\{F\}$ is the force vector, $[K]$ is the stiffness matrix, and $\{u\}$ is the displacement vector. The form of $[K]$ results from the variation of Eq. (2.17) and is given as

$$[K] = \int_{vol} [B]^T [E] [B] dv \quad (2.19)$$

which for the CST element becomes

$$[K] = [B]^T [E] [B] A t \quad (2.20)$$

where A is the area and t is the thickness.

The procedure then becomes to assemble the stiffness matrix $[K]$, element by element. These are used to assemble the global stiffness matrix for the entire system. Boundary conditions must be applied to the assembled system of equations of the form of Eq. (2.18) before these equations are solved for $\{u\}$. If strain or stress values are desired Eq. (2.12) and Eq. (2.3) may then be applied.

This procedure is then automated, and the analyst only need describe the geometry in terms of elements and nodes and boundary conditions.

The programs that incorporate this development are described in the next chapter.

CHAPTER III

FINITE ELEMENT FRACTURE PROGRAMS

III.1 Introduction

Three two-dimensional plane stress finite element programs are developed herein to predict yield and fracture under monotonically increasing loads. These programs are:

1. FRACTURE: This finite element program is developed to analyze point loaded tensile and notched specimens. Engineering stress-strain relations are used; however, the model geometry is not updated during each load increment.
2. PANEL1: This program is a modification of FRACTURE and is used to analyze uniformly loaded panel specimens.
3. PANEL2: This is a modification of PANEL1 which uses incremental geometry changes and true stress-strain relationships.

Input was obtained from a mesh generation program, and all input data was plotted as a check for errors. All of the programs were run on the University of Oklahoma's Merrick Center IBM 370/158 computer.

The programs contained in this work are not optimized or even necessarily efficient from the programming point of view.

III.2 Formulation

The basis of the formulation of the programs developed herein is that each element of the finite element mesh has its own material properties (modulus and Poisson's ratio) based on its state of strain. These "local" properties should approximate those of the actual structure. Furthermore, these properties will be those of a uniaxial tensile test specimen of the same material under the same state of strain; that is, when an element has a principal strain equal to the uniaxial yield strain of the material, the element yields (changes tangent modulus and Poisson's ratio). In a similar manner, an element fractures (changes modulus to zero) when its maximum principal strain is equal to the strain at which the tensile specimen fractures.

To apply these concepts to an operational program, it is necessary to have the entire stress-strain curve from the elastic region all the way to fracture (while stress-strain curves are readily available, strain at fracture is not). The stress-strain curve is then divided into a series of linear segments as shown in Figure 3.1. From this linearized curve, values for modulus are obtained as

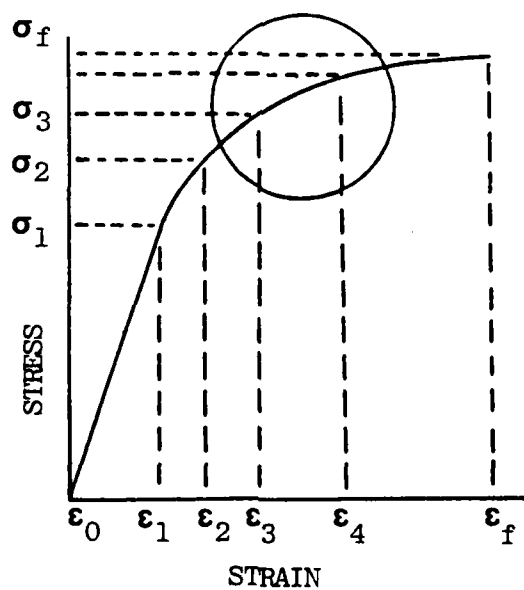
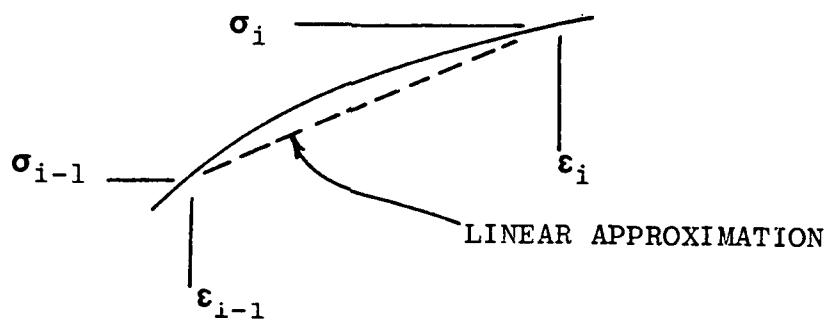


Figure 3.1. Linear Approximation of a Stress-Strain Curve.

$$E_i = \frac{\sigma_i - \sigma_{i-1}}{\epsilon_i - \epsilon_{i-1}} \quad (3.1)$$

where σ_i and ϵ_i are the engineering stress and strain, respectively.

The values of Poisson's ratio (μ) in the plastic range were calculated from the equation given by Bert, Mills, and Hyler¹³ as proposed by Nadai:¹⁴

$$\mu = \frac{1}{2} - (\frac{1}{2} - \mu_e)(E_S/E_e) \quad (3.2)$$

where μ_e is the elastic Poisson's ratio, E_S is the secant modulus, and E_e is the elastic modulus. For any section, the secant modulus is taken as the average stress in the interval divided by the average strain in that interval; that is,

$$E_{S_i} = \frac{\sigma_i + \sigma_{i-1}}{\epsilon_i + \epsilon_{i-1}} \quad (3.3)$$

Therefore, the incremental Poisson's ratio (μ_i) becomes

$$\mu_i = \frac{1}{2} - \frac{(\frac{1}{2} - \mu_e)}{E_e} \frac{(\sigma_i + \sigma_{i-1})}{(\epsilon_i + \epsilon_{i-1})} \quad (3.4)$$

These material properties along with the terminal strains (ϵ_i) for each interval are stored in the program and referenced by an element material pointer. The properties for a fractured element are also stored, with the tangent modulus set to zero and Poisson's ratio equal to 0.5. As an example Table 3.1 gives the tabulated steel and aluminum properties used in the program FRACTURE.

With the material properties tabulated and referenced by strain level, the material nonlinearity of the problem

TABLE 3.1
EXAMPLE OF TABULATED MATERIAL PROPERTIES

| Pointer | Region | E_i | μ_i | ϵ_i |
|---------|-----------|-----------|---------|--------------|
| 1,1* | Elastic | 29000000. | 0.318 | 0.00200 |
| 1,2 | Elastic | 10500000. | 0.313 | 0.00472 |
| 2,2 | 1st yield | 1183000. | 0.375 | 0.00753 |
| 3,2 | 2nd yield | 462000. | 0.443 | 0.01814 |
| 4,2 | 3rd yield | 271000. | 0.467 | 0.03286 |
| 5,2 | 4th yield | 152000. | 0.484 | 0.07817 |
| 6,2 | 5th yield | 65000. | 0.491 | 0.14291 |
| 7,2 | Fracture | 0. | 0.500 | 999. |

*First #=Region, Second #=Material (1=Steel, 2=Aluminum)

is approximated by considering the structure to be analyzed as a composite of a finite number (n) of elements with appropriate properties. At the start of the analysis, the entire composite is assumed to have the same properties (those of the elastic portion of the stress-strain curve). As the load increases, one element (say the k -th element) will reach a total principal strain value equal to the yield strain. This k^{th} element's properties (modulus and Poisson's ratio) are modified; therefore, the composition of the structure is $n-1$ elastic elements and one element with a reduced (plastic) modulus. Since the response of each element is again linear, the usual elastic finite element

analysis can be used until another element yields or the k^{th} element reaches the strain at which next modulus change occurs. The process is repeated until at least one element fractures. The total load to this point is the sum of the incrementally applied loads, and the total deflections at any node are the sum of the incremental deflections.

At fracture, the procedure described above must be modified, since the loads carried by the fractured element to this point must now be carried by the remaining structure. In Ref. 10 and 11 the crack is advanced by removing the constraint at the fractured node and redistributing the force on that node to the remaining nodes along the appropriate line of symmetry; however, as Miller¹¹ points out, there is no obvious rationale which appears to govern the redistribution, while the effects of the redistribution method are significant. In the present program, a new and completely general procedure is applied. When an element reaches the strain for transition to fracture, the structure is unloaded following the elastic response of the unfractured specimen while retaining each element's progress along the stress-strain curve. It is then reloaded with the fracture surface extended. Any effects due to compression during this unloading are ignored since the actual structure never undergoes this unload reload cycle. If the main diagonal stiffness coefficient corresponding to a node is reduced to zero (the node is unconnected) as a result of a modulus change

at fracture, the node is constrained.

If another element fractures before the maximum load is reached, then the crack growth is unstable but may become stable again if the load subsequently increases over the previous maximum fracture load. Figure 3.2 illustrates this procedure for a stress-strain curve with 3 linear plastic regions. A sample mesh at a crack tip is shown in Figure 3.2 along with four sample elements numbered. The bottom four curves are plots of typical stress-strain responses of the four elements as load increases. Numbers along the curves indicate the load level at that point. At level 1, element 1 at the crack tip enters the first yield region. There is less stress (strain) concentration at the other three elements; therefore, they advance only partially along the elastic portion of the curve. At load level 2, element 1 changes modulus again, even before any of the other three elements have yielded for the first time. The load continues to increase to level 3, at which point the principal strain of element 2 indicates it has reached the transition strain for first yield. This continues through levels 4, 5, and 6. At level 7, element 1 has reached the fracture strain. The entire model is then unloaded (artificially). The modulus for element 1 is set to zero and reloading begins with all unfractured elements having an elastic modulus. Stress remains at the unloaded value for element 1, since all incremental stresses are zero. Strains

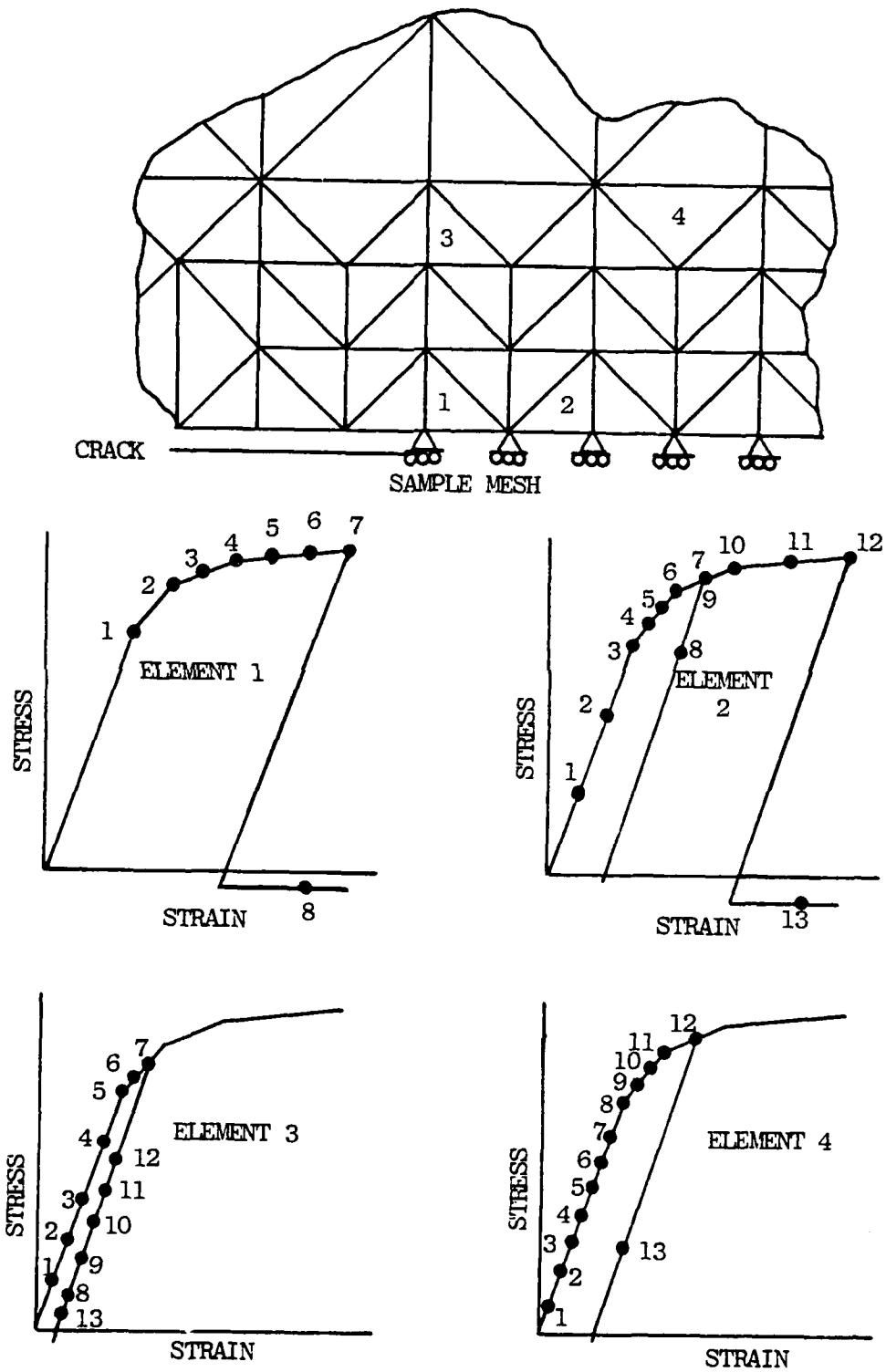


Figure 3.2. Typical Element Response, "Zero Modulus-Unload Reload" Method

for element 1, however, continue to increase. At level 8 element 4 changes modulus for the first time. At level 9, the stress and strain, but not the load, at element 2 equals the equivalent values at level 7. Here the element's properties, just at the elastic values, return to those of yield zone 2. Elements 3 and 4 retain the elastic modulus and Poisson's ratio. At level 10, element 2 enters the 3rd yield zone and at 11, element 4 enters the 2nd yield zone. At level 12, element 2 fractures and the structure is again artificially unloaded. Note that element 3 properties have remained elastic since element 1 fractured. At 13, reloading has begun but at a slower rate for element 3 due to the low strain behind the crack tip. If the load at level 12 is larger than the load at 7, then fracture at 7 is stable. On the other hand, if load 7 exceeds level 12, then fracture is unstable. This process continues until the stiffness matrix is no longer invertible.

The "zero modulus-unload reload" method just described has the following advantages over the nodal release-load redistribution approach of Ref. 10 and 11:

1. The method of redistribution is not arbitrary, but based on cracked specimen geometry.

2. Failures can occur anywhere in the model. With sufficiently small elements, the zero modulus elements act as the crack. Not only is the nodal release method incapable of predicting general crack growth, it is specifically

restricted to the study of fracture along axes of symmetry.

3. The "zero modulus-unload reload" method described herein is element oriented, whereas the load redistribution method is node oriented. Since only deflections are specified at the nodes and stresses and strains are specified over the elements, stress or strain data must be arbitrarily distributed to the nodes in the load redistribution method so that the failure criteria may be applied.

The current method does require the extra time used to unload and reload the structure.

This study uses maximum strain criteria both for yielding and fracture. Newman¹⁰ and Miller et al.¹¹ both use maximum strain for fracture, but use von Mises criteria for yielding. A problem with the stress formulation of von Mises criteria is that not all practical materials (for example mild steel) have unique strains for a given stress. Thus if the material stress-strain curve is as shown in Figure 3.3, and one linearized section is taken from a to b, then the modulus for section ab is zero. The incremental stress for an element with properties in this portion of the curve will always be zero. Therefore, under the stress formulation of von Mises criteria, the stress will never advance past point b. This problem could be circumvented by reformulating von Mises criteria in terms of strain. Since the specimens for this study were uniaxially loaded and the minimum stress was low compared to the maximum stress, maximum strain

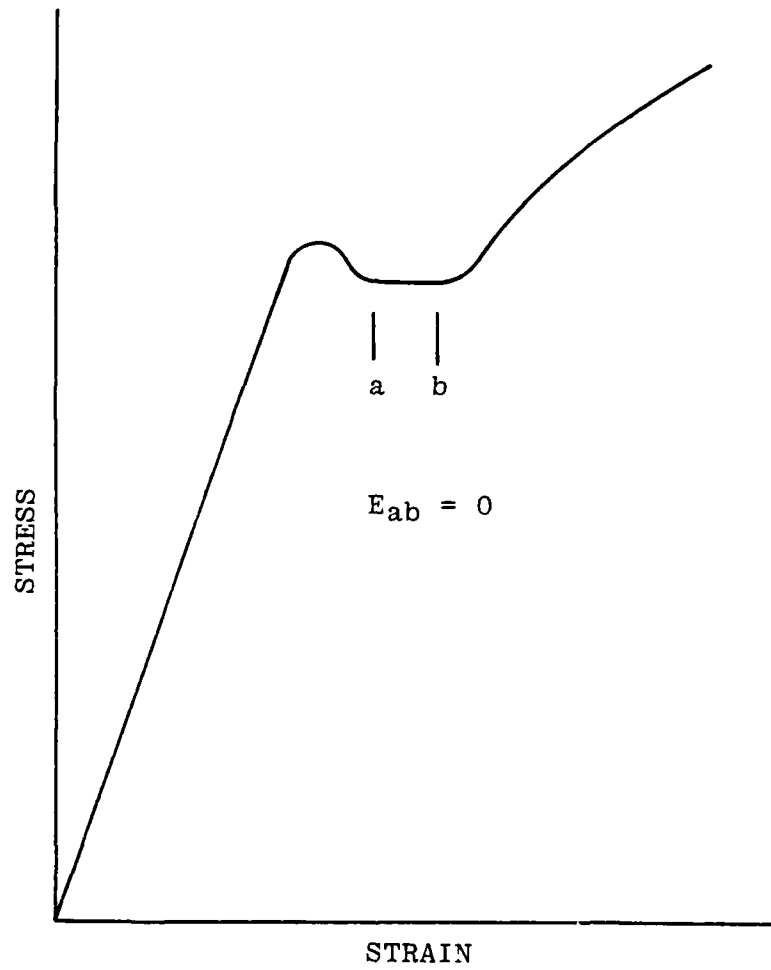


Figure 3.3. Stress-Strain Curve with Zero Modulus Section.

criteria and von Mises criteria are very similar, and therefore, this reformulation was not attempted. It should be remembered, however, that for geometries and/or loadings which result in approximately equal principal stresses, the principal strain criteria used in this program will introduce significant error.

As described in Chapter II, the programs developed here utilize a standard constant strain (linear deflection) triangular element, CST, under plane stress conditions. This element enables the use of a large number of elements in a given area with minimum storage requirements and mesh refinement is easier to accomplish. The predicted rate of crack growth must be independent of the element size (crack growth of 0.001 inches cannot be predicted using elements with sides 0.1 inches long); therefore, many small elements are needed along anticipated crack paths. If higher order elements (e.g., the linear strain triangle) are used in such a dense mesh, storage requirements become excessive. Therefore, the simplest two dimensional element (the CST) is used.

In the experimental procedure, the tensile specimens are loaded through a steel pin in the center of the head of the specimens. To realistically simulate this composite structure, the finite element analysis includes the pin as part of the system. One half of the pin is divided into six elements in the one quadrant models, and a full pin is divided into twelve elements in the half specimen models.

A unit load is applied to the center of the pin to distribute the load. In programs PANEL 1 and PANEL 2, the load is uniformly distributed to the nodes along the edge of the panel.

III.3 Description of the Computer Programs

Each of the three programs consists of a main program and six major subroutines as shown in Figure 3.4. Subroutines FAIL and CHANGE are the only routines not common to a standard elastic finite element analysis. Appendix I contains a listing of FRACTURE with significant differences between FRACTURE, PANEL1, and PANEL2 discussed in this section.

The main program first calls IREAD, which reads in the geometric description (nodal locations and element conductivity) from the mesh generator as well as the nodal constraints. IREAD also prints out the data as a check on proper input.

The subroutine PROP sets up the material property matrix. This matrix contains the modulus, Poisson's ratio, and strain for next transition indexed by a pointer and type of material. Recall that programs FRACTURE and PANEL use material properties that are based on the engineering stress-strain relation while program PANEL2 uses the true stress-strain relation. The subroutines IREAD and PROP are called

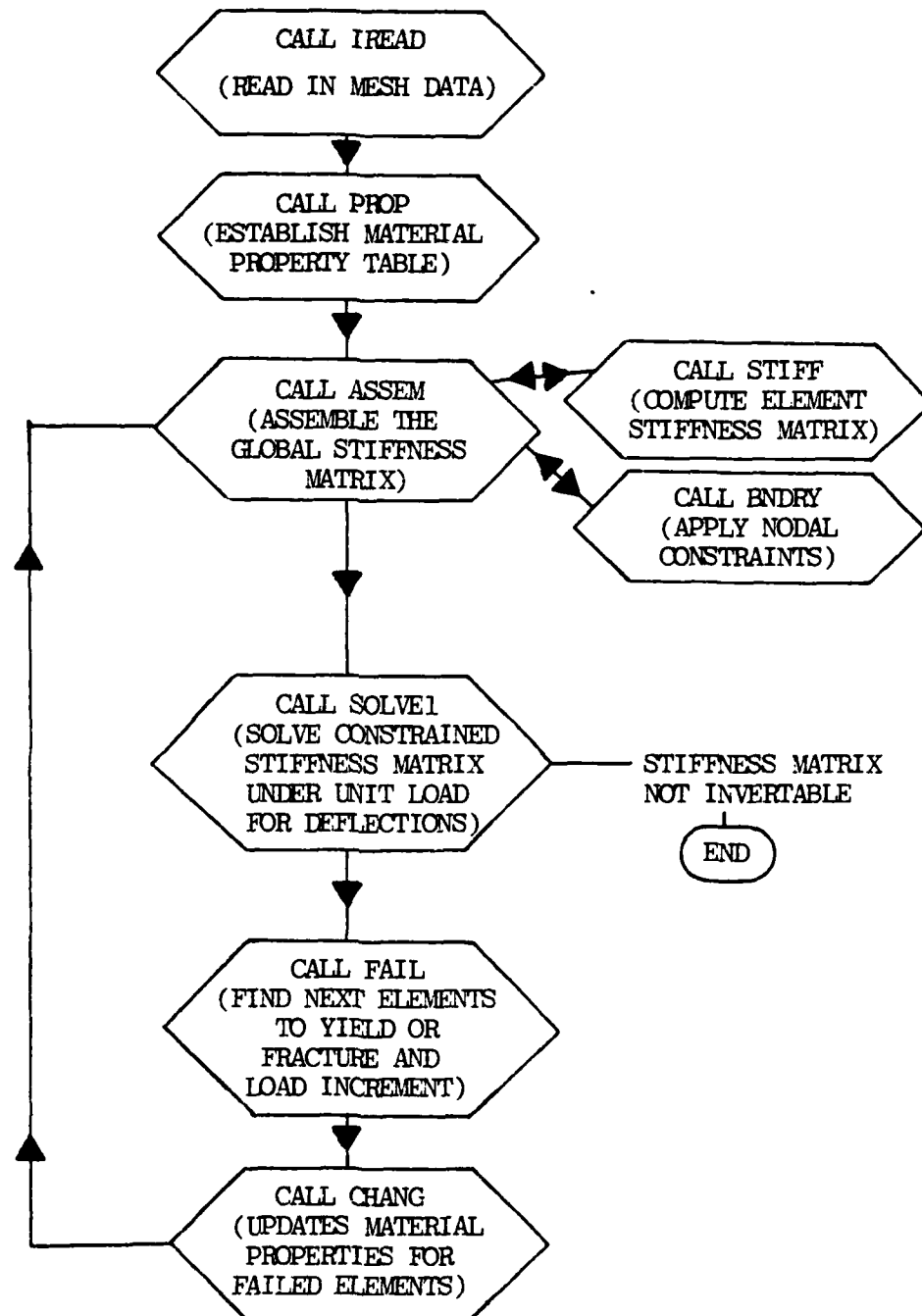


Figure 3.4. Flow Chart for the Program FRACTURE.

only once in the program and no further reference is made to them later in the program.

The subroutine ASSEM assembles the element stiffness properties to obtain the global stiffness matrix, GSTIF. For each element, ASSEM calls STIFF which calculates the element stiffness matrix. The global stiffness is stored in a banded form in the interest of storage and computational efficiency. The appropriate boundary conditions on the nodal deflections are then applied by calling the subroutine BNDRY. Finally, a check is made to insure that no main diagonal terms are zero. This occurs if the stiffness contribution of each element touching the node is zero; if any diagonal term is zero, the node is condensed out by BNDRY.

Subroutine SOLVE1 solves the banded system of equations,

$$\{F\} = [K] \{u\} \quad (3.4)$$

for the unknown displacements $\{u\}$. Here $\{F\}$ is the nodal force vector and $[K]$ is the global stiffness matrix. The program was originally developed using a Gauss-Seidel iterative solution technique since $[K]$ and $\{u\}$ change very little from load increment to increment. This eliminates the need to reassemble the stiffness matrix for each load increment. For a small mesh, the iterative method converged rapidly for the first few iterations, but the time required for accurate solutions greatly exceeded that required for the Gauss

elimination method. As a result, the Gauss elimination method was used exclusively in this study; however, for the very large meshes used in the following chapters, this iterative scheme may deserve more attention. When the specimen fails, the stiffness matrix is no longer invertible and the computation is terminated. The load matrix for FRACTURE consists of a unit load applied to the center node of the pin (used to distribute the load to the specimen) in the longitudinal direction. For the PANEL programs, where the specimen is uniformly loaded, the unit load is divided between the top five nodes of the specimen in ratios of $1/8$, $1/4$, $1/4$, $1/4$, and $1/8$ starting from the edge node. Double precision is used in this subroutine and throughout the program to reduce roundoff errors.

Subroutine FAIL is the first non-standard subroutine of FRACTURE; i.e., it cannot be found with the usual finite element analysis programs. First, FAIL calculates the unit strains in the x and y directions along with the shear strains for each element. These are a function of the deflections calculated in SOLVE1. The first time through FAIL, all elements are in the elastic range and the initial strains are zero. Therefore, the principal strains for a unit load are calculated and the load at first yield is taken to be the tabulated strain at first yield divided by the maximum principal strain for a unit load. Next, the unit strains are multiplied by the calculated load to obtain

the total strains for each element at first yield.

For subsequent calls to FAIL, the total strains for each element are not zero and their directions are not the same as those of the incremental strains. This makes direct calculation of the next yield or fracture load impossible; therefore, an incremental scheme must be used to predict the next load increment. This is accomplished by storing the next strain for modulus change for each element in an array called ECH, and calculating the incremental principal strain (DEPR) and total principal strain (EPRI). If the incremental principal strains are in the same direction as the total principal strains, the incremental load (LI) for the next failure is given by

$$LI = (ECH - EPRI) / DEPR \quad (3.5)$$

Since EPRI and DEPR are not in general in the same direction, Eq. (3.5) is only an approximation. This calculation is made for each element and the smallest load increment is then used as the trial load increment which will cause the next element to change modulus. In order to reduce the computational time, this increment may be increased to cause more elements to fail for each solution of Eq. (3.4). With the incremental load now calculated, the total strains are set equal to the previous total strains plus the incremental strains times the incremental load. The total principal strains for each element are then calculated and compared

with the tabulated strains for next modulus change. If no elements exceed the next change strains, the incremental strains are again multiplied by the incremental load and added to the total strains. The principal strains are again calculated and are compared to the tabulated values. The cycle continues until at least one value of the tabulated maximum allowable strain for the interval is exceeded. All such elements are printed along with the new total load and the corresponding property intervals. If only yielding has occurred, control is returned to the main program. If fracture has occurred, the total strains are reduced by the elastic response due to a unit load times the total load at fracture, and then control is returned to the main program.

Subroutine CHANG was originally conceived to update the global stiffness matrix for failed elements in conjunction with the SOLVE (Gauss-Seidel) iterative routine. Since the entire stiffness matrix must now be regenerated (because it is changed during the Gauss elimination in SOLVE1) for each pass, the function of CHANG has been reduced to updating the material pointer for failed elements. Element thickness was also updated in CHANG for the PANEL2 program.

The program continues to cycle from ASSEM to SOLVE1 to FAIL to CHANG until the stiffness matrix can no longer be inverted or the program exceeds the estimated time limit.

CHAPTER IV

CRACKED PANEL ANALYSIS

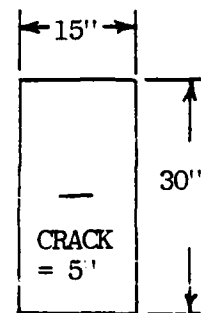
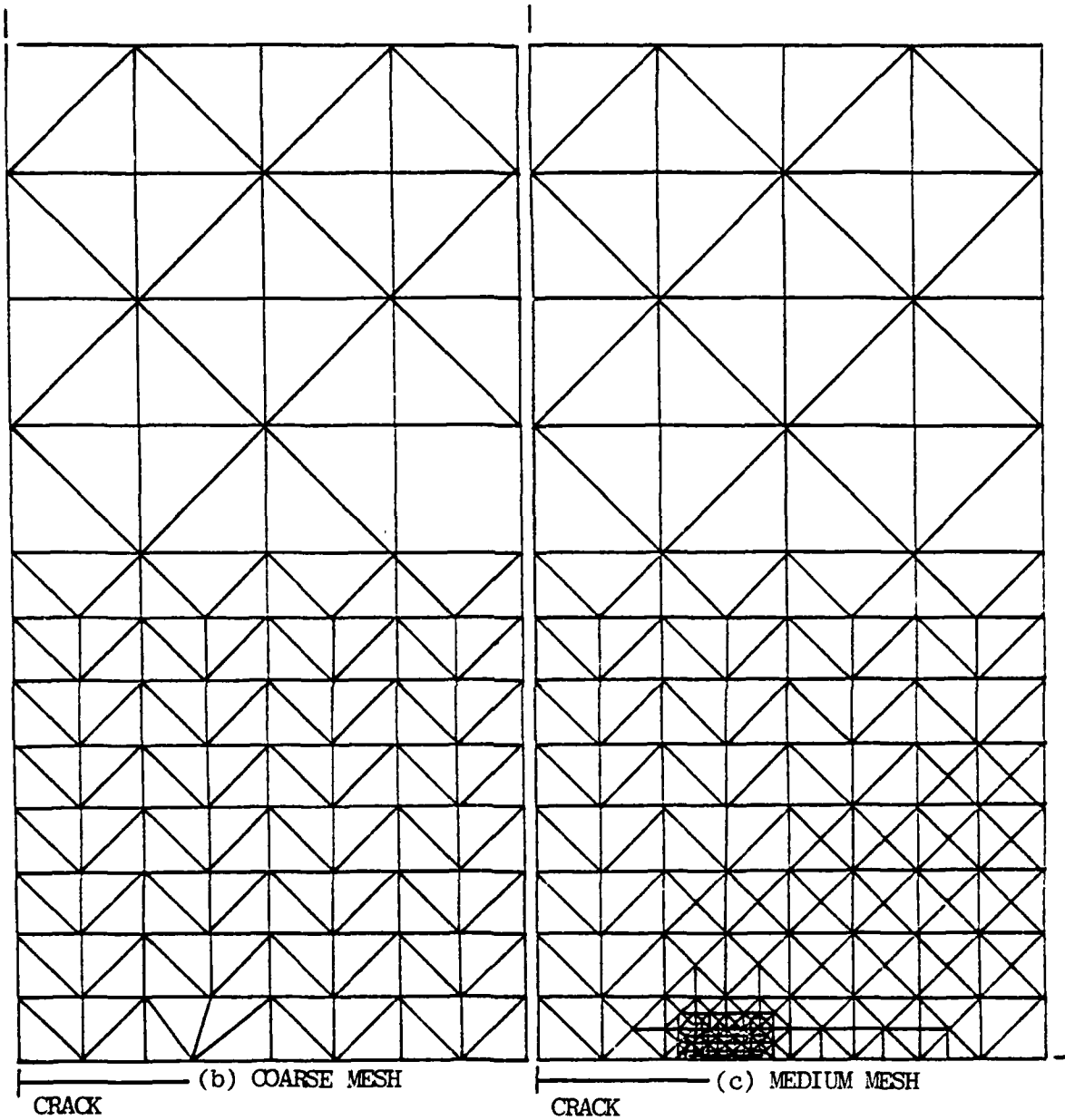
IV.1 Introduction

After the present study was undertaken, and the FRACTURE program was completed, the article by Miller¹¹ on fracture prediction became available. Miller's work raised two questions pertinent to the present study. First, can the present program improve on Miller's prediction of fracture load, and second, can the program accurately predict the experimental results presented by Miller?

To answer these questions and to determine the parameters that effect FEM fracture prediction, a modification of FRACTURE, called PANEL1, was made. The essential differences between FRACTURE and PANEL1, the method of load application and the size of the incremental load steps, are minor. A third program, PANEL2, used true stress-strain relations and updated geometric coordinates and element thicknesses for each load increment.

IV.2 Finite Element Analysis

Due to the geometric and loading symmetry of the panel, only one quadrant of the panel is used in the finite element analysis. Figure 4.1a shows the dimensions of the 0.10", 2024-T3 aluminum test panel. A nonuniform finite element mesh of the panel is shown in Figure 4.1b. To predict the response at the crack tip more accurately, further refinement was made there, as shown in Figure 4.1c. The crack-tip portion is blown up in Figure 4.1d to show the mesh details. The stress-strain curve data for the material was obtained from published data¹⁵. Some error is introduced by this selection since the exact material properties are not known. The stress-strain curve was then divided into one elastic and three linearly plastic regions. The panel was first analyzed using a coarse mesh. Subsequent refinements of the mesh were made at the crack tip. The loads predicted by each of these meshes are shown in Figure 4.2 as a function of the minimum element area at the crack tip. Entry into each plasticity region of the stress-strain curve is shown by the lower three curves with initial fracture and final fracture shown in the top curves. The horizontal line represents Miller's¹¹ experimental results. The elements on the right side of the figure are too large to predict stable fracture; therefore, only initial fracture is shown in this area. As can be seen in the figure, as element size becomes smaller at the tip, the load at entry into each of the



(a) DIMENSIONS

Figure 4.1. Cracked Panel Dimensions and FEM Models.

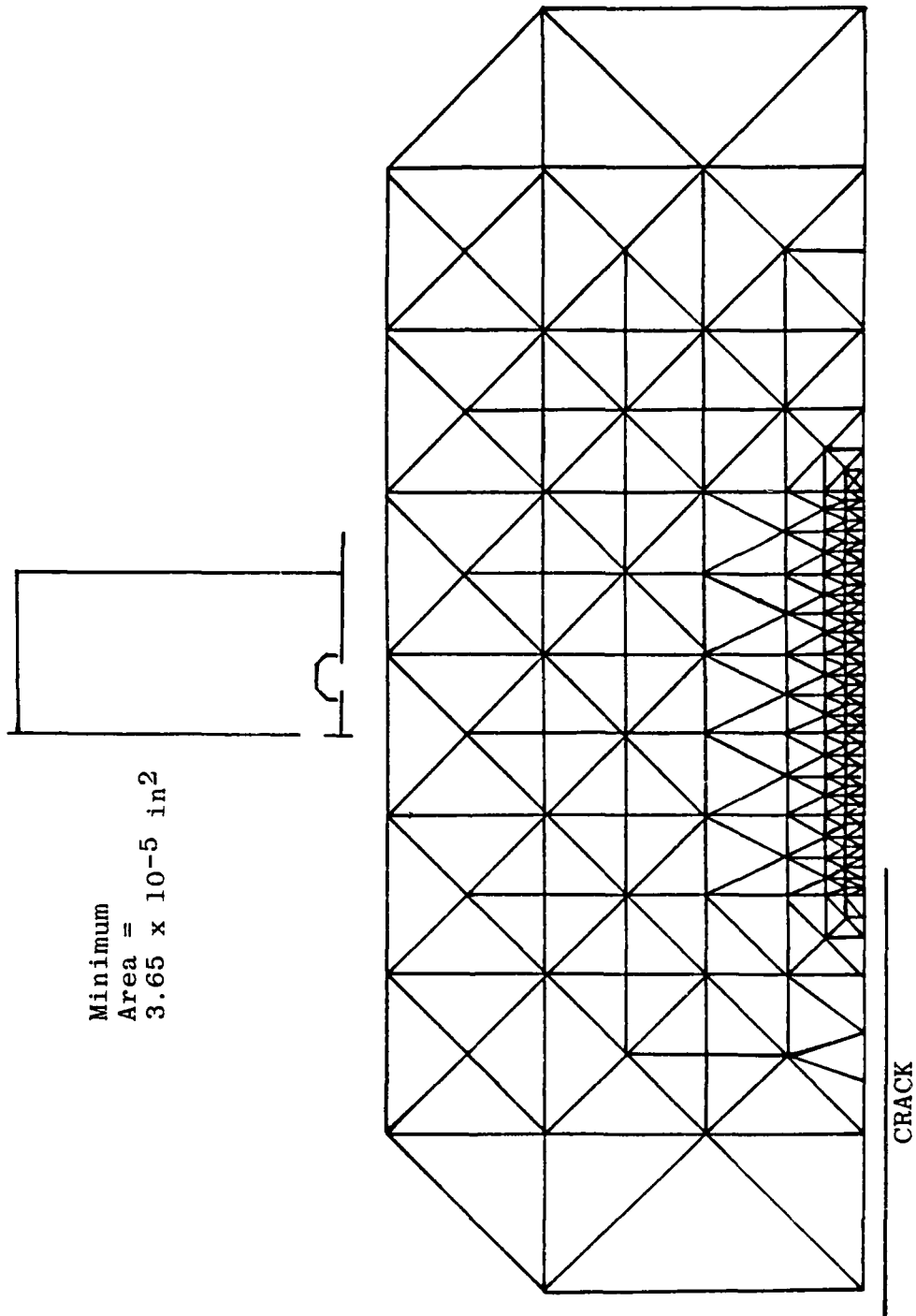


Figure 4.1d. Details of the Fine Mesh (c).

plasticity regions decreases, and the predicted final fracture curve converges to the experimental value. Note that there is no significant difference in the present solution and that of Miller's for equivalent mesh sizes. The large differences between Miller's experimental and numerical results appears to be due solely to the refinement of the mesh. While the methods do appear to have similar accuracies, it should be remembered from earlier discussions that Miller's method only applies to failure along lines of symmetry, and load redistribution procedures are arbitrary.

For stable fracture prediction, the mesh not only needs to be refined at the crack tip, but also along the projected crack path. The element meshes for the data shown in Figure 4.2 are basically the same except for refinements at the crack tip. The mesh shown in Figures 4.1c and 4.1d, however, is refined along the entire path of anticipated stable fracture. While the element size at the crack tip is larger for this fine mesh than those at the extreme left of Figure 4.2, the predictions are more accurate as can be seen in Figure 4.3. This refined mesh also predicted the crack growth as a function of load as shown in Figure 4.4. While no experimental data is available to confirm these predictions, it is interesting to note that each increment of crack growth advanced over several nodes.

Element orientation also plays a role in fracture load prediction. Figure 4.5 shows one example of this effect.

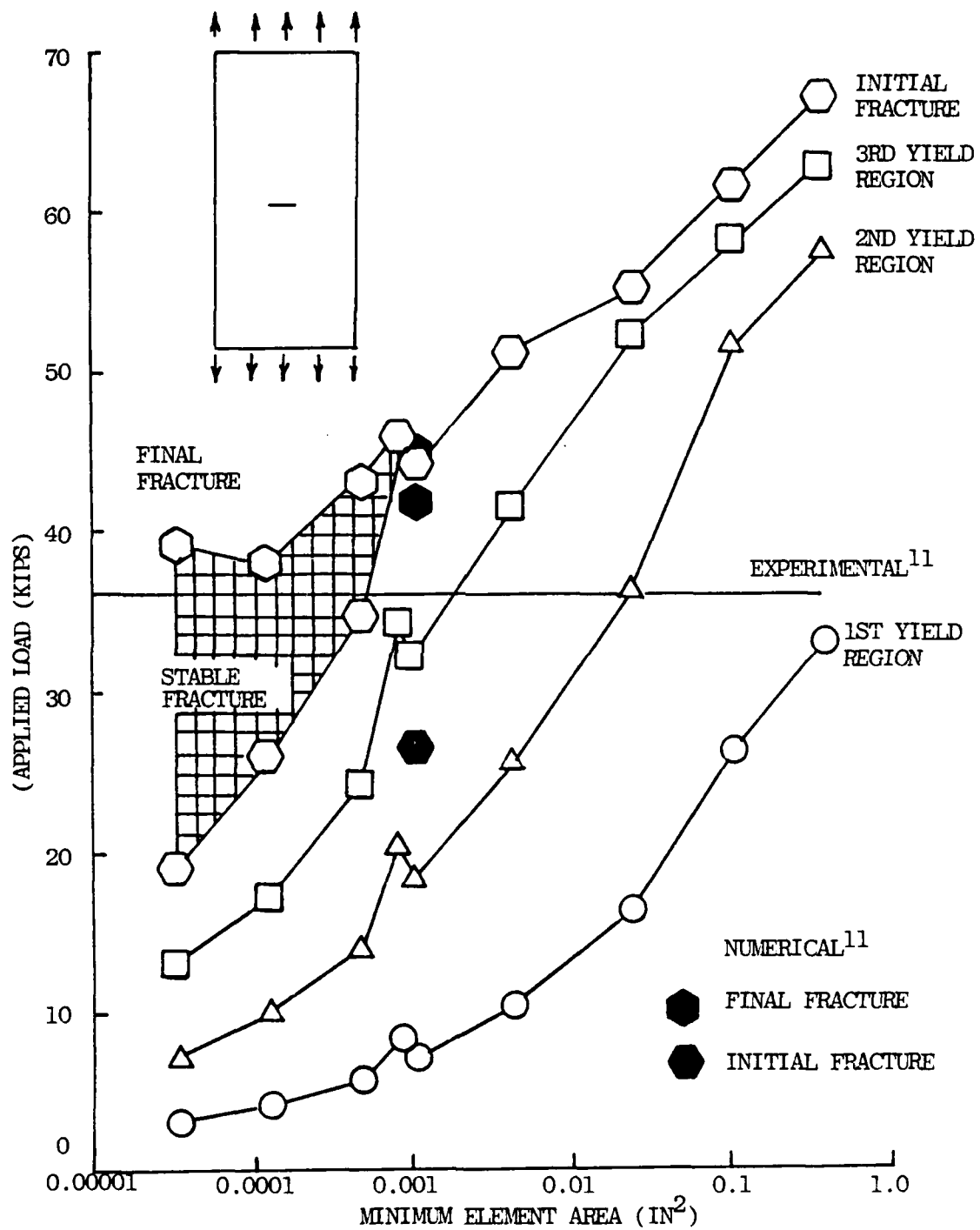


Figure 4.2. Numerical Convergence, Cracked Panel Study.

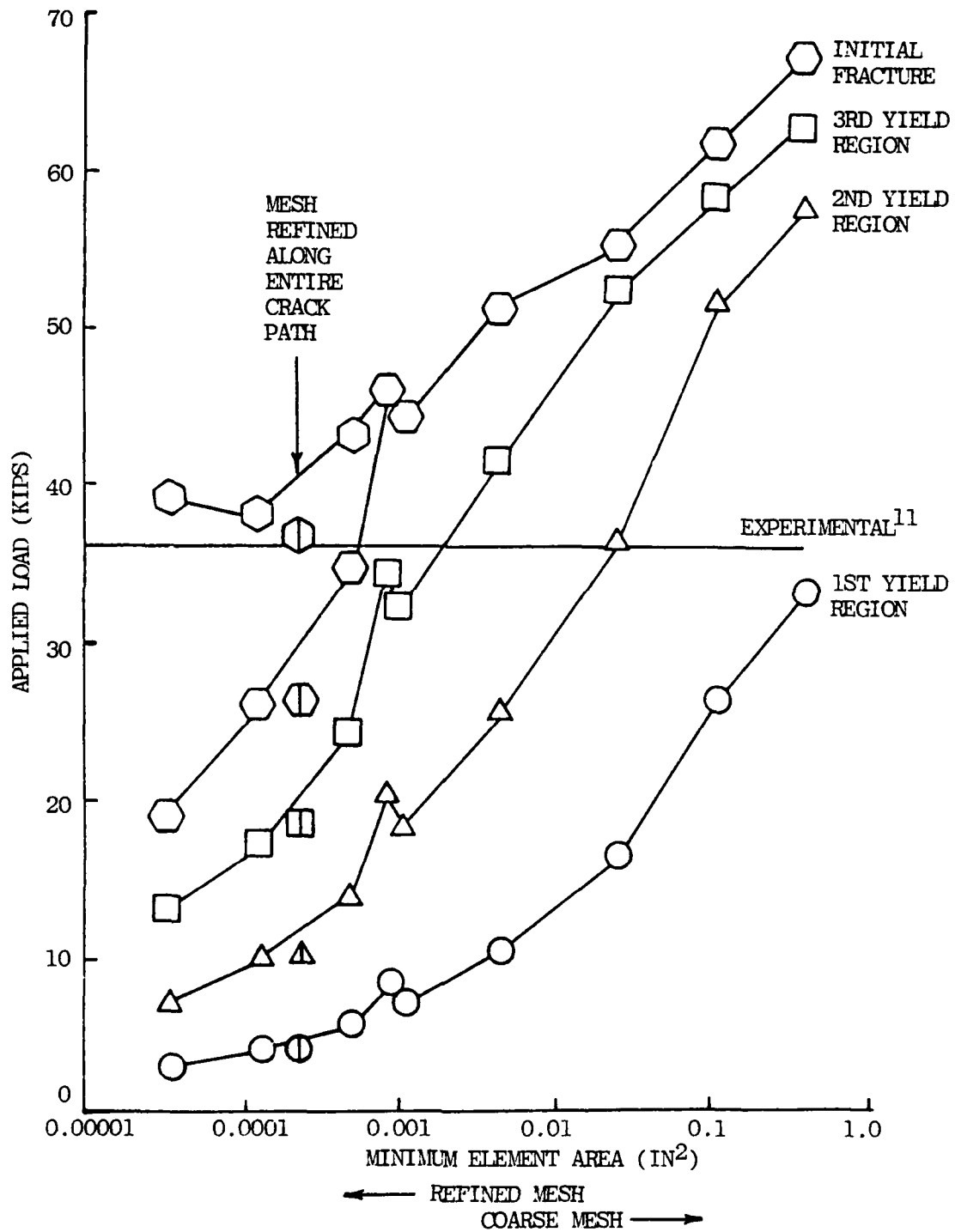


Figure 4.3. Effect of Mesh Refinement Along the Crack Path

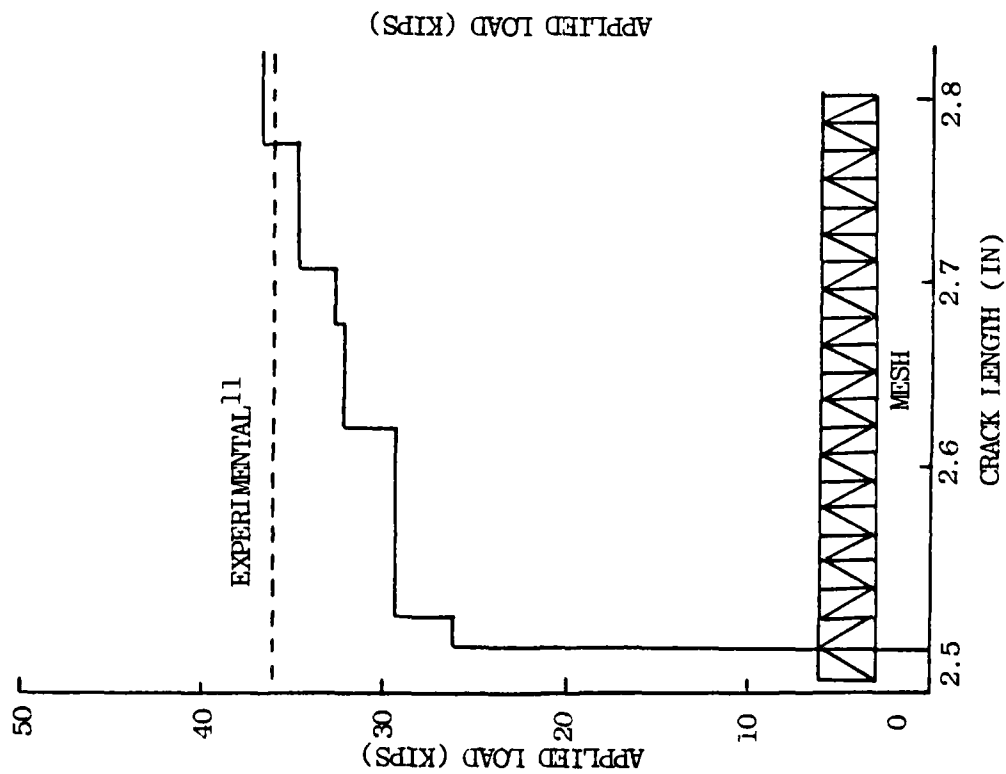


Figure 4.4. FEM Crack Growth Prediction.

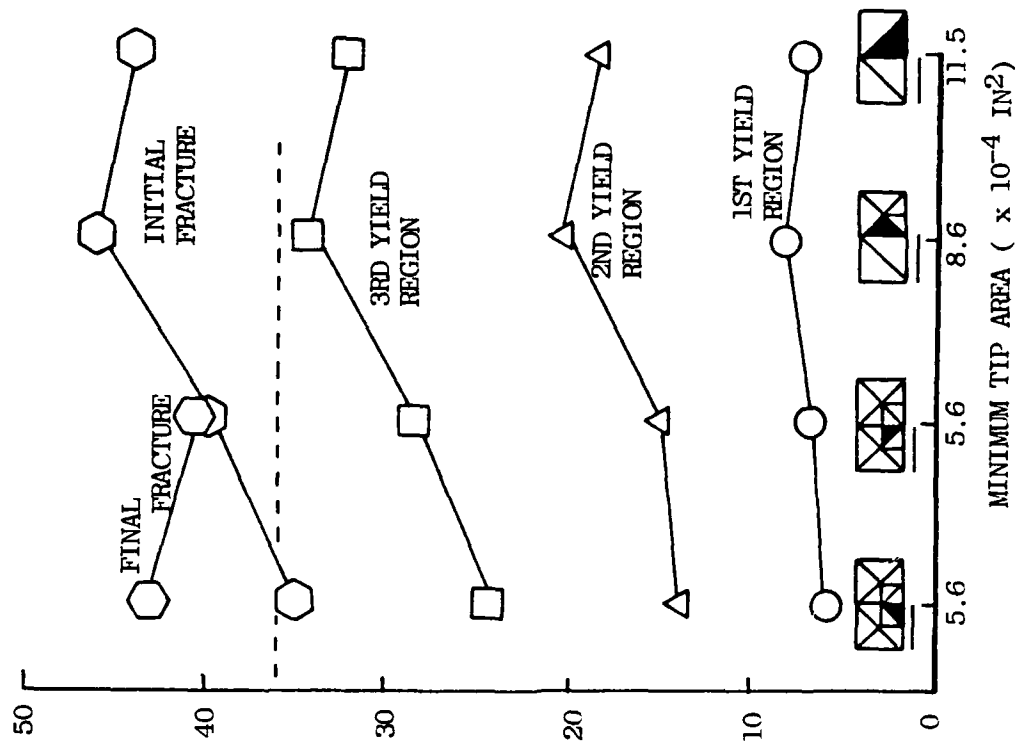


Figure 4.5. Effects of Element Orientation.

This difference in element orientation accounts for the slight upswing near the middle of Figure 4.2.

Finally, the program shows the material state of each element as the load increases. This data is plotted at selected load intervals in Figure 4.6. Part (a) shows the initial formation of the plastic zone at a load of 10,000 pounds. As the load increases to 20,000 pounds (Part (b)), the region of the specimen with properties in the first plasticity section increases and a small region in the second and third sections begin to form at the crack tip. Part (c) shows the expansion of all three regions just prior to initial fracture. One quadrant of the specimen is also shown in (c) to indicate the relative size of the plasticity zones. Figure 4.6d shows the plasticity zones after a significant amount of stable cracking. Note that after initial fracture and unloading, an element may go directly from an elastic response into any of the plasticity sections depending on its previous progress along the stress-strain curve (strain hardening). Note also that the plasticity zone is still increasing in size as the crack advances. In Figures 4.6e and 4.6f the plasticity zones move partially outside the magnified area of the crack tip with the region shown in Figure 4.6f being the plasticity zone at fracture.

PANEL2 was also used to analyze several panel meshes to determine the effects of using true stress-strain and updating specimen geometry during each load increment. No

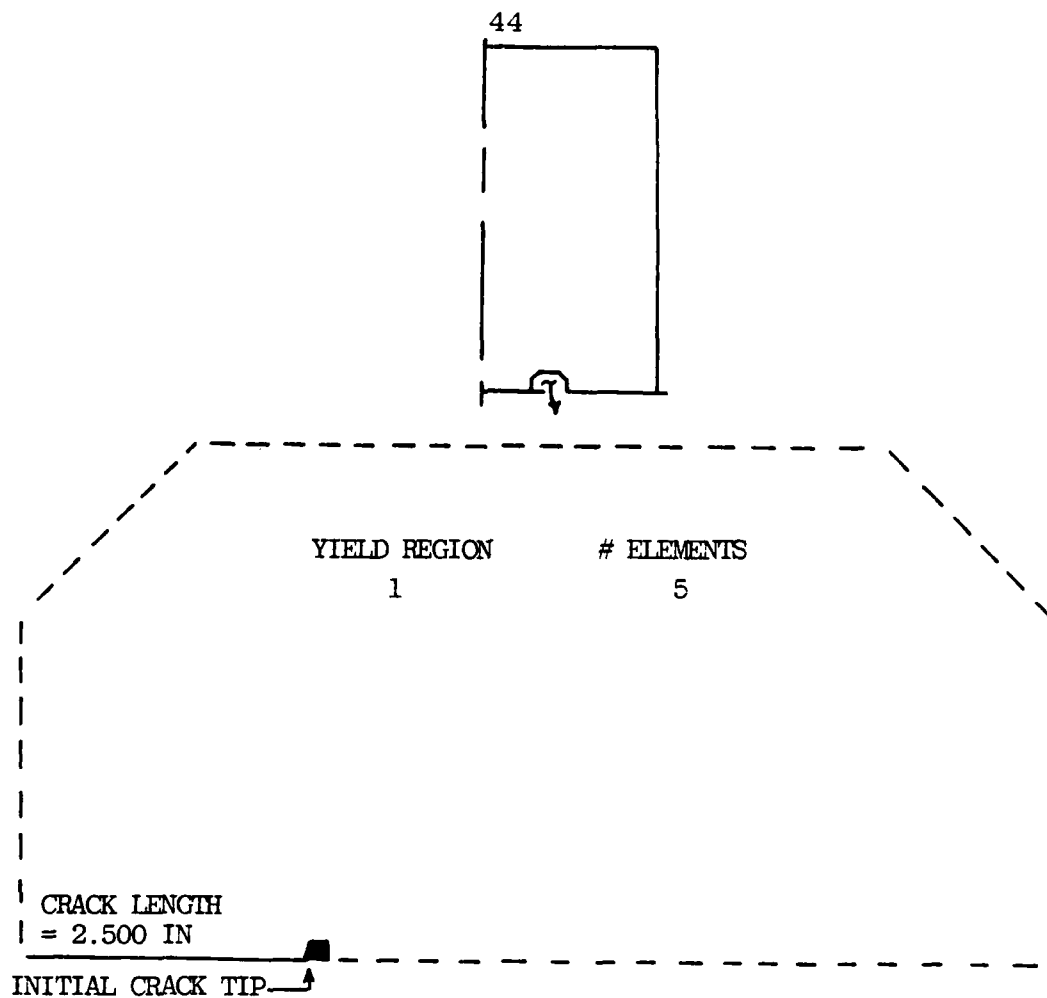


Figure 4.6a. Plastic Regions - Load = 10,000 LB.

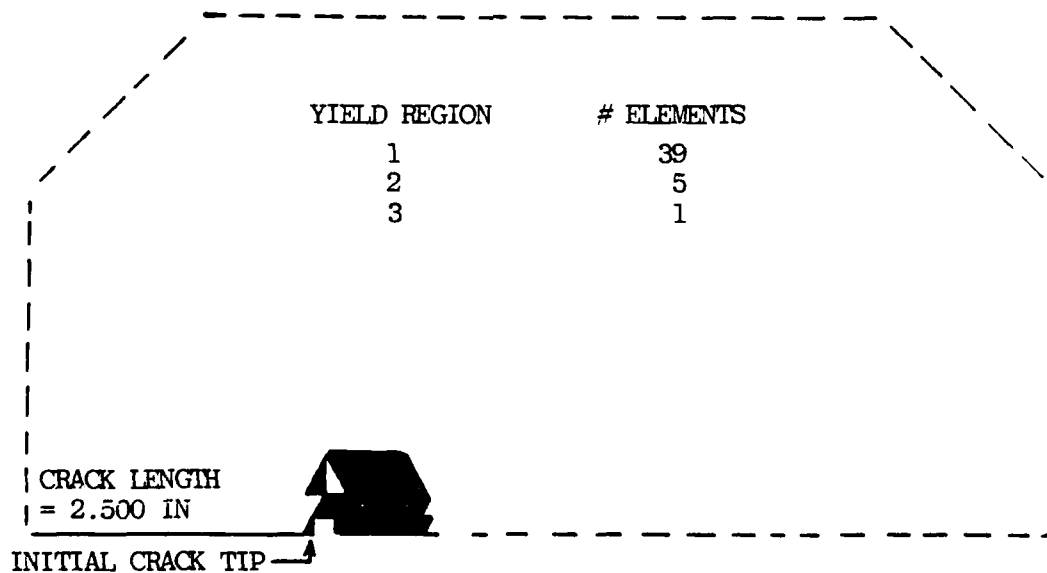


Figure 4.6b. Plastic Regions - Load = 20,000 LB.

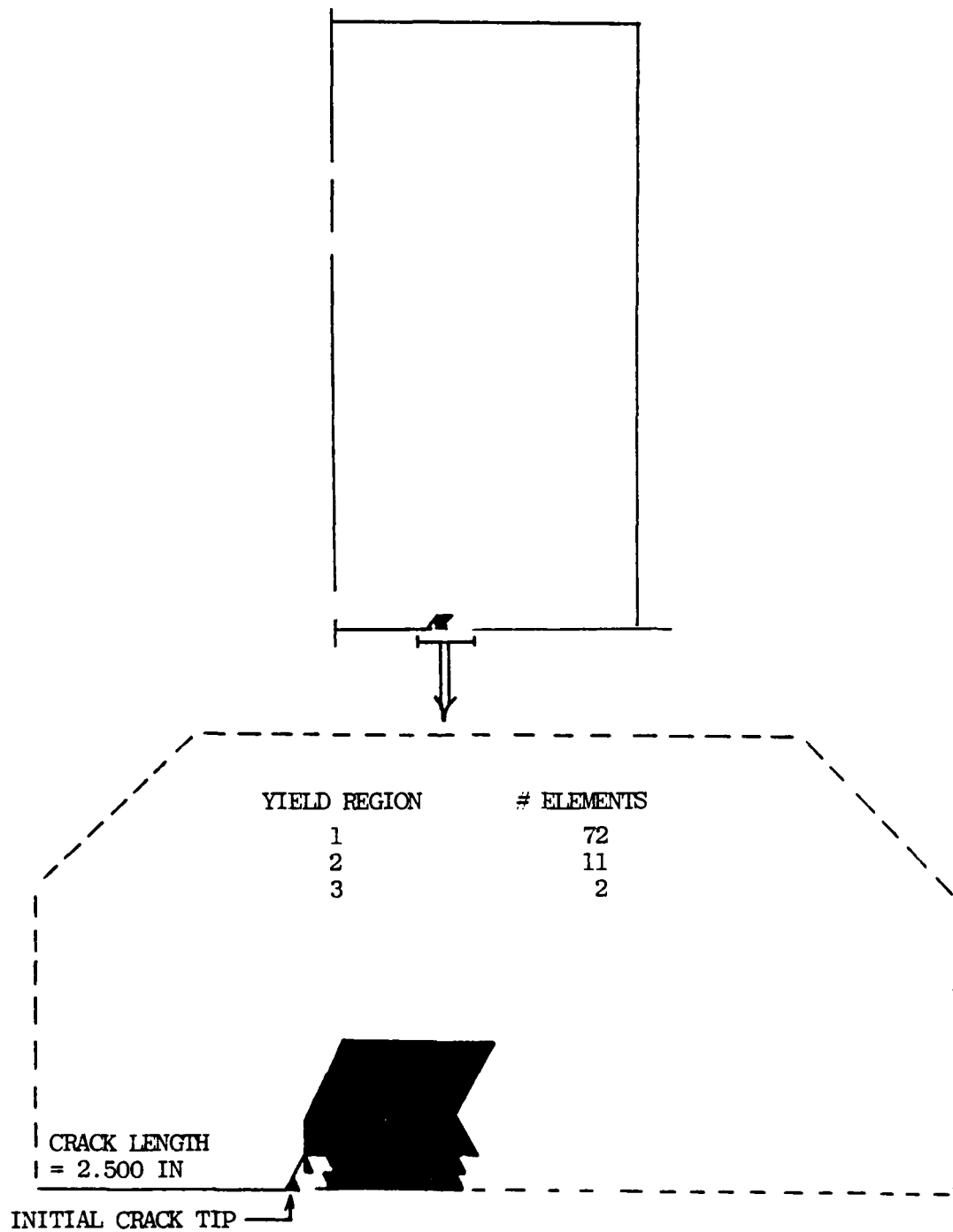


Figure 4.6c. Plastic Regions - Load = 25,000 LB.

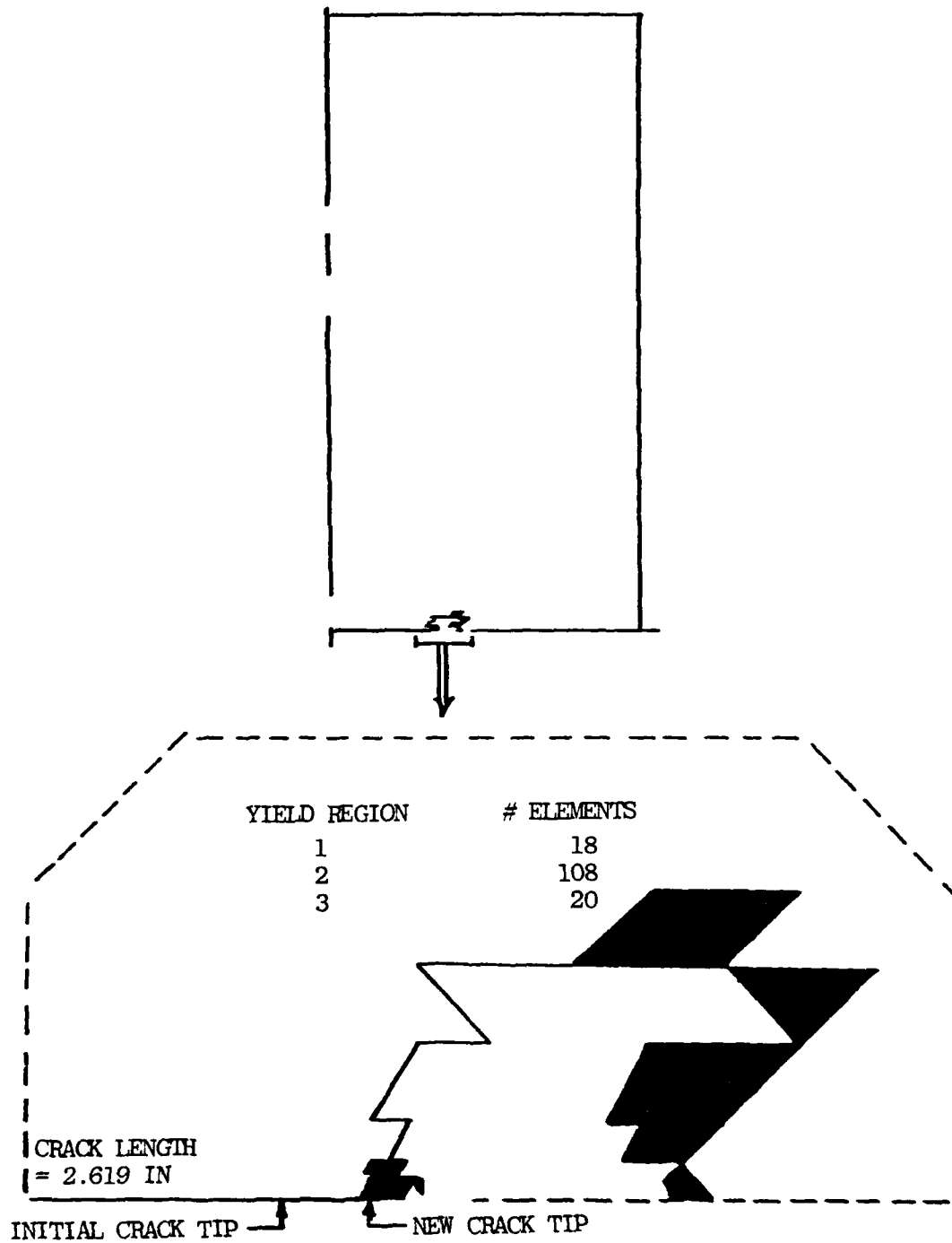


Figure 4.6d. Plastic Regions - Load = 30,000 LB.

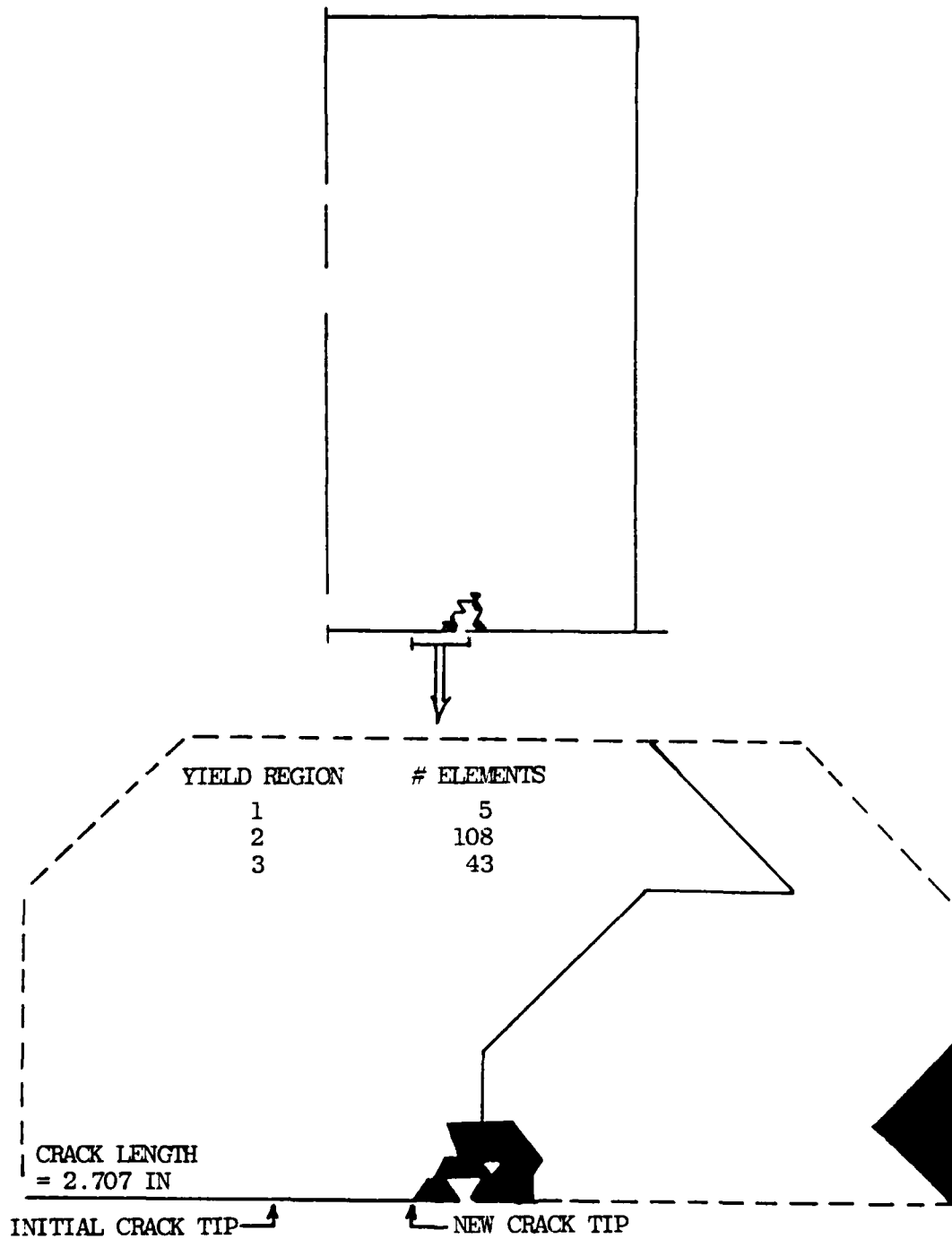


Figure 4.6e. Plastic Regions - Load = 34,000 LB

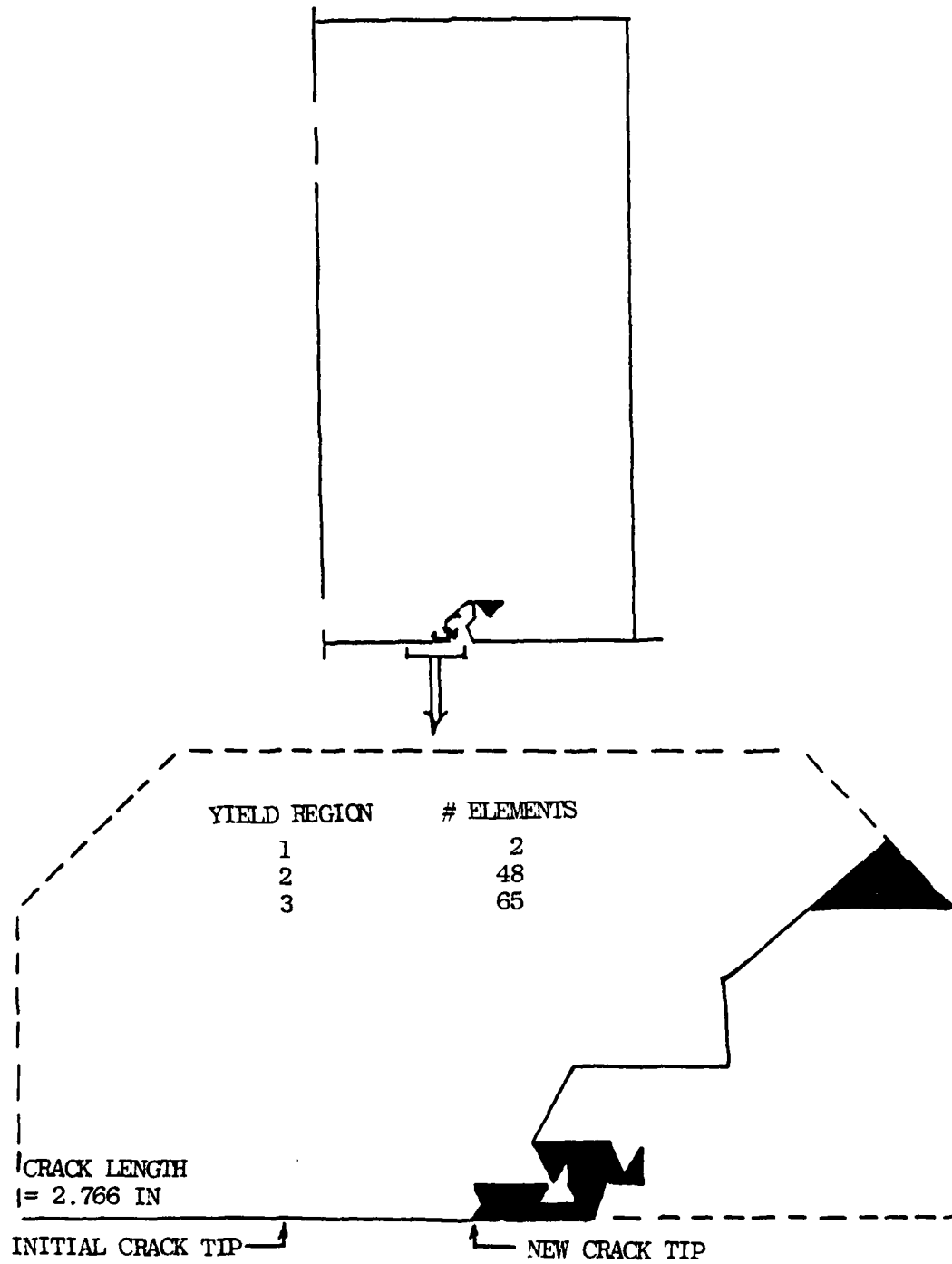


Figure 4.6f. Plastic Regions - Load = 36087 LB.

significant improvement was noted; therefore, only the engineering stress-strain programs, PANEL1 and FRACTURE, were used in the subsequent analyses.

IV.3 Cracked Panel Summary

The analysis of a centrally cracked panel under monotonically increasing load using the modified finite element program, PANEL, demonstrated that unstable fracture prediction using the FEM is highly dependent on the mesh size at the crack tip. Additionally, the prediction of stable fracture requires that a suitably refined mesh be extended along the entire length of the anticipated crack growth. For monotonically increasing load, accurate predictions can be made using the engineering stress-strain relation and initial specimen geometry.

CHAPTER V

TENSILE SPECIMEN ANALYSIS

V.1 Introduction

As mentioned in Chapter IV, the fracture prediction programs require stress-strain data all the way to ultimate load. This data is not generally published for the high strain range. Even if it were, the scatter in properties might introduce error into the analysis since published stress capabilities are normally statistical minimums. Therefore, the entire stress-strain curve was determined experimentally for the 2024-T3 sheet from which experimental specimens were fabricated. This data was converted to sectional modulus and Poisson's ratio which were then used in the program. Models of the tensile test specimens were also run in FRACTURE to evaluate the effectiveness of the program.

V.2 Experimental Study

The stress-strain relation for the 0.125 inch thick, 2024-T3 aluminum sheet used in the fractured specimen analysis (Chapter VI) was obtained from uniaxial tensile tests on specimens whose dimensions are shown in Figure 5.1. These specimens were loaded to fracture on a Riehle test machine which provides calibrated load data. Pin to pin deflections for the specimens were obtained from a spring loaded potentiometer attached to the pins. These deflections were recorded as a function of the applied load. The resultant load-deflection curves are plotted in Figure 5.2.

The loads (L) were converted to engineering stress (σ) by dividing by the original cross sectional area (A_0):

$$\sigma = L / A_0 \quad (5.1)$$

Only pin to pin deflection data was obtained to avoid damage to instrumentation when specimens were loaded to catastrophic failure. It was therefore necessary to adjust the pin to pin deflection (D_{pp}) to a gage deflection (D_g). This was accomplished by selecting a two inch gage length on the neck section and assuming that outside this region the material remained elastic. An elastic finite element program, based on published Young's modulus and Poisson's ratio,¹⁶ was then used to determine the relative elastic deflections between the pin and a point on the gage boundary

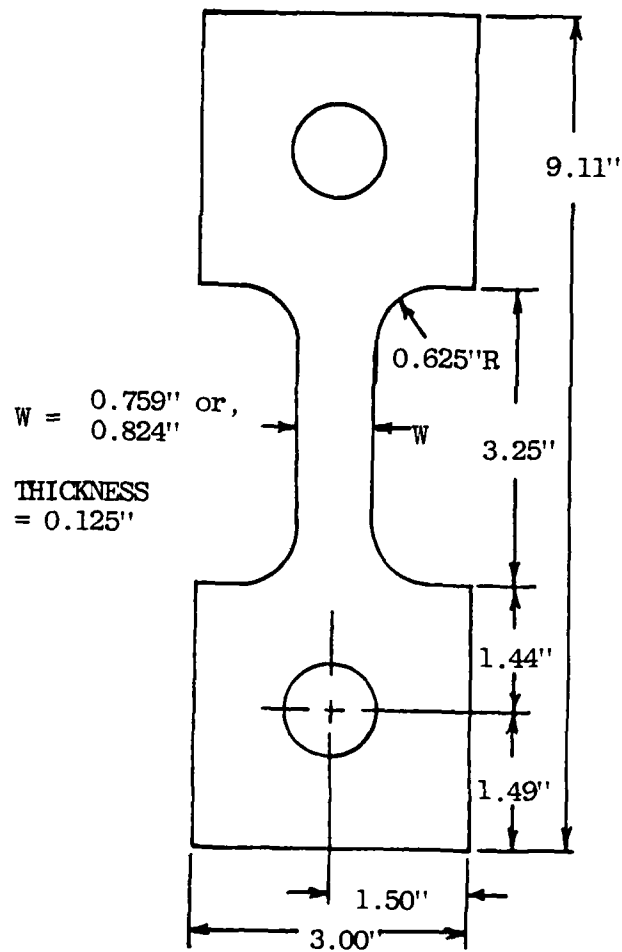


Figure 5.1. Tensile Test Specimen Dimensions.

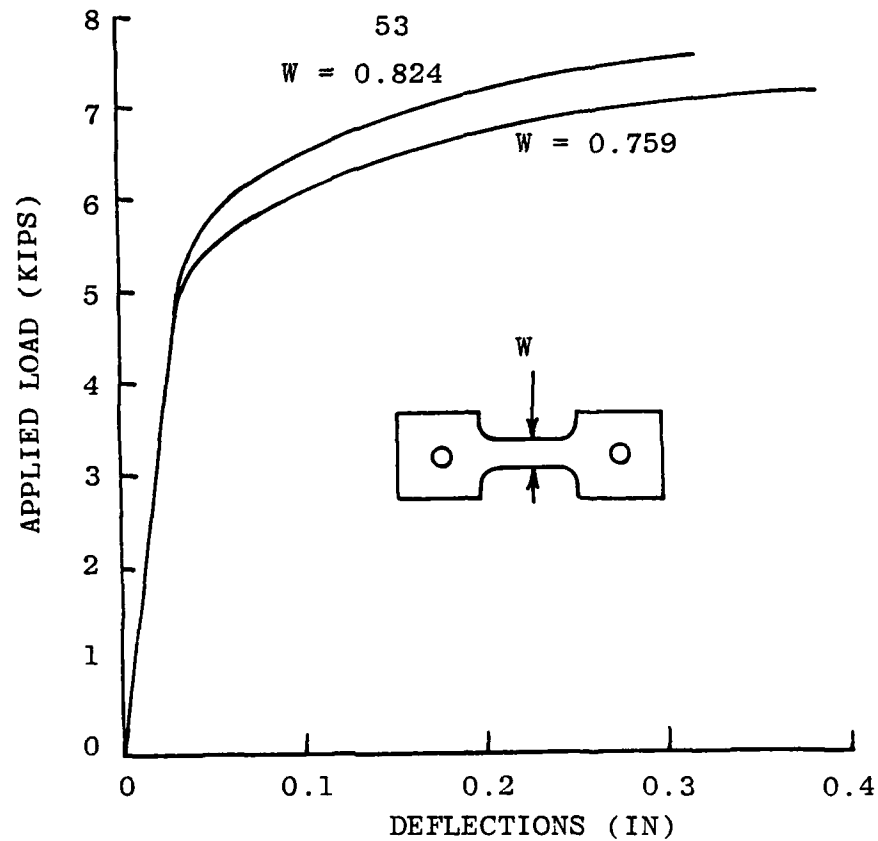


Figure 5.2. Tensile Test Load Deflection Curves.

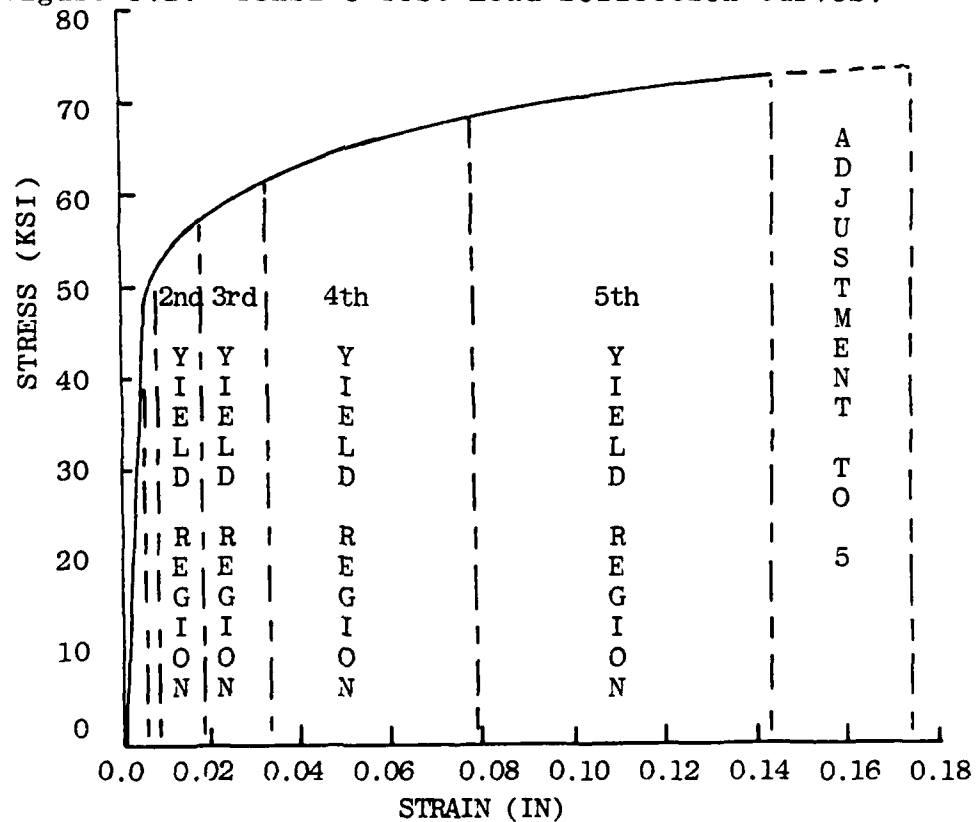


Figure 5.3. Linearized Stress-Strain Curve.

as a function of load. Calling this deflection D_r , the gage deflection is approximated by

$$D_g(L) \approx D_{pp}(L) - 2.0 D_r(L) L \quad (5.2)$$

The factor two in Eq. (5.2) results from there being two pin to gage boundary regions. While, as will be shown shortly, some plastic region exists outside of this gage region, the error is considered small. This results in a strain (ϵ) of the form

$$\epsilon = D_g/2.0 \quad (5.3)$$

or, in view of (5.2),

$$\epsilon = (D_{pp}/2.0) - D_r L \quad (5.4)$$

The resulting stress-strain curve is shown as the solid line in Figure 5.3. Note that the strain at fracture was initially determined from the 0.824 inch width specimen. The stress-strain curve was then approximated by the six linear sections as shown in Figure 5.3.

V.3 Finite Element Analysis

The finite element models from the mesh generator program were run in the FRACTURE program to test its ability to duplicate the load deflection curves which generated the stress-strain data used in the program. Figure 5.4a shows the original coarse mesh and Figure 5.4b shows a medium mesh. The medium mesh is refined in the area of the fillet and pin sections. The fine mesh is used at the midsection

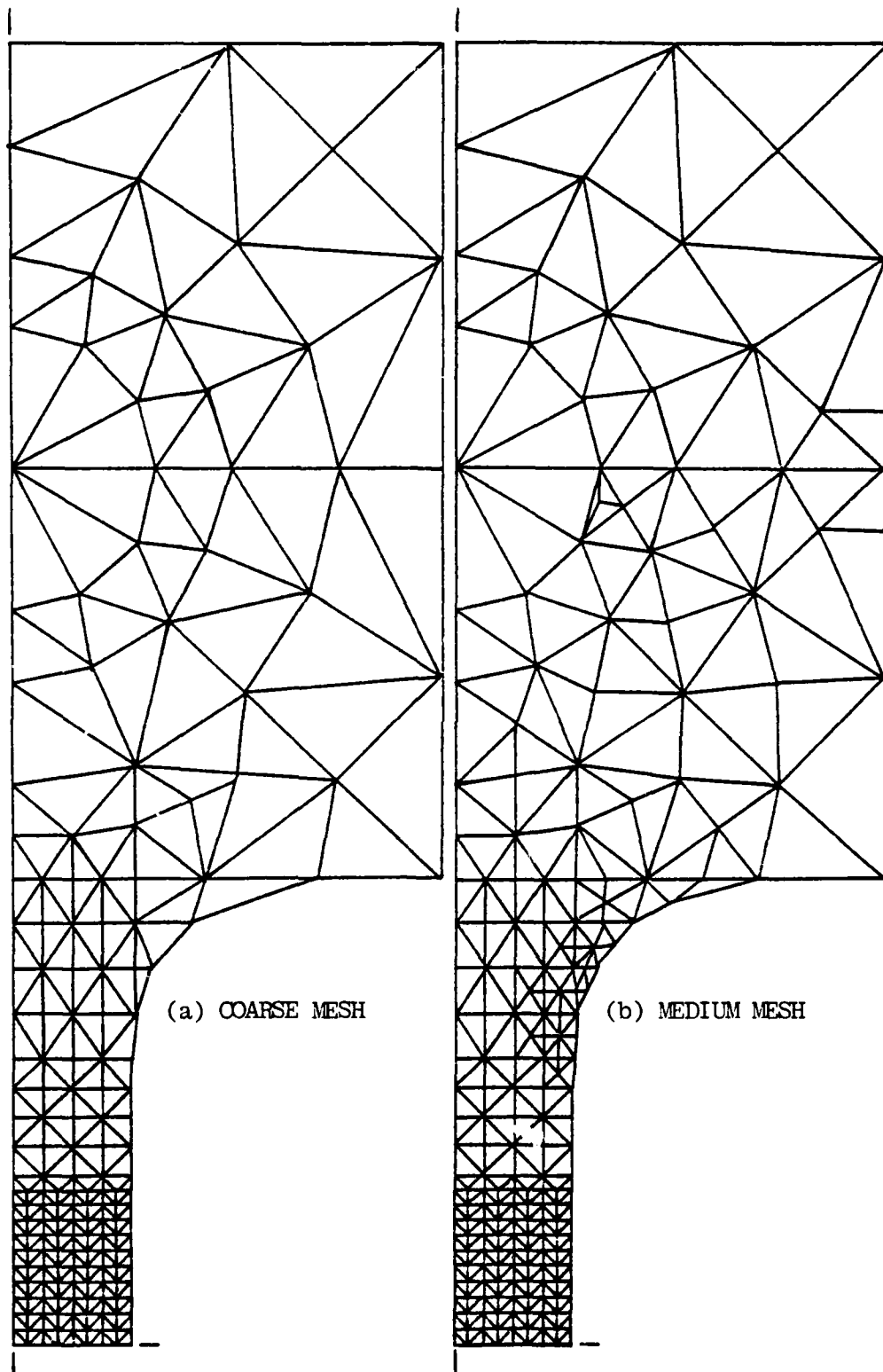


Figure 5.4. Tensile Test FEM Models.

in both models in anticipation of fracture in this area. Again, only one quadrant of the specimen was modeled due to symmetry.

Figure 5.5 shows a comparison of the results of the FEM analysis with the experimental loads and deflections. For the 0.824 inch wide specimen (used to obtain the stress-strain curve for the program), the results obtained from both meshes are very accurate; however, the medium mesh, with refinements in the pin and fillet areas, gives slightly more accurate results in the elastic and fracture regions. A further refinement of the mesh in the neck area was found to have negligible effect on the results. The results obtained for 0.759 inch wide coarse model shows good agreement with experimental results except at fracture, even though the material properties were obtained from the wider specimen. When a medium mesh (results not shown for clarity) was run for the 0.759" model, fracture occurred at approximately the same deflection as the 0.824" model, as opposed to the larger deflection of the test specimen. This suggests that, if the FEM analysis is assumed to be correct, the difference in deflections at fracture for the two experimental specimens is not accurate; indeed, the difference was traced to a slight anomaly in width of the 0.824" specimen. To compensate, the 0.824" load-deflection curve was extrapolated out to the 0.759" deflection at failure, and an adjustment, shown in Figure 5.3, was made to the program's

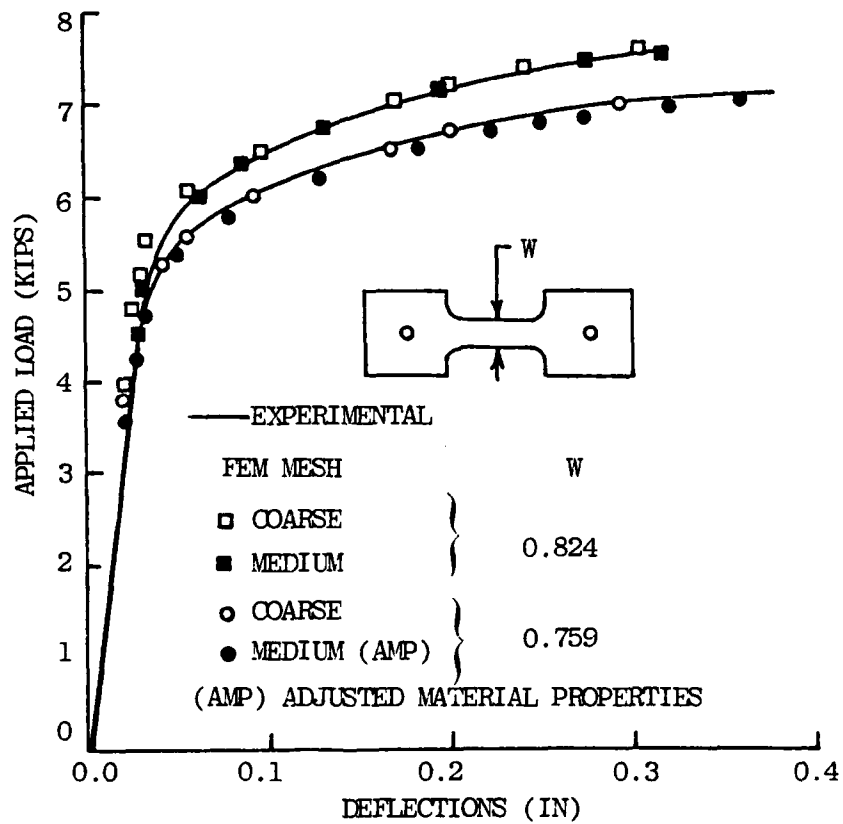


Figure 5.5. FEM Load Deflection Predictions for Tensile Test Specimens.

stress-strain data. The medium mesh was then used in the program with the new yield region 5 material properties. Correlation with the experimental results was much better. The remaining difference is most probably due to the fact that the deflection at fracture should be higher for the 0.824" specimen than for the 0.759" specimen since there is additional deflection in the elastic region for the 0.824" specimen due to its increased load carrying capability at fracture. The adjusted stress-strain curve was then used for the fracture studies of Chapter VI.

Not only did the program demonstrate the ability to accurately predict the load-deflection curves which generated its material properties, it also yielded the following important and useful data: First, note on Figure 5.5 that local yielding occurred well before yielding became apparent in the load deflection curve. Second, the program provided data on the progression of yield through the specimen. Figure 5.6 shows the smoothed yield response. Initial yielding occurs at the fillet as shown in Figure 5.6a. At a load of approximately 1000 pounds below the apparent yield, this region spreads through the fillet area and begins at the edge of the pin (while the yielding at the pin was confirmed by measuring the hole after fracture, the coarseness of the mesh in this region may not have given an accurate map of the yield zone). In Figure 5.6c, one element at the fillet has moved into the second yield region, the

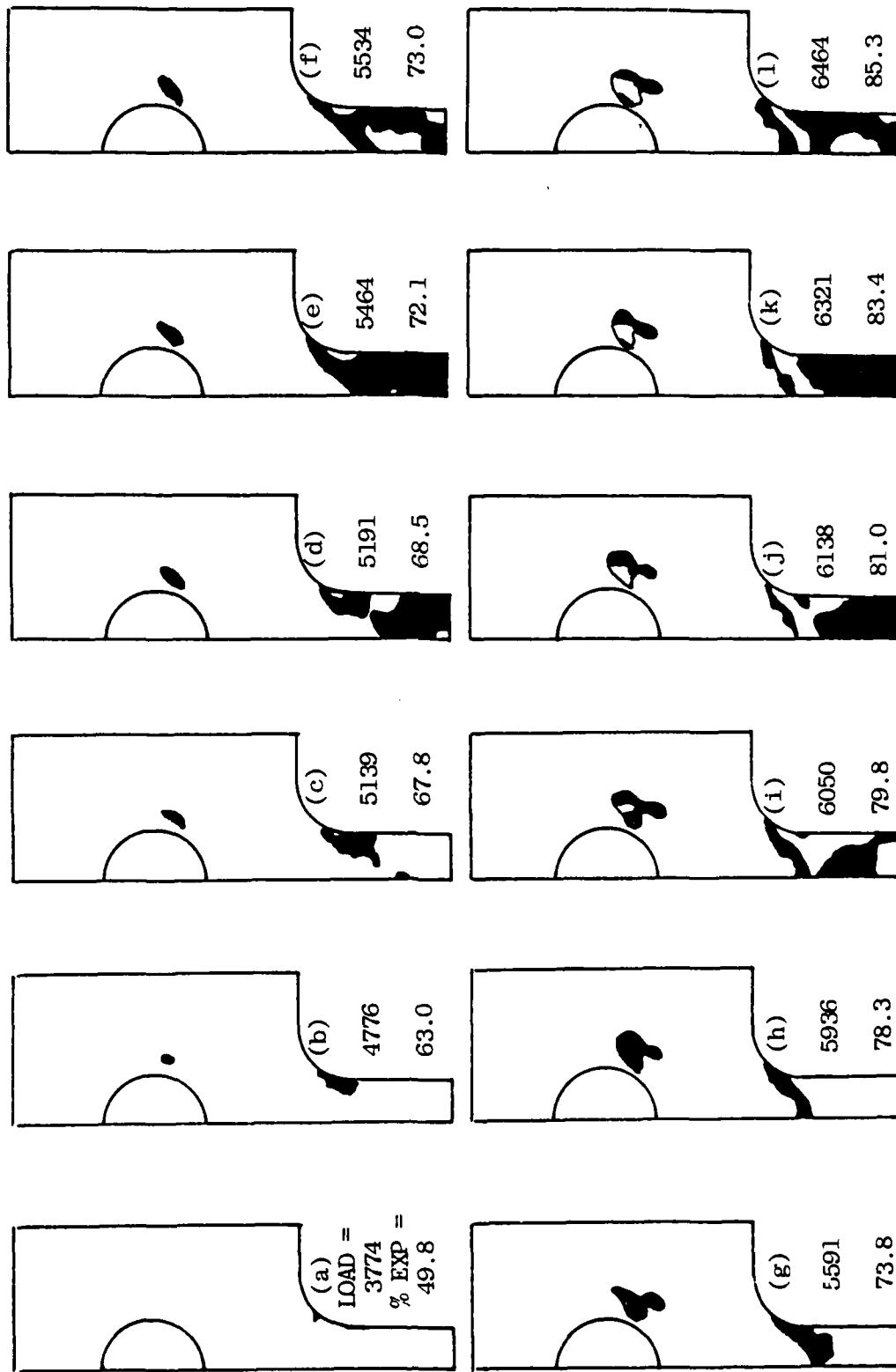
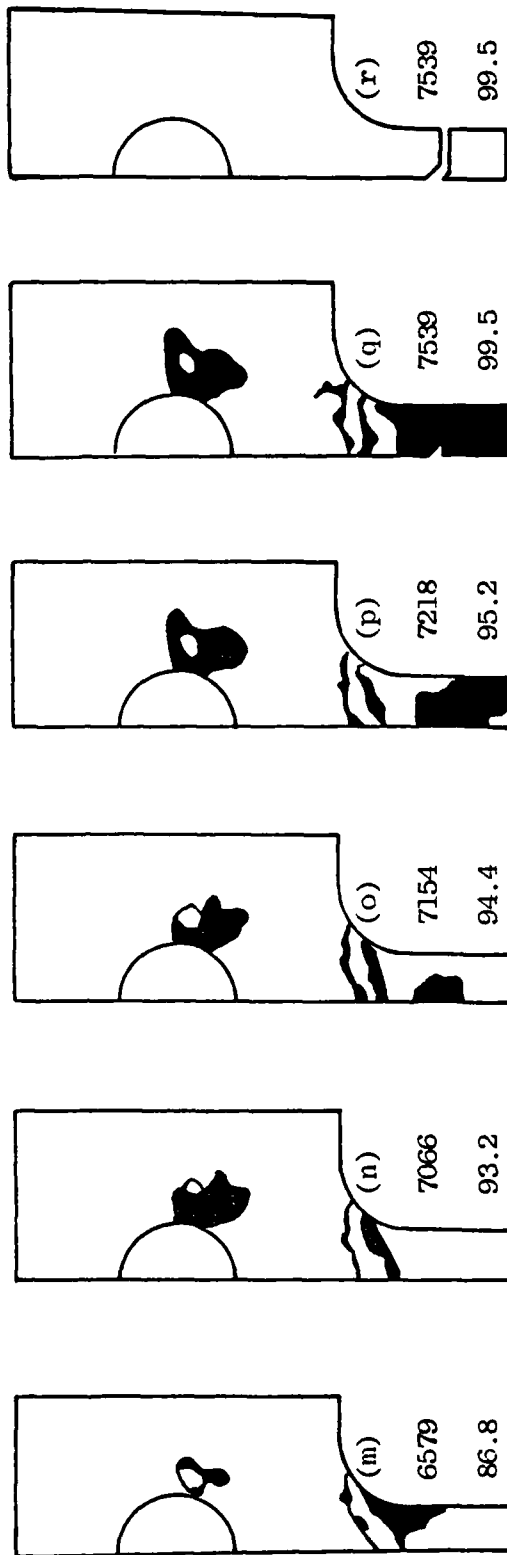


Figure 5.6. Yield Regions for Tensile Test Specimens.



EXPERIMENTAL LOAD (EXP) = 7580 LB

FIGURE FIRST ENTRY INTO

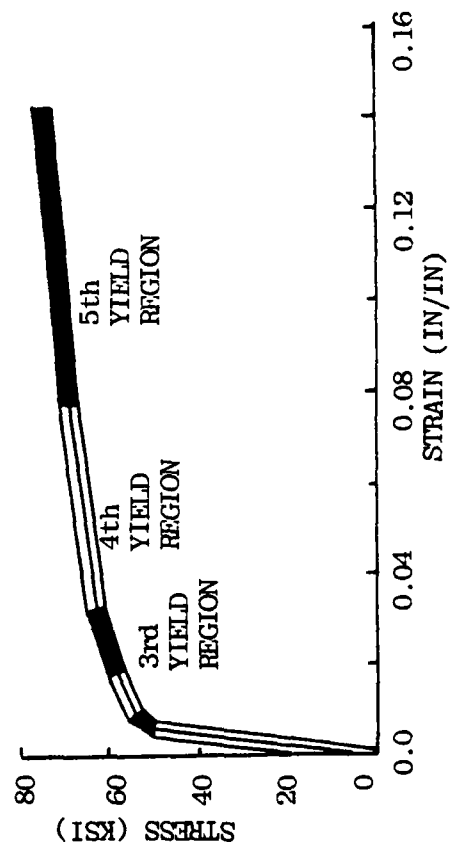


Figure 5.6 (cont). Yield Regions, Tensile Test Specimen.

fillet yield region has expanded, and yielding has begun on the center axis. In Figure 5.6d, the neck area is almost entirely involved in the first yield region. The two large white areas in the neck are still elastic. In Figure 5.6e, the entire neck is involved in the first yield region, the second yield region at the fillet is expanding, and second yield has occurred at the center axis. The second region at the fillet is expanding in Fig. 5.6f, g and h with the first yield region moving up to the base of the neck while the first yield zone spreads at the pin. In Figure 5.6i, third yield (dark area) is progressing in much the same way as the second did in Figure 5.6f. Also in Figure 5.6i, the second yield region is entered at the pin. Figure 5.6j and k show the further expansion of the third yield zone with Figure 5.6(l) showing the beginning of the fourth yield region. The first, second, and third yield zones are compressed toward the base of the neck as zone four expands in Figure 5.6m and n, with the pin zone continuing to expand. Fifth yield initiates from the center axis as shown in Figure 5.6(o). In Figure 5.6p the pin zone increases further along with the fifth yield region while zones one, two, three and four are pushed further toward the base of the neck. Initial fracture occurs in Figure 5.6q initiating from the center axis and propagating unstably to the edge as shown in Figure 5.6r. Note that the FEM prediction for fracture load is 99.5% of the experimentally obtained load.

Third, as mentioned above, the FEM analysis predicted an initiation and unstable propagation of the crack from a point on the longitudinal centerline of the specimen. This phenomenon was confirmed on the test specimens by placing the fractured surfaces together and observing that the end sections fit together while the center sections did not. This is due to the increased plastic strain on the outer sections after the center section failed and unloaded. Failure of mildly notched tensile specimens from the center axis has also been reported by Drucker.¹⁷ Since initial yield occurred at the fillet, and fracture initiated on the center axis, it can readily be seen that fracture initiation location can not be predicted by using the maximum elastic stress location. Fourth, while the mesh was refined on the mid-section in anticipation of failure along the centerline, the FEM prediction showed that fracture occurred off the mid-section centerline as shown in Figure 5.6r. Each of the tensile test specimens also broke along a line off the centerline. Figure 5.7 shows the location of fracture predicted by the FEM analysis and as occurred in the tensile tests. The test specimens failed on a 45° line through the thickness. This is the scatter band shown in the figure with the experimental location shown in both the deflected and undeflected geometries. Note that the FEM prediction indicates that a perfect specimen would break into three pieces. As can be seen, the FEM accurately predicts the failure location.

Finally, the load and deflection at fracture for both the experimental test and the FEM analysis are shown in Table 5.1. The load predictions for the medium mesh models are extremely accurate (less than three percent for the 0.759" specimen and less than one percent for the 0.824" specimen), and deflections are also a good approximation of measured values (about four percent and one percent for the two respective specimens). As previously discussed, accurate prediction of fracture deflection is highly dependent on accurate material maximum strain data.

V.4 Tensile Test Analysis Summary

The finite element program, FRACTURE, demonstrated the following capabilities for the analysis of two tensile test specimens:

1. Ability to predict load-deflection curves,
2. Ability to demonstrate the importance of local material properties,
3. Ability to provide data on the complete field response for the specimen, thus a better understanding of the failure process,
4. Ability to predict fracture initiation location, both with respect to the midsection and longitudinal axis, and
5. Ability to predict load and deflection at fracture.

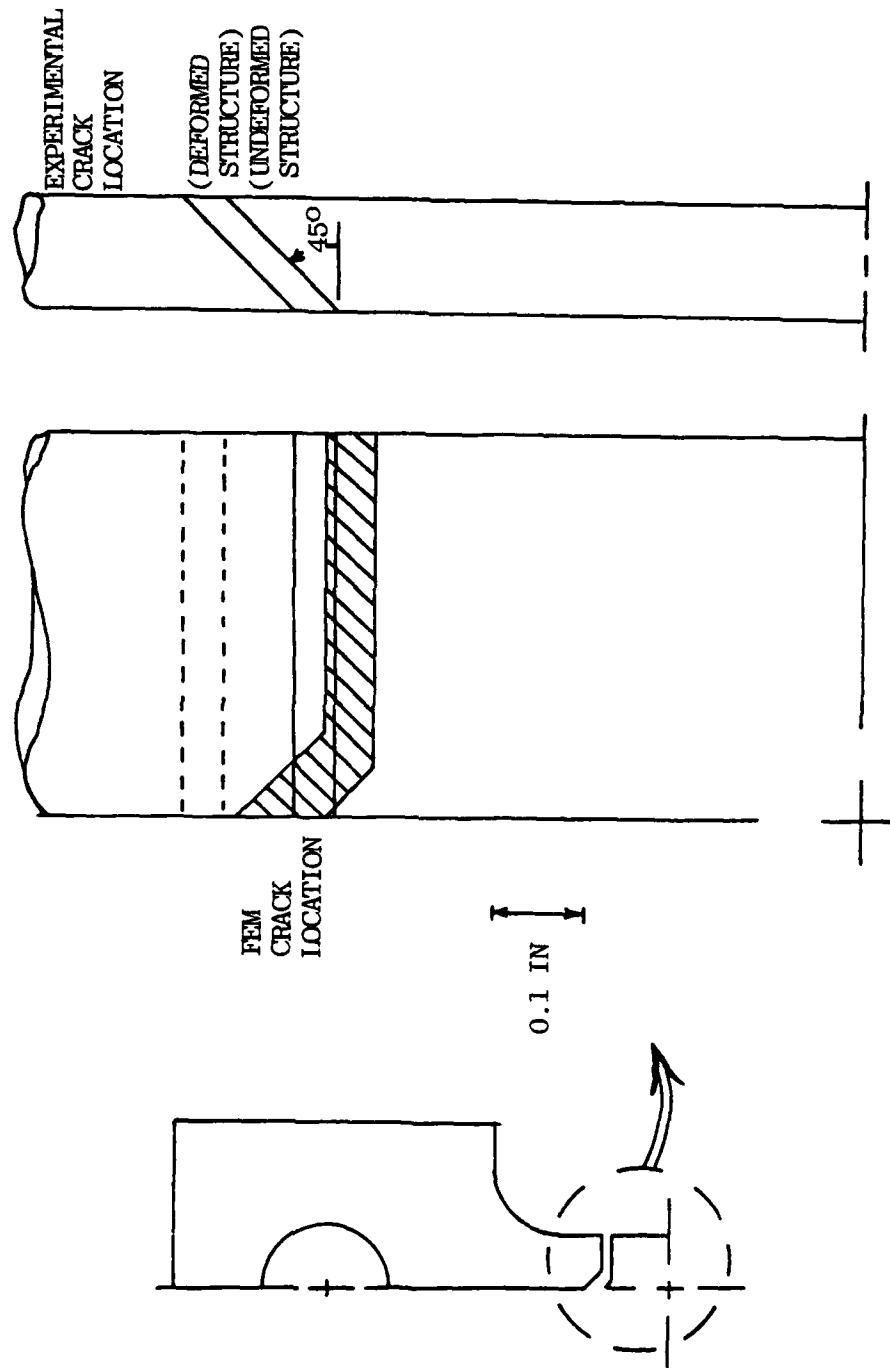


Figure 5.7. Crack Locations, FEM Predictions and Experimental Results for Tensile Test Specimen.

TABLE 5.1
COMPARISON OF EXPERIMENTAL AND FEM LOADS
AND DEFLECTION AT FRACTURE

| SPECIMEN | 0.759" | | 0.824" | |
|------------------|--------------|---------------|--------------|---------------|
| | LOAD (lb) | DEFL. (in) | LOAD (lb) | DEFL. (in) |
| EXPERIMENTAL | 7180 | 0.3750 | 7580 | 0.3125 |
| COARSE MESH | 6953 | 0.2928 | 7532 | 0.3035 |
| PERCENT ERROR | 3.16 | 21.92* | 0.63 | 2.88 |
| MEDIUM MESH | 7015 | 0.3588 | 7539 | 0.3158 |
| PERCENT ERROR | 2.30 | 4.32 | 0.54 | 1.06 |

*Based on uncorrected stress-strain data.

CHAPTER VI

CRACKED SPECIMEN ANALYSIS

VI.1 Introduction

The tensile test specimen analysis demonstrated the effectiveness of the current method in predicting experimental behavior for mild stress concentrations and the panel study showed that for sufficiently fine meshes, this method can also predict load at fracture in specimens with severe stress concentrations (cracks). Unfortunately, no experimental deflection data was presented for the panel study; therefore, the ability of the program to predict load deflection curves for severely notched specimens could not be addressed without further testing. To obtain the needed data, three tensile test specimens were notched and loaded to fracture. Comparisons of this experimental data and the finite element predictions were made and are presented in this chapter.

VI.2 Experimental Tests

The testing procedure for notched specimens was the same as that presented in Chapter V, and the three specimens tested were made from blanks of the same dimensions as the 0.824" wide specimen of Chapter V. Sharp notches of lengths 0.008", 0.023", and 0.129" were then introduced in the blanks on one edge of the neck at the centerline. The 0.003" and 0.023" cracks were obtained using an X-Acto knife blade, and the 0.129" crack was machined on a band saw with the final tip also being formed by an X-Acto knife.

VI.3 Finite Element Analysis

Introduction of the single edge notch (SEN) in the specimen removed one plane of symmetry necessitating the use of a two quadrant finite element model. The overall mesh is shown in Figure 6.1a with details for the different crack lengths shown in Figure 6.1b, c, and d.

Figure 6.2 shows the same type of result that was demonstrated in Chapter IV, Figure 4.2; that is, the accuracy of the FEM predictions of fracture load is highly dependent on the element size at the tip of the crack.

The load deflection curves for two different size elements are shown in Figure 6.3. Note that the shape of the predicted curves are essentially the same. With large elements at the tip, the CST elements can not model the large

gradients at the tip, and therefore, the load and deflection exceed the experimental values. The slight upward trend in the load for the finer mesh is due to the size of the minimum load increments used to reduce the computational time. As the mesh is refined, the computational time increases due to increased band width of the stiffness matrix and the increased number of nodes and elements. The computational time can be reduced by increasing the minimum load increment; however, the predicted load and deflection at fracture are affected since elements tend to remain stiffer during the loading process.

The load deflection curves for the three different size notches are shown in Figure 6.4. The results improve as the crack size increases. This can be attributed to increasing the minimum load increment to allow enough time to advance the crack along the additional specimen width for smaller cracks. Also the deflections are slightly low for each given load. This same effect can be observed in Figure 5.5 for the tensile specimen coarse mesh. As discussed in Chapter V, the tensile predictions were improved by refining the mesh in the area of the fillet and pin.

Finally, the yield regions for a 0.023" initial crack size are plotted for selected loads in Figure 6.5. The initial yield zone formation is shown in Figure 6.5a and b. Figure 6.5c and d show the first, second, third and fourth yield regions expanding outward from the crack tip. At the

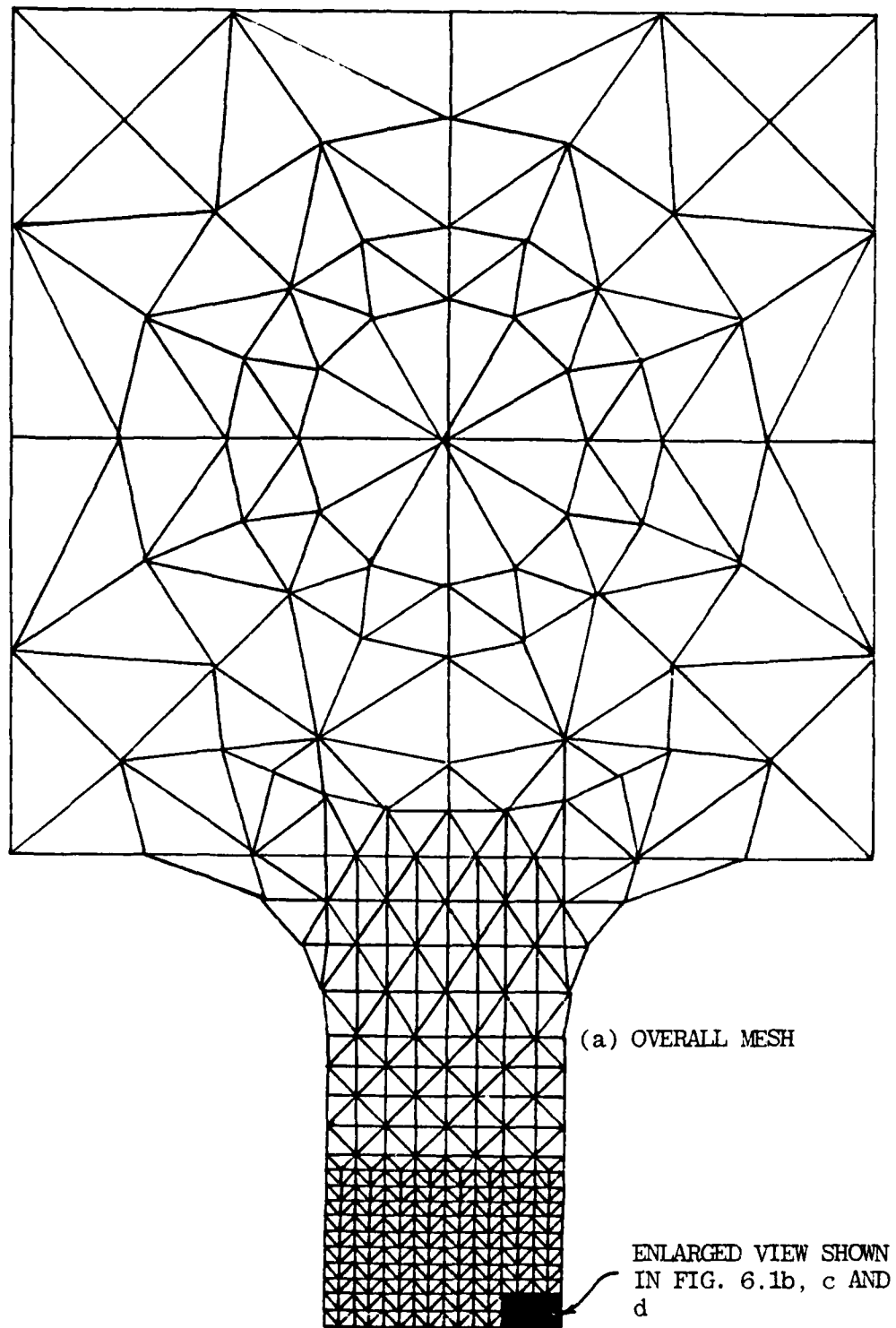
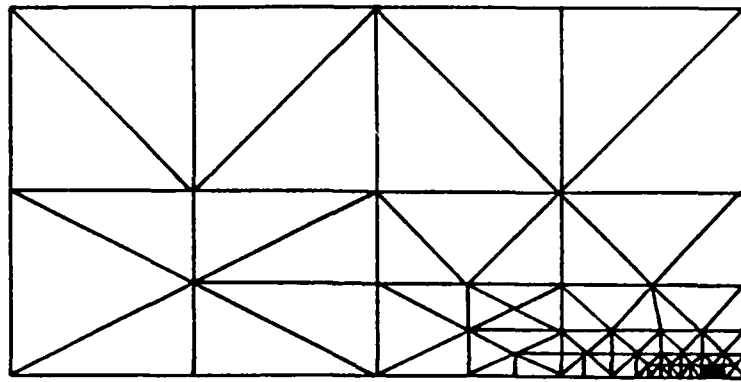
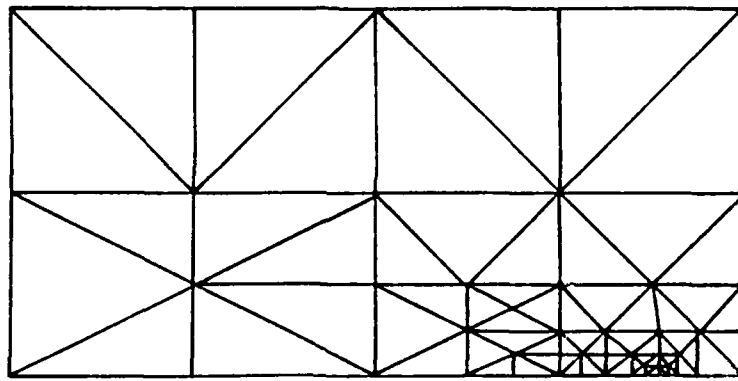


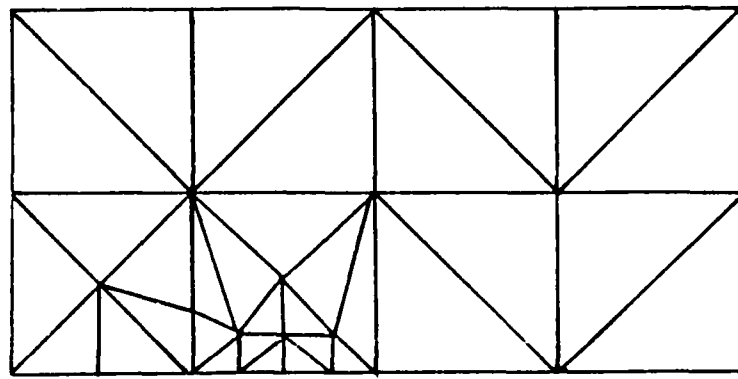
Figure 6.1. FEM Models of Cracked Specimens.



(b) Detail of Mesh for 0.008 In. Crack



(c) Detail of Mesh for 0.023 In. Crack



(d) Detail of Mesh for 0.129 In. Crack

Figure 6.1 (cont). FEM Models of Cracked Specimens.

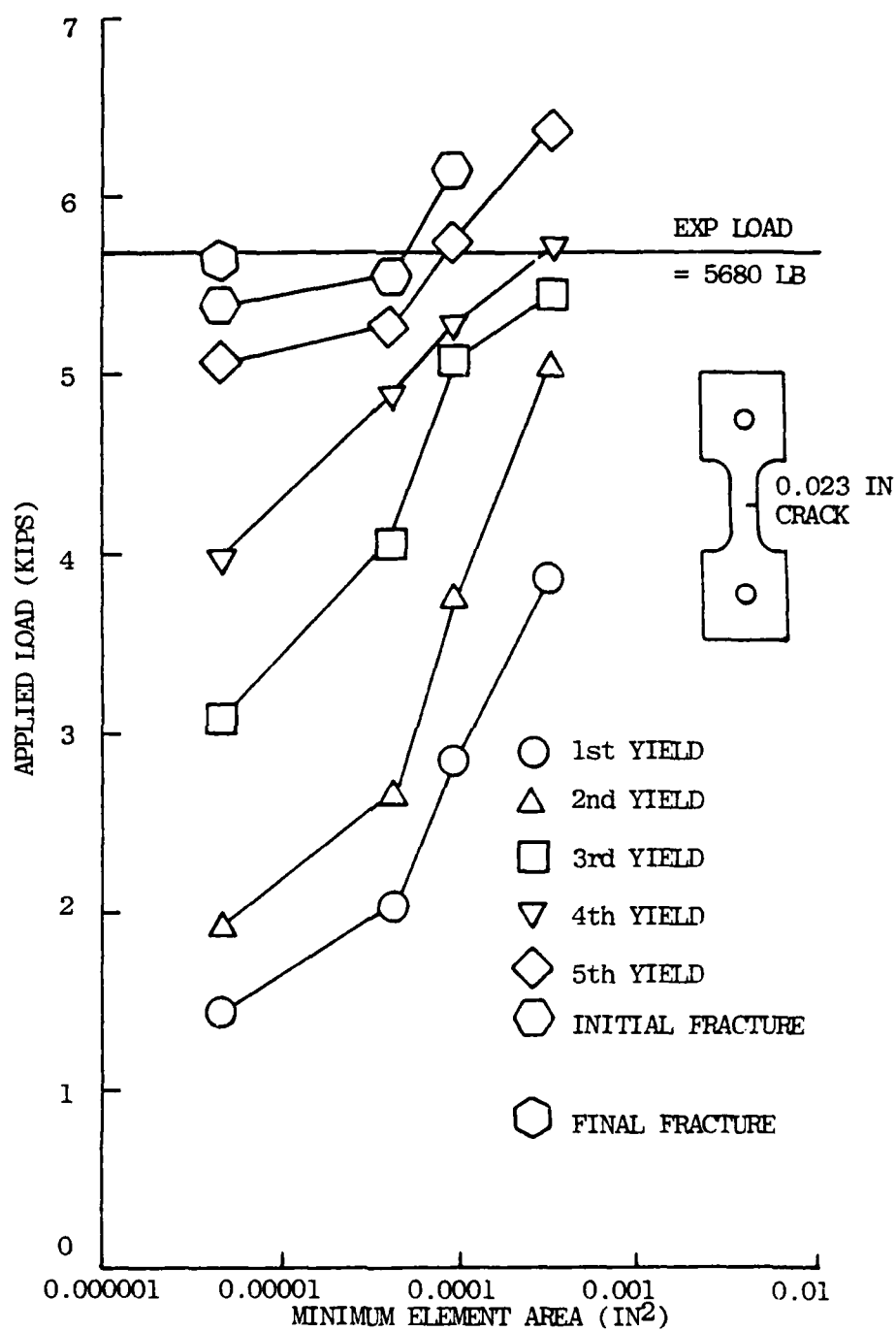


Figure 6.2. Numerical Convergence, Cracked Specimen Analysis.

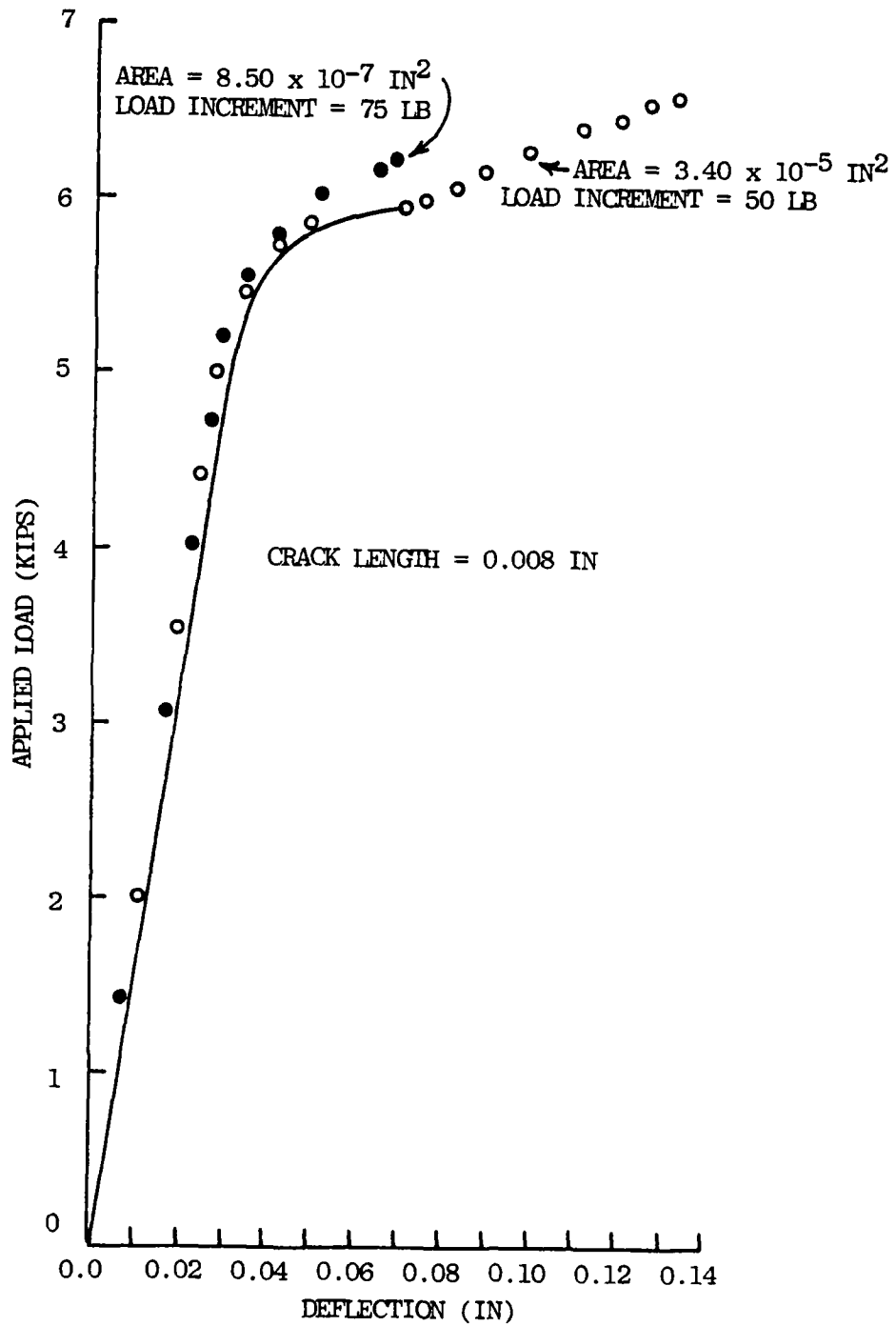


Figure 6.3. Effects of Load Increment and Element Size for the Cracked Specimen Analysis.

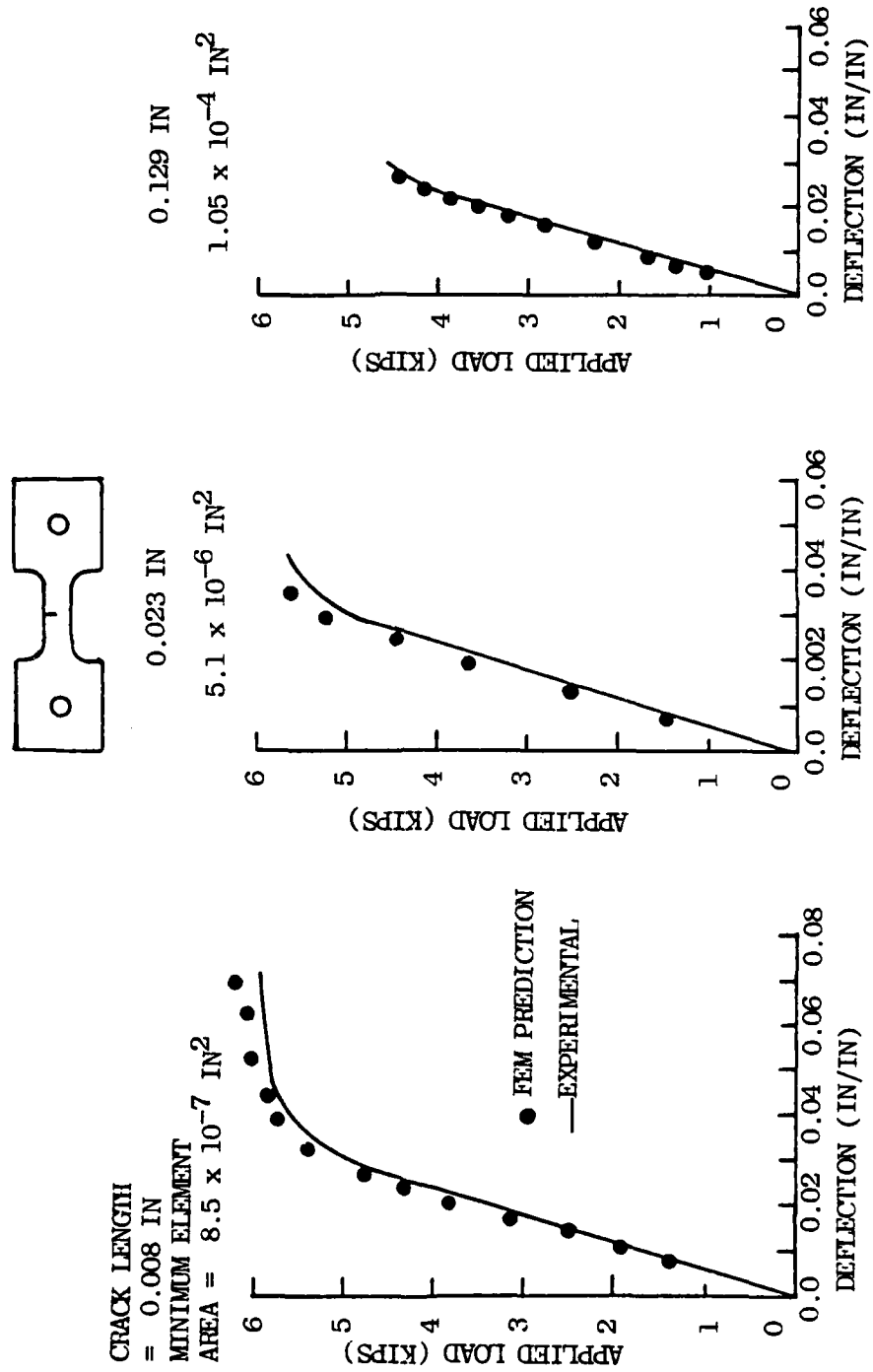
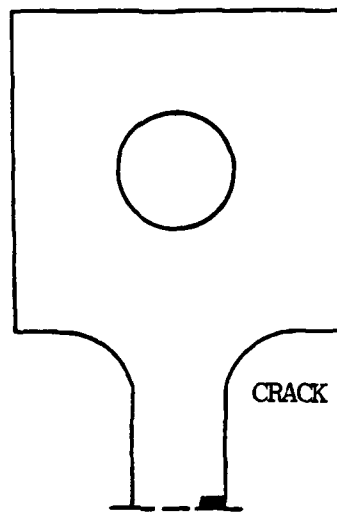


Figure 6.4. Load Deflection Curves for Cracked Specimen Analysis.



CRACK = 0.023 IN.



Figure 6.5a. Yield Regions, Load = 1806 LB.



Figure 6.5b. Yield Regions, Load = 3020 LB.



Figure 6.5c. Yield Regions, Load = 4000 LB.

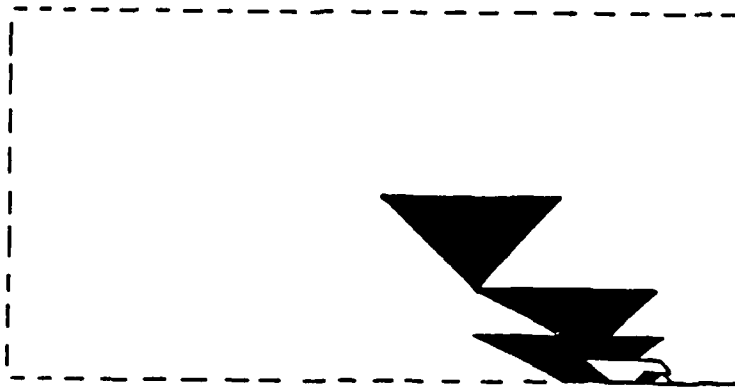


Figure 6.5d. Yield Regions, Load = 4500 LB.

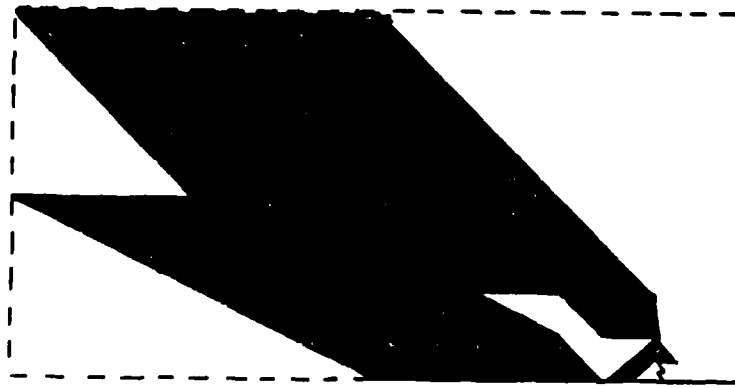


Figure 6.5e. Yield Regions, Load = 5000 LB.

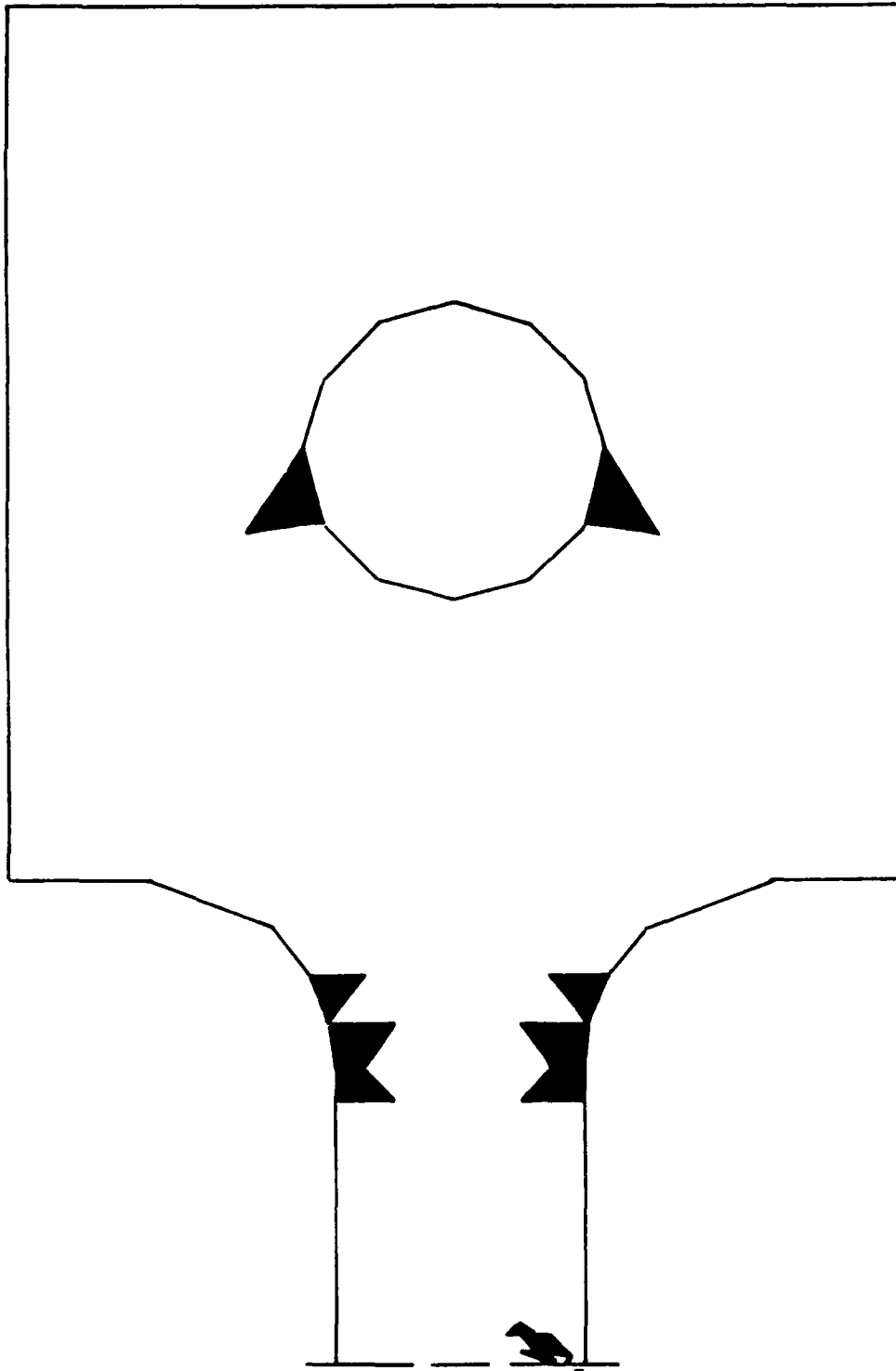


Figure 6.5f. Yield Regions, Load = 5000 LB, Overall Results.



Figure 6.5g. Yield Regions, Load = 5200 LB.

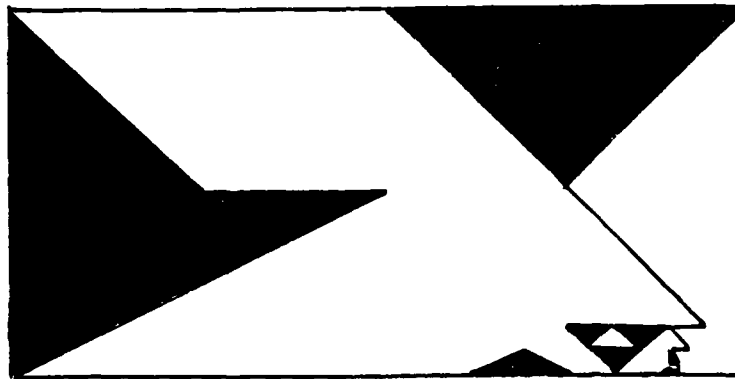


Figure 6.5h. Yield Regions, Load = 5325 LB.

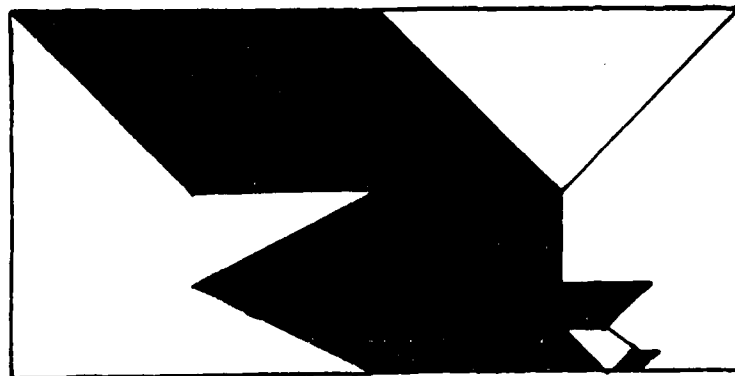


Figure 6.5i. Yield Regions, Load = 5433 LB.

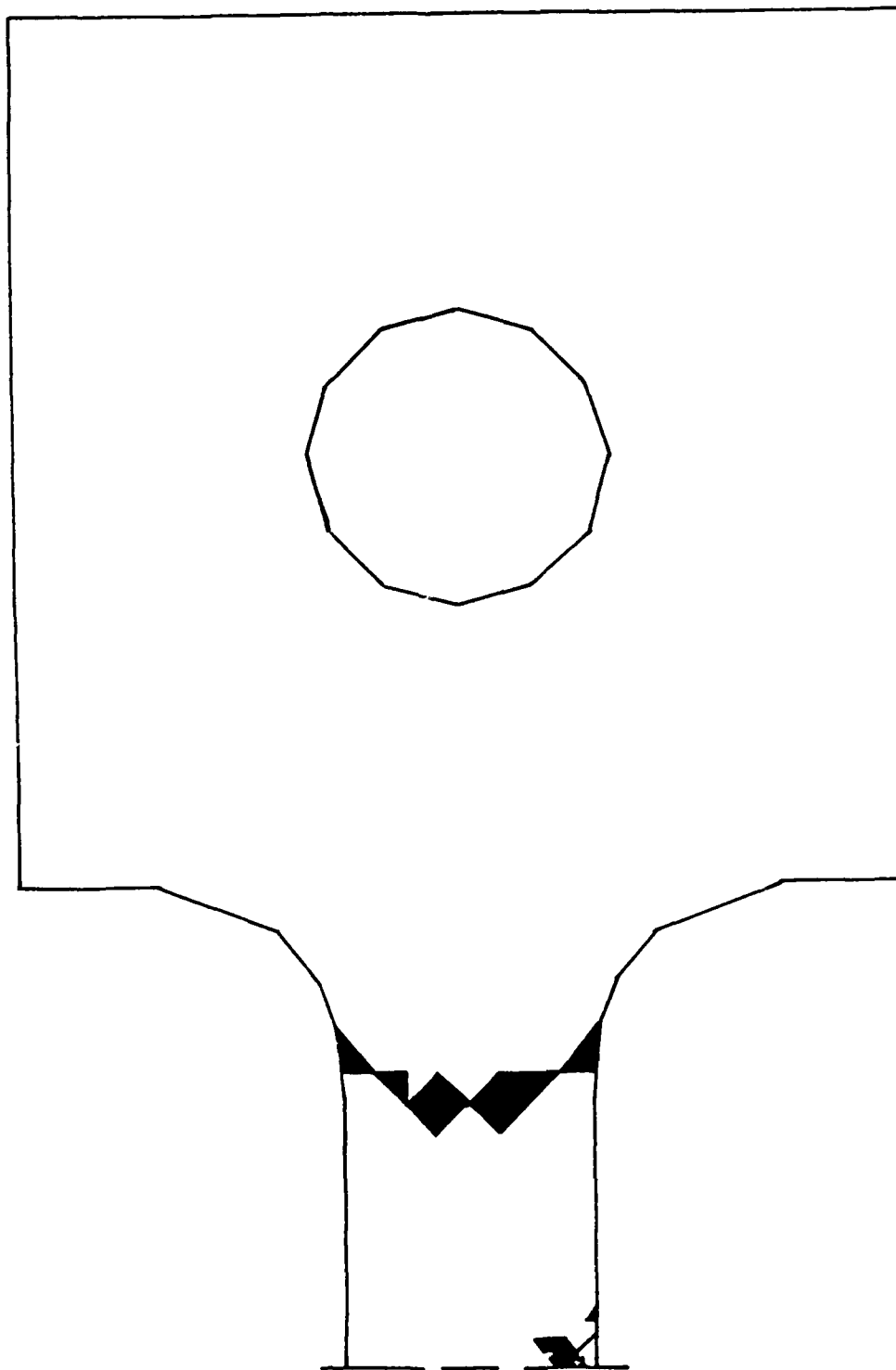


Figure 6.5j. Yield Regions, Load = 5433 LB, Overall Results.

load that corresponds to Fig. 6.5c, yielding also begins at the hole. The first yield zone extends past the enlarged area of the figure (as shown in Figure 6.5e) with the entire specimen shown in Figure 6.5f for the same load. Figures 6.5g, h and i show the further advance of the yield zones as load increases. At load level corresponding to Figure 6.5g, all five zones are present. In Figure 6.5h, the specimen has reached the load at which initial fracture occurs and Figure 6.5i shows the zones just prior to unstable fracture. Notice that the entire neck, except at the tip, is in the second yield region.

VI.4 Cracked Specimen Analysis Summary

The FEM analysis of the sharply notched specimens described in this chapter further verifies the abilities demonstrated in the previous two chapters, and confirms the ability to predict specimen deflections for sharply notched specimens.

CHAPTER VII

CONCLUSIONS AND RECOMMENDATIONS

The finite element program developed during this study has been shown to predict load deflection curves, load and deflection at fracture, fracture paths, initiation sites, crack growth, and stable or unstable crack propagation. The accuracy of the method is highly dependent on the element size along the crack path. The use of properly refined meshes yields accurate results.

The method is completely general in that it can analyze any two-dimensional isotropic structure subjected to plane stress and uniaxial loading. The loading restriction can be removed by substituting a failure criterion which is more suitable than the maximum strain criterion. While this method represents a valuable design tool for a limited class of problems, it more importantly demonstrates the potential of the finite element method for the direct prediction of fracture. The current program required only minor alterations to a standard plane stress finite element program to

give accurate analysis of elasto-plastic fracture problems. Since finite element programs have already been written to analyze plane strain, three dimensional and thermal loading problems, if similar modifications could be made to these programs, then it would be possible to directly predict fracture for these cases under monotonically increasing load. The only restriction on this approach appears to be the computer storage and computational time. These become less significant as the program effectiveness improves, refinements such as substructuring are incorporated, better solution techniques are found, and as computer capabilities continue to expand.

The direct prediction of cyclic fracture would be an even more valuable application of the approach contained in this work. Again the basic procedures developed in this study should apply with appropriate modifications.

Each of these capabilities needs to be verified, but the excellent results obtained in the present study suggest that the concept is valid and worthy of further development. The rewards for such a work could be enormous.

BIBLIOGRAPHY

1. Wood, H. A., and Trapp, W. J. "Research and Application Problems in Fracture of Materials and Structures in the United States Air Force." Engineering Fracture Mechanics, Vol. 5, 1973, pp. 119-145.
2. Hoepfner, D. W., and Krupp, W. E. "Prediction of Component Life by Application of Fatigue Crack Growth Knowledge." Engineering Fracture Mechanics, Vol. 6, 1974, pp. 47-70.
3. Boyd, G. M. "From Griffith to COD and Beyond." Engineering Fracture Mechanics, Vol. 4, 1972, pp. 459-482.
4. Anderson, H. "A Finite-Element Representation of Stable Crack Growth." J. Mech. Phys. Solids, Vol. 21, 1973, pp. 337-356.
5. Light, M. F., Luxmore, A., and Evans, W. T. "Prediction of Slow Crack Growth by a Finite Element Method." International Journal of Fracture, Vol. 11, 1975, p. 1045.
6. Newman, J. C. Jr., and Arman, H. Jr. "Elastic-Plastic Analysis of Propagating Crack under Cyclic Loading." AIAA Journal, Vol. 13, No. 8, 1975, pp. 1017-1023.
7. Ogura, K., and Ohji, K. "FEM Analysis of Crack Closure and Delay Effect in Fatigue Crack Growth under Variable Amplitude Loading." Engineering Fracture Mechanics, Vol. 9, 1977, pp. 471-480.
8. Ohji, K., Ogura, K., and Ohkubo, Y. "Cyclic Analysis of a Propagating Crack and its Correlation with Fatigue Crack Growth." Engineering Fracture Mechanics, Vol. 7, 1975, pp. 457-464.

9. Socie, D. F. "Prediction of Fatigue Crack Growth in Notched Members under Variable Amplitude Loading Histories." Engineering Fracture Mechanics, Vol. 9, 1977, pp. 849-865.
10. Newman, J. C. Jr. "Finite-Element Analysis of Crack Growth under Monotonic and Cyclic Loading." ASTM STP 637, American Society for Testing and Materials, 1977, pp. 56-80.
11. Miller, R. E. Jr., Backman, B. F., Hansteen, H. B., Lewis, C. M., Samuel, R. A., and Varanasi, S. R. "Recent Advances in Computerized Aerospace Structural Analysis and Design." Computers and Structures, Vol. 7, 1977, pp. 315-326.
12. Zienkiewicz, O. C. The Finite Element Method in Engineering Science. London: McGraw-Hill, 1971.
13. Bert, C. W., Mills, E. J., and Hyler, W. S. "Effect of Variation in Poisson's Ratio on Plastic Tensile Instability." Journal of Basic Engineering, Trans. ASME, Vol. 89D, 1967, pp. 35-39.
14. Nadai, A. Theory of Flow and Fracture of Solids. Vol. 1, 2nd ed. New York: McGraw-Hill, 1950, pp. 379-387.
15. Aerospace Structural Metals Handbook, Vol. II. Syracuse: Syracuse University Press, 1963.
16. MIL-HDBK-5. Department of Defense, 1962.
17. Drucker, D. C. "A Continuum Approach to the Fracture of Metals." Fracture of Solids, Proceedings, Institute of Metals Division, American Institute of Mining, Metallurgical, and Petroleum Engineers, 1962, pp. 3-50.

AD-A105 500

AIR FORCE INST OF TECH WRIGHT-PATTERSON AFB OH
FRACTURE PREDICTION IN PLANE ELASTO-PLASTIC PROBLEMS BY THE FIN--ETC(U)
1978 R G BELIE
AFIT-CI-79-2610

F/G 20/11

FIN--ETC(U)

UNCLASSIFIED

NL

2 OF 2
AD-A
101-00



| | | | | | | | | | | | | |
|--|--|--|--|--|--|--|--|--|--|--|--|--|
| | | | | | | | | | | | | |
| | | | | | | | | | | | | |
| | | | | | | | | | | | | |

END

DATE

FILED

DTIC

11-81

APPENDIX I

THE FINITE ELEMENT PROGRAM, FRACTURE

This appendix contains the finite element FRACTURE.
A sample of the program output is also included at the end
of the program.


```

0001 SUBROUTINE IREAD(NNM,NEM,NRM,NMAX,ACMAX,NOF,NPE,NBDY,NHBY,NEQ,NRMAX,
      INEMAX,X,Y,NOD,VBDY,IBDY,ISTYPE)
      C
      C THIS SUBROUTINE READS AND PRINTS OUT GEOMETRIC AND CONSTRAINT
      C DATA, AND CALCULATES THE HALF BAND WIDTH, NHBW
      C
      IMPLICIT REAL*8(A-H,O-Z)
      DIMENSION X(NRM,NEM),Y(NRM,NEM),NOD(NEM,NPE),VBDY(100),IBDY(100)
      ...READ IN DATA FROM THE MESH GENERATOR...
      READ(5,900)ISTYPE,1DIV,DCRACK,NBAR,DHBAR,WHTOP,OTOP,DHOLE,RHOLE,R
      IFIL
      900 FORMAT(11,12,F8.4)
      GO TO (1,2,3,4),ISTYPE
      1 WRITE(6,981)
      GO TO 5
      2 WRITE(6,982)
      GO TO 5
      3 WRITE(6,983)
      GO TO 5
      4 WRITE(6,984)
      5 1DIV=1DIV*8
      WRITE(6,985)1DIV,NBAR,DHBAR,WHTOP,OTOP,RHOLE,DHOLE,RFIL
      981 FORMAT(1H1,48X,MESH FOR FRACTURE STUDY',//,48X,'SINGLE EDGE NOTC'
      1,M SPECIMEN'//)
      982 FORMAT(1H1,48X,MESH FOR FRACTURE STUDY',//,48X,'DOUBLE EDGE NOTC'
      1,M SPECIMEN'//)
      983 FORMAT(1H1,48X,MESH FOR FRACTURE STUDY',//,48X,'90 DEG EDGE NOTC'
      1,M SPECIMEN'//)
      984 FORMAT(1H1,48X,MESH FOR FRACTURE STUDY',//,48X,'ASYMM EDGE NOTC'
      1,M SPECIMEN'//)
      985 FORMAT(1H1,15X,'DIVISIONS AT CENTER SECTION = ',13,
      1', BAR HALF WIDTH = ',F8.4',', BAR HALF LENGTH = ',F8.4,/,16X,
      2'TOP HALF WIDTH = ',F8.4',', TOP LENGTH = ',F8.4',', HOLE RADIUS = ',
      3',F8.4',', LOCATION FROM THE TOP = ',F8.4',/,16X,'FILLET RADIUS'
      4',S = ',F8.4,/,//)
      READ(5,932)NNM
      WRITE(6,932)NNM
      902 FORMAT(1H,'THE NUMBER OF NODES = ',14,/,1H,3('NODE',9X,'X',15X,
      1,Y',12X)/)
      NN=NNM-2
      DO 15 I=1,NN,3
      READ(5,933) N,X(N),Y(N),NI,X(NI),Y(NI),NNN,X(NNN),Y(NNN)
      WRITE(6,931)N,X(N),Y(N),NI,X(NI),Y(NI),NNN,X(NNN),Y(NNN)
      15 CONTINUE
      930 FORMAT(3(14,2F10.4))
      931 FORMAT(1H,3(14,2(13X,E12.5),8X))
      NNN=NNM/3
      NNN=NNN*3
      IF(NNM.EQ.NNM-1) READ(5,930)N,X(NI),Y(NI)
      IF(NNM.EQ.NNM-1)WRITE(6,931)N,X(NI),Y(NI)
      IF(NNM.EQ.NNM-2) READ(5,930)N,X(NI),Y(NI),NI,X(NI),Y(NI)
      IF(NNM.EQ.NNM-2)WRITE(6,931)N,X(NI),Y(NI),NI,X(NI),Y(NI)
0002
0003
0004
0005
0006
0007
0008
0009
0010
0011
0012
0013
0014
0015
0016
0017
0018
0019
0020
0021
0022
0023
0024
0025
0026
0027
0028
0029
0030
0031
0032
0033
0034
0035
0036

```



```

0301 SUBROUTINE PROP(ET,XNUT,STRAIN,IEP,NEMAX,ECH)
C
C THIS SUBROUTINE TABULATES THE MATERIAL PROPERTIES
C
      IMPLICIT REAL*8(A-H,O-Z)
      DIMENSION ET(10,2),XNUT(10,2),STRAIN(10,2),IEP(NEMAX),ECH(NEMAX)
      DO 1 I=1,NEMAX
1    IEP(I)=1
C
C      .... STEEL PROPERTIES ....
C      ET(1,1)=29000000.
C      XNUT(1,1)=0.318
C      STRAIN(1,1)=0.002
C
C      .... ALUMINUM PROPERTIES ....
C      ET(1,2)=10500000.
C      ET(2,2)=1183000.
C      ET(3,2)=462000.
C      ET(4,2)=271000.
C      ET(5,2)=152000.
C      ET(6,2)=50300.
C      ET(6,2)=65000.
C      ET(7,2)=0.0
C      XNUT(1,2)=0.313
C      XNUT(2,2)=0.375
C      XNUT(3,2)=0.443
C      XNUT(4,2)=0.467
C      XNUT(5,2)=0.484
C      XNUT(6,2)=0.491
C      XNUT(7,2)=0.5
C      STRAIN(1,2)=0.00472
C      STRAIN(2,2)=0.00753
C      STRAIN(3,2)=0.01814
C      STRAIN(4,2)=0.03286
C      STRAIN(5,2)=0.07817
C      STRAIN(6,2)=0.17483
C      STRAIN(6,2)=0.14291
C      STRAIN(7,2)=999.
C      DO 3 I=1,6
3    ECH(I)=STRAIN(I,1)
      DO 2 I=7,NEMAX
2    ECH(I)=STRAIN(I,2)
      RETURN
      END
0302
0303
0304
0305
0306
0307
0308
0309
0310
0311
0312
0313
0314
0315
0316
0317
0318
0319
0320
0321
0322
0323
0324
0325
0326
0327
0328
0329
0330
0331
0332
0333
0334
0335
0336
0337

```

```

0001 SUBROUTINE ASSEM(NMH,NEM,NRMAX,NCMAX,NDF,NPE,NBDY,NMBW,NEQ,NRMAXH,
      INEMMAX,X,Y,NOD,GSTIF,8,C,VBDY,IBDY,ET,XNUT,IEP,ITFAIL,ECN,ITIME,
      ZSTRAIN)
      ** MODIFICATION OF A PROGRAM BY J.N. REDDY **
      C
      C THIS SUBROUTINE ASSEMBLES THE GLOBAL STIFFNESS MATRIX
      C
      IMPLICIT REAL*8(A-H,O-Z)
      DIMENSION X(NRMAXH),Y(NRMAXH),NOD(NEMMAX,NPE),VBDY(100),
      1GSTIF(NRMAX,NCMAX),
      2XNUT(10,2),IBDY(100),IEP(NEMMAX),ECN(NEMMAX),STRAIN(10,2),
      3,8(NEMMAX,3),C(NEMMAX,3),BETA(3),GAMA(3)
      C ..... INITIALIZE THE GLOBAL STIFFNESS MATRIX .....
      DO 50 I=1,NEQ
      DO 50 J=1,NMBW
      DO 50 K=1,NMBW
      50 GSTIF(I,J)=0.0
      NN=NDF*NPE
      DO 150 N=1,NEM
      INTYPE=1
      IF(N,GT,6)INTYPE=2
      IF(STRAIN(IEP(N),INTYPE).EQ,999)GO TO 52
      IF(STRAIN(IEP(N),INTYPE).EQ,ECN(N))GO TO 57
      E=ET(I,INTYPE)
      XNU=XNUT(I,INTYPE)
      GO TO 55
      57 E=ET(IEP(N),INTYPE)
      XNU=XNUT(IEP(N),INTYPE)
      GO TO 55
      52 E=0.0
      XNU=0.5
      55 CONTINUE
      DO 60 I=1,NPE
      NI=NOD(N,I)
      ELXY(I,1)=X(NI)
      60 ELXY(I,2)=Y(NI)
      CALL STIFF (NPE,NN,ELXY,ELSTIF,E,XNU,BETA,GAMA,DET)
      DO 65 I=1,3
      B(N,I)=BETA(I)/DET
      65 C(N,I)=GAMA(I)/DET
      C ..... ASSEMBLE ELEMENT STIFFNESS MATRICES TO GET GLOBAL STIFFNESS
      DO 140 I=1,NPE
      NR=(NOD(N,I)-1)*NDF
      DO 140 II=1,NDF
      NR=NR+II
      L=(I-1)*NDF+II
      DO 130 J=1,NPE
      NCL=(NOD(N,J)-1)*NDF
      DO 120 JJ=1,NDF
      M=(J-1)*NDF+JJ
      NC=NCL+JJ+1-NR
      IF (NC) 120,120,110
      110 GSTIF(NR,NC)=GSTIF(NR,NC)+ELSTIF(L,M)
      0002
      0003
      0004
      0005
      0006
      0007
      0008
      0009
      0010
      0011
      0012
      0013
      0014
      0015
      0016
      0017
      0018
      0019
      0020
      0021
      0022
      0023
      0024
      0025
      0026
      0027
      0028
      0029
      0030
      0031
      0032
      0033
      0034
      0035
      0036
      0037
      0038
      0039
      0040
      0041

```



```

0042 120 CONTINUE
0043 130 CONTINUE
0044 140 CONTINUE
0045 150 CONTINUE
C      .... IMPOSE BOUNDARY CONDITIONS .....
      DO 170 I=1,NBDY
      IE=IBDY(I)
      VE=VB DY(I)
      170 CALL BNDRY (NRMAX,NCMAX,NEG,NHBM,GSTIF,GF,IE,VE)
      DO 180 I=1,NEO
      IF(GSTIF(I,I).NE.0.0)GO TO 180
      CALL BNDRY(NRMAX,NCMAX,NEG,NHBM,GSTIF,GF,I,0.0)
      WRITE(6,900)I
      900 FORMAT(1H 'ROW ',I5,' HAS BEEN CONSTRAINED')
      180 CONTINUE
      RETURN
      END
0046
0047
0048
0049
0050
0051
0052
0053
0054
0055
0056
0057

```

```

0001 SUBROUTINE STIFF(NPE,NN, ELXY,ELSTIF,E,ANU,BETA,GAMA,DET)
C ** MODIFICATION BASED ON SUBROUTINE STIFF BY J.N. REDDY **
C
C THIS SUBROUTINE CALCULATES THE ELEMENT STIFFNESS MATRIX
C
0002 IMPLICIT REAL*8(A-H,O-Z)
0003 DIMENSION ELXY(3,2),ELSTIF(NN,NN),X(3),Y(3)
0004 DIMENSION B(3,6),BT(6,3),STRI(3,6),D(3,3)
0005 DIMENSION GAMA(3),BETA(3)
0006 T=0.127
0007 DO 10 I=1,3
0008 DO 10 J=1,3
0009 DO 10 I(J)=0.0
C
C ***** PLANE STRESS CASE (ISOTROPIC) *****
C
0010 CI=E/(1.0-ANU*ANU)
0011 D(1,1)=CI
0012 D(1,2)=ANU*CI
0013 D(3,3)=0.5*(1.0-ANU)*CI
0014 D(2,1)=D(1,2)
0015 D(2,2)=D(1,1)
C
C ***** STIFFNESS MATRIX FOR CONSTANT STRAIN TRIANGLE CASE *****
C
0016 DO 70 I=1,NPE
0017 X(I)=ELXY(I,1)
0018 Y(I)=ELXY(I,2)
0019 DO 60 K=1,NN
0020 B(1,K)=0.0
0021 DO 70 CONTINUE
0022 DO 80 I=1,NPE
0023 J=I+1
0024 IF (J.GT.NPE) J=J-NPE
0025 K=J+1
0026 IF (K.GT.NPE) K=K-NPE
0027 BETA(I)=Y(J)-Y(K)
0028 GAMA(I)=X(K)-X(J)
0029 DO 80 CONTINUE
0030 DET=X(1)*Y(2)-Y(3)*X(2)+Y(3)*X(1)+X(3)*Y(1)-Y(2)*X(3)
0031 DO 100 I=1,NPE
0032 J=2*(I-1)+1
0033 L=2*I
0034 B(1,J)=BETA(I)/DET
0035 B(3,J)=GAMA(I)/DET
0036 B(2,L)=GAMA(I)/DET
0037 B(3,L)=BETA(I)/DET
0038 DO 100 CONTINUE
C
C FOR CONSTANT STRAIN TRIANGLE CASE THE STIFFNESS MATRIX IS EQUAL TO
C K = A*E*(BT)*(D)*(B)
C
0039 DO 110 I=1,3
0040 DO 110 J=1,NN
0041 BT(I,J)=0.5*DET*(I,J)
0042 CALL MATMUL (D,3,3,B,NN,STR)
0043 CALL MATMUL (BT,NN,3,STR,NN,ELSTIF)
0044 RETURN
0045 END

```

```

0001 SUBROUTINE MATMUL (A,M,N,B,L,C)
      ** MODIFICATION BASED ON SUBROUTINE MATMUL BY J.N. REDDY **
      SUBROUTINE FOR MATRIX MULTIPLICATION
      THIS PROGRAM MULTIPLIES A (M,N) BY B(N,L) TO GIVE C(M,L)
      IMPLICIT REAL*8(A-H,O-Z)
      DIMENSION A(M,N),B(N,L),C(M,L)
      DO 10 I=1,M
      DO 10 J=1,L
        C(I,J)=0.
      DO 10 K=1,N
        C(I,J)=C(I,J)+A(I,K)*B(K,J)
      10 RETURN
      END
0002
0003
0004
0005
0006
0007
0008
0009
0010

```

```

0001 SUBROUTINE BNDRY (NRMAX,NCMAX,NEQ,NHBW,S,SL,IE,SVAL)
      ** MODIFICATION BASED ON SUBROUTINE BNDRY BY J.N. REDDY **
0002 C THIS PROGRAM IMPUTES THE PRESCRIBED BOUNDARY CONDITIONS ON THE
0003 C THE SYSTEM MATRIX(BANDED SYMMETRIC MATRIX)
0004 C S IS THE SYSTEM MATRIX (STIFFNESS MATRIX)
0005 C SL IS THE LOAD VECTOR
0006 C IE IS THE LABEL OF THE VARIABLE THAT IS PRESCRIBED
0007 C SVAL IS THE VALUE OF THE PRESCRIBED VARIABLE
0008 C IMPLICIT REAL*8(A-M,O-Z)
0009 C DIMENSION S(NRMAX,NCMAX)
0010 C IT=NHBW-1
0011 C I=IE-NHBW
0012 C DO 10 II=1,IT
0013 C I=I+1
0014 C IF (I-LI,1) GO TO 10
0015 C J=IE-I+1
0016 C S(I,J)=0.0
0017 C 10 CONTINUE
0018 C S(IE,1)=1.0
0019 C I=IE
0020 C DO 20 II=2,NHBW
0021 C I=I+1
0022 C IF (I-GI,NEQ) GO TO 20
0023 C S(IE,II)=0.0
0024 C 20 CONTINUE
0025 C RETURN
0026 C END

```

```

0001 SUBROUTINE SOLVE1(NRM,NCM,NEQNS,NBW,BAND,RHS)
0002 99 MODIFICATION BASED ON SUBROUTINE SOLVE BY J.N. REDDY **
0003 THIS PROGRAM SOLVES A Banded Symmetric System of Equations
0004 C THE Banded Matrix is Input Through BAND(NEQNS,NBW)
0005 RHS IS THE RIGHT HAND SIDE (FORCE VECTOR) OF THE SYSTEM
0006 C NEQNS IS THE NO. OF EQUATIONS (EQUAL TO ACTUAL NO. OF ROWS)
0007 C NBW IS THE HALF BANDWIDTH OF THE SYSTEM
0008 IMPLICIT REAL*8(A-H,O-Z)
0009 DIMENSION BAND(NRM,NCM),RHS(NRM)
0010 DO 5 I=1,NEQNS
0011 5 RHS(I)=0.0
0012 RHS(2)=1.0
0013 MEQNS=NEQNS-1
0014 DO 30 NPIV=1,MEQNS
0015 NPIVOT=NPIV+1
0016 LSTSUB=NPIV+NBW-1
0017 IF (LSTSUB.GT.NEQNS) LSTSUB=NEQNS
0018 DO 20 NROW=NPIVOT,LSTSUB
0019 INVERT ROWS AND COLUMNS FOR ROW FACTOR
0020 NCOL=NROW-NPIV+1
0021 FACTOR=DAND(NPIV,NCOL)/BAND(NPIV,1)
0022 ICOL=NCOL-NROW+1
0023 JCOL=NCOL-NPIV+1
0024 BAND(NROW,ICOL)=BAND(NROW,ICOL)-FACTOR*BAND(NPIV,JCOL)
0025 20 RHS(NROW)=RHS(NROW)-FACTOR*RHS(NPIV)
0026 30 CONTINUE
0027 DO 90 IJK=2,NEQNS
0028 NPIV=NEQNS-IJK+2
0029 RHS(NPIV)=RHS(NPIV)/BAND(NPIV,1)
0030 C ALTHOUGH ZEROING ELEMENTS IN MATRIX, DONT BOTHER TO OPERATE ON IT
0031 LSTSUB=NPIV-NBW+1
0032 IF (LSTSUB.LT.1) LSTSUB=1
0033 NPIVOT=NPIV-1
0034 DO 80 JK=LSTSUB,NPIVOT
0035 NROW=NPIVOT-JK+LSTSUB
0036 NCOL=NPIV-NROW+1
0037 FACTOR=BAND(NROW,NCOL)
0038 80 RHS(NROW)=RHS(NROW)-FACTOR*RHS(NPIV)
0039 90 CONTINUE
0040 RHS(1)=RHS(1)/BAND(1,1)
0041 RETURN
0042 END
0043

```

```

0001 SUBROUTINE FAIL(ITIME,U,NRMAX,XLOAD,B,C,NEM,XNU,STRAIN,IEF,NEMMAX,
      1 EYT,EYT,GXYT,NEF,NOD,IFT,FLUAD,XLOAD1,EXEL,EYEL,EZEL,GXYEL,
      2 IFTYPE,ISTYPE,ECH,U1,U11)
      3 .... THIS SUBROUTINE DETERMINES 1) THE NEXT ELEMENT(S) TO YIELD,
      4 CHANGE MODULUS, OR FRACTURE 2) THE LOAD FOR THIS FAILURE,
      5 AND 3) THE DEFLECTION AT THE PIN CENTER NOD ....
      6 IMPLICIT REAL*8(A-H,O-Z)
      7 DIMENSION U(NRMAX),B(NEMMAX,3),C(NEMMAX,3),EX(800 ),EY(800),
      8 1 GXY(800 ),XNU(10,2),STRAIN(10,2),IEF(300),EZ(800),
      9 2 EYT(NEMMAX),GXYT(NEMMAX),EXT(NEMMAX),NOD(NEMMAX,3),
      0 3 EXEL(NEMMAX),EYEL(NEMMAX),EZEL(NEMMAX),GXYEL(NEMMAX),
      1 4 EYT(NEMMAX),IFT(NEMMAX),EPRIN(3),ECH(NEMMAX)
      2 .... CALCULATE INCREMENTAL STRAIN IN X AND Y DIRECTION AND
      3 SHEAR STRAIN ....
      4 IFTYPE=2
      5 DO 10 I=7,NEM
      6 CCNU=XNU(IFT(I),IMTYPE)/(1.0-(XNU(IFT(I),IMTYPE))**2)
      7 EX(I)=0.0
      8 EY(I)=0.0
      9 EZ(I)=0.0
      0 GXY(I)=0.0
      1 DO 11 J=1,3
      2 NODE2=NOD(I,J)*2
      3 NODE1=NODE2-1
      4 EX(I)=EX(I)+B(I,J)*U(NODE1)
      5 EY(I)=EY(I)+C(I,J)*U(NODE2)
      6 GXY(I)=GXY(I)+B(I,J)*U(NODE2)+C(I,J)*U(NODE1)
      7 11 CONTINUE
      8 10 CONTINUE
      9 IF(ITIME.EQ.1.OR.IFTYPE.EQ.1)U11=U(2)
      0 EMAX=0.0
      1 IF(ITIME.NE.1)GO TO 20
      2 IFTIME=2
      3 .... CALCULATE FIRST ELEMENT TO YIELD ....
      4 .... MAX NORMAL STRAIN CRITERIA ....
      5 IFTYPE=0
      6 DO 30 I=7,NEM
      7 EPLUS=EX(I)+EY(I)
      8 EMINUS=EX(I)-EY(I)
      9 ESORT=((EMINUS)*2+(GXY(I)**2)**0.5
      0 EPRIN1)=0.5*(EPLUS+ESORT)
      1 EPRIN2)=0.5*(EPLUS-ESORT)
      2 EPRIN3)=EZ(I)
      3 DO 30 I1=1,3
      4 IF(EPRIN(I1)-EMAX)J0=I0.50
      5 40 NEF=NEF+1
      6 IF(NEF.EQ.301)GO TO 60
      7 IEF(NEF)=I
      8 GO TO 30
      9 60 WRITE(6,902)
      0 902 FORMAT(1H '.... MORE THAN 300 ELEMENTS FAILED ....')

```

```

0040 CALL EXIT
0041 50 NEF=1
0042 IF(NEF)=1
0043 EMAX=EPRIN(1)
0044 30 CONTINUE
0045 XLOAD=STRAIN(1,2)/EMAX
0046 UT1=U(2)*XLOAD
0047 DO 70 I=7,NEM
0048 EX(I)=EX(I)*XLOAD
0049 EY(I)=EY(I)*XLOAD
0050 EZ(I)=EZ(I)*XLOAD
0051 GXY(I)=GXY(I)*XLOAD
0052 EXEL(I)=EX(I)
0053 EYEL(I)=EY(I)
0054 EZEL(I)=EZ(I)
0055 GXYEL(I)=GXY(I)
0056 70 CONTINUE
0057 IF(ISTYPE.EQ.2.OR.ISTYPE.EQ.3)XLOAD=XLOAD*2.0
0058 XLOAD=XLOAD
0059 WRITE(6,903)XLOAD,UT1
0060 %60 FORMAT(1H1.4X,'LOAD DEFLECTION HISTORY',///,1H,'FAILURE ',
1,' INITIAL YIELD ) OCCURRED AT A LOAD OF ',F12.2,' WITH A ',
2,' DEFLECTION AT THE PIN OF ',E12.5)
DO 150 I=1,NEF
150 WRITE(6,930)IEF(I),IFT(I)
WRITE(6,980)
RETURN
20 INCR=0
C ....CALCULATE NEXT ELEMENTS TO YIELD. CHANGE MODULUS. OR FRACTURE
X1=1.0
NEF=0
XFMIN=999999.
C ....APPROXIMATE NEXT FAILURE LOAD....
DO 22 I=7,NEM
IF(ECH(I).EQ.999)GO TO 22
DEPR=-5*(EX(I)+EY(I))*((EX(I)-EY(I))*2+(GXY(I))*2)*0.5)
EPRI=-5*(EX(I)+EY(I))*((EX(I)-EY(I))*2+(GXY(I))*2)*0.5)
XF=(ECH(I)-EPRI)/DEPR
IF(XF.LE.0.0)GO TO 23
IF(XF.LT.XFMIN)XFMIN=XF
23 IF(ISTYPE.NE.1)GO TO 22
EXEL(I)=EX(I)
EYEL(I)=EY(I)
EZEL(I)=EZ(I)
GXYEL(I)=GXY(I)
22 CONTINUE
ALINCR=XFMIN*5.0
C IF(ALINCR.LT.50.)XLINCR=50.
WRITE(6,970)XLINCR
970 FORMAT(1H,'LOAD INCREMENT = ',E12.5)
100 IOUT=0
IF(INCR.NE.0)X1=0.2

```

```

0087 IF(XLINCR.LT.200.0)XI=1.0
0088 DO 80 I=7,NEM
0089   EMAX=UCHI(I)
0090   IF(ISTRAIN(I).2).EQ.999.0)GO TO 80
0091   EXT(I)=EXT(I)+EX(I)*XLINCR*XI
0092   EYT(I)=EYT(I)+EY(I)*XLINCR*XI
0093   EZT(I)=EZT(I)+EZ(I)*XLINCR*XI
0094   GRAY(I)=GRAY(I)+GX(I)*XLINCR*XI
0095   EPLUS=EXT(I)+EYT(I)
0096   EMINUS=EXT(I)-EYT(I)
0097   ESORT=((EMINUS)*.2+(GYT(I)*.2)*.00.5
0098   EPRIN(1)=0.5*(EPLUS+ESORT)
0099   EPRIN(2)=0.5*(EPLUS-ESORT)
0100   EPRIN(3)=EZ(I)
0101   DO 81 I=1.3
0102     IF(EPRIN(I)).LT.LMAX)GO TO 81
0103     NEF=NEF+1
0104     IOUT=1
0105     IF(NEF.NE.30)GO TO 82
0106     WRITE(6.902)
0107     DO 83 J=1.99
0108       83 WRITE(6.951)IEF(J)
0109       951 FORMAT(1H 'ELEMENT ',15,' FAILED')
0110       CALL EXIT
0111       82 IEF(NEF)=1
0112       81 CONTINUE
0113       80 CONTINUE
0114       INCN=INCN+1
0115       IF(IOUT.EQ.0)GO TO 100
0116       XINCR=INCN-1
0117       XINCR=XINCR*XLINCR*XI*XLINCR
0118       UTI=UTI+UT(2)*XINCR
0119       IF(UTYPE=0)
0120         IF(ISTYPE.EQ.2.0H.1)ISTYPE=EQ.3)XINCR=XINCR*2.0
0121         XLAD=XLAD+XINCR
0122         WRITE(6.915)NEF
0123         915 FORMAT(1H '13.' ELEMENT'S FAILED DURING THIS LOAD STEP')
0124         WRITE(6.910)XLAD,UTI
0125         910 FORMAT( 1H 'FAILURE (YIELD OR FRACTURE) OCCURRED AT A LOAD OF '
0126           1.F12.2.' WITH A DEFLECTION AT THE PIN OF '.E12.5)
0127         DO 120 I=1.NEF
0128           IF(ISTRAIN(I).EQ.999.0)GO TO 130
0129           WRITE(6.930)IEF(I),IFT(IEF(I))
0130           930 FORMAT(1H 'ELEMENT ',15,' YIELDED FOR THE '.15,' TIME')
0131           GO TO 120
0132           130 WRITE(6.940)IEF(I)
0133           940 FORMAT(1H 'ELEMENT ',15,' FRACTURED')
0134           IF(UTYPE=1)
0135             WRITE(6.980)
0136             980 FORMAT(//.1H '53A.'*****//)
0137           IF(IFTYPE.EQ.0)RETURN

```



```

0138 IF(XLOAD,LT,FLOAD)WRITE(6,950)FLOAD
0139 950 FORMAT(///,1H,'***** CRACK INSTABILITY OCCURRED AT A LOAD OF ',
0140 IF12.2,' *****',//)
0141 FLOAD=XLOAD
0142 UT1=UT1-UT11*FLOAD
0143 XLOAD=0.0
0144 ***** UNLOAD SPECIMEN ALONG ELASTIC SLOPE ****
0145 XSTYPE=1.0
0146 IF(1STYPE.EQ.2.OR.1STYPE.EQ.3)XSTYPE=.5
0147 DO 140 I=7,NEM
0148 IF(1STRAIN(IFT(I),2).EQ.999.1GO TO 145
0149 DO 147 I1=1,NF
0150 IF(1IEF(I1).EQ.1)GO TO 145
0151 147 CONTINUE
0152 IF(1STRAIN(IFT(I),2).NE.ECH(I))GO TO 145
0153 IF(IFT(I).EQ.1)GO TO 145
0154 EPLUS=EXT(I)+EY(I)
0155 EMINUS=EXT(I)-EY(I)
0156 ESORT=((EMINUS)**2+(GXYT(I)**2)**0.5
0157 EPRIN(I)=0.5*(EPLUS+ESORT)
0158 ECH(I)=EPRIN(I)
0159 145 EXT(I)=EXT(I)-EXEL(I)*FLOAD*XSTYPE
0160 EYT(I)=EY(I)-EYEL(I)*FLOAD*XSTYPE
0161 EZT(I)=EZT(I)-EZEL(I)*FLOAD*XSTYPE
0162 GXYT(I)=GXY(I)-GXEL(I)*FLOAD*XSTYPE
0163 140 CONTINUE
0164 RETURN
0165 END

```

```

0001 SUBROUTINE CHANG(IEF,IFT,NEF,NEMMAX,ECH,STRAIN)
0002 IMPLICIT REAL*8(A-H,O-Z)
0003     DIMENSION IFT(NEMMAX),ECH(NEMMAX),STRAIN(10,2),IEF(300)
0004     IMTYPE=2
0005     ... UPDATES THE TANGENT MATERIAL LOCATION INDEX ...
0006     DO 80 N=1,NEF
0007         IF(STRAIN(IFT(IEF(N))+1,2).EQ.999.)IFT(IEF(N))=IFT(IEF(N))+1
0008         IF(STRAIN(IFT(IEF(N)),IMTYPE).NE.ECH(IEF(N)))GO TO 85
0009         IFT(IEF(N))=IFT(IEF(N))+1
0010         ECH(IEF(N))=STRAIN(IFT(IEF(N)),IMTYPE)
0011     80 CONTINUE
0012     RETURN
        END

```

C

MESH FOR FRACTURE STUDY
DOUBLE EDGE NOTCH SPECIMEN

DIVISIONS AT CENTER SECTION = 8, BAR HALF WIDTH = 0.4120, BAR HALF LENGTH = 4.5550
TOP HALF WIDTH = 1.4970, TOP LENGTH = 2.9310, HOLE RADIUS = 0.5000, LOCATION FROM THE TOP = 1.4850
FILLET RADIUS = 0.6250

THE NUMBER OF NODES = 226

| NODE | X | Y | NODE | X | Y | NODE | X | Y |
|------|-------------|-------------|------|--------------|--------------|------|-------------|-------------|
| 1 | 0.0 | 0.307000 01 | 2 | 0.0 | 0.357000 01 | 3 | 0.250000 00 | 0.350300 01 |
| 4 | 0.433000 00 | 0.332000 01 | 5 | 0.500000 00 | 0.307000 01 | 6 | 0.433000 00 | 0.282000 01 |
| 7 | 0.250000 00 | 0.263700 01 | 8 | 0.0 | 0.257000 01 | 9 | 0.433000 00 | 0.282000 01 |
| 10 | 0.250000 00 | 0.263700 01 | 11 | 0.0 | 0.257000 01 | 12 | 0.0 | 0.382000 01 |
| 13 | 0.287000 00 | 0.376200 01 | 14 | 0.530300 00 | 0.360000 01 | 15 | 0.692900 00 | 0.335700 01 |
| 16 | 0.750000 00 | 0.307000 01 | 17 | 0.692900 00 | 0.278300 01 | 18 | 0.530300 00 | 0.251970 01 |
| 19 | 0.237000 00 | 0.237710 01 | 20 | 0.0 | 0.232000 01 | 21 | 0.483000 00 | 0.294060 01 |
| 22 | 0.596500 00 | 0.292650 01 | 23 | 0.213600 00 | 0.217800 01 | 24 | 0.479000 00 | 0.228660 01 |
| 25 | 0.213600 00 | 0.199500 01 | 26 | 0.891200 00 | 0.285620 01 | 27 | 0.741500 00 | 0.253140 01 |
| 28 | 0.0 | 0.418750 01 | 29 | 0.427600 00 | 0.410240 01 | 30 | 0.793200 00 | 0.386020 01 |
| 31 | 0.133240 01 | 0.369700 01 | 32 | 0.1111750 01 | 0.307000 01 | 33 | 0.103240 01 | 0.264230 01 |
| 34 | 0.790200 00 | 0.227900 01 | 35 | 0.427600 00 | 0.203760 01 | 36 | 0.0 | 0.192250 01 |
| 37 | 0.0 | 0.455500 01 | 38 | 0.748500 00 | 0.455500 01 | 39 | 0.112270 01 | 0.418370 01 |
| 40 | 0.149700 01 | 0.381250 01 | 41 | 0.149700 01 | 0.307000 01 | 42 | 0.149700 01 | 0.232750 01 |
| 43 | 0.112270 01 | 0.195630 01 | 44 | 0.775200 00 | 0.195630 01 | 45 | 0.597500 00 | 0.191380 01 |
| 46 | 0.419600 00 | 0.183080 01 | 47 | 0.209900 00 | 0.178820 01 | 48 | 0.0 | 0.178820 01 |
| 49 | 0.149700 01 | 0.455500 01 | 50 | 0.149700 01 | 0.162400 01 | 51 | 0.126470 01 | 0.328380 01 |
| 52 | 0.126470 01 | 0.285620 01 | 53 | 0.112270 01 | 0.232750 01 | 54 | 0.309000 00 | 0.162400 01 |
| 55 | 0.206000 00 | 0.162400 01 | 56 | 0.103000 00 | 0.162400 01 | 57 | 0.0 | 0.162400 01 |
| 58 | 0.103700 01 | 0.162400 01 | 59 | 0.149700 01 | 0.328380 01 | 60 | 0.662000 00 | 0.162400 01 |
| 61 | 0.149700 01 | 0.285620 01 | 62 | 0.412000 00 | 0.162400 01 | 63 | 0.906100 00 | 0.181050 01 |
| 64 | 0.849500 00 | 0.162400 01 | 65 | 0.537000 00 | 0.162400 01 | 66 | 0.623600 00 | 0.146770 01 |
| 67 | 0.495700 00 | 0.131150 01 | 68 | 0.755700 00 | 0.155710 01 | 69 | 0.517820 00 | 0.154590 01 |
| 70 | 0.517800 00 | 0.146770 01 | 71 | 0.559700 00 | 0.140250 01 | 72 | 0.485600 00 | 0.138560 01 |
| 73 | 0.453900 00 | 0.131150 01 | 74 | 0.463800 00 | 0.124810 01 | 75 | 0.412000 00 | 0.146770 01 |
| 76 | 0.309000 00 | 0.146770 01 | 77 | 0.206000 00 | 0.146770 01 | 78 | 0.103000 00 | 0.146770 01 |
| 79 | 0.0 | 0.146770 01 | 80 | 0.412000 00 | 0.131150 01 | 81 | 0.309000 00 | 0.131150 01 |
| 82 | 0.206000 00 | 0.131150 01 | 83 | 0.103000 00 | 0.131150 01 | 84 | 0.0 | 0.131150 01 |
| 85 | 0.412000 00 | 0.138960 01 | 86 | 0.300500 00 | 0.138960 01 | 87 | 0.432900 00 | 0.124810 01 |
| 88 | 0.360500 00 | 0.124810 01 | 89 | 0.431800 00 | 0.115520 01 | 90 | 0.309000 00 | 0.123340 01 |
| 91 | 0.257500 00 | 0.123340 01 | 92 | 0.309000 00 | 0.107710 01 | 93 | 0.257500 00 | 0.107710 01 |
| 94 | 0.370400 00 | 0.999000 00 | 95 | 0.370400 00 | 0.5947500 00 | 96 | 0.309000 00 | 0.115520 01 |
| 97 | 0.206000 00 | 0.115520 01 | 98 | 0.103000 00 | 0.115520 01 | 99 | 0.0 | 0.115520 01 |

| | | | | | | |
|-----|-------------|-------------|-------------|-------------|-------------|-------------|
| 100 | 0.370400 00 | 0.115420 01 | 0.416900 00 | 0.107710 01 | 0.370400 00 | 0.107710 01 |
| 103 | 0.412000 00 | 0.999000 00 | 0.309000 00 | 0.999000 00 | 0.206000 00 | 0.999000 00 |
| 106 | 0.103000 00 | 0.999000 00 | 0.00 | 0.999000 00 | 0.412000 00 | 0.696000 00 |
| 109 | 0.309000 00 | 0.896000 00 | 0.206000 00 | 0.896000 00 | 0.103000 00 | 0.896000 00 |
| 112 | 0.00 | 0.896000 00 | 0.412000 00 | 0.412000 00 | 0.793000 00 | 0.793000 00 |
| 115 | 0.206000 00 | 0.793000 00 | 0.103000 00 | 0.793000 00 | 0.00 | 0.793000 00 |
| 118 | 0.412000 00 | 0.696000 00 | 0.309000 00 | 0.696000 00 | 0.206000 00 | 0.696000 00 |
| 121 | 0.103000 00 | 0.999000 00 | 0.00 | 0.999000 00 | 0.412000 00 | 0.587000 00 |
| 124 | 0.309000 00 | 0.896000 00 | 0.206000 00 | 0.896000 00 | 0.103000 00 | 0.587000 00 |
| 127 | 0.00 | 0.896000 00 | 0.412000 00 | 0.412000 00 | 0.360500 00 | 0.535500 00 |
| 130 | 0.309000 00 | 0.535500 00 | 0.257500 00 | 0.535500 00 | 0.206000 00 | 0.535500 00 |
| 133 | 0.103000 00 | 0.535500 00 | 0.103000 00 | 0.535500 00 | 0.515000-01 | 0.535500 00 |
| 136 | 0.00 | 0.535500 00 | 0.412000 00 | 0.412000 00 | 0.360500 00 | 0.481900 00 |
| 139 | 0.309000 00 | 0.481900 00 | 0.257500 00 | 0.481900 00 | 0.206000 00 | 0.481900 00 |
| 142 | 0.103000 00 | 0.481900 00 | 0.103000 00 | 0.481900 00 | 0.515000-01 | 0.481900 00 |
| 145 | 0.00 | 0.481900 00 | 0.412000 00 | 0.428400 00 | 0.360500 00 | 0.428400 00 |
| 148 | 0.309000 00 | 0.428400 00 | 0.257500 00 | 0.428400 00 | 0.206000 00 | 0.428400 00 |
| 151 | 0.103000 00 | 0.428400 00 | 0.103000 00 | 0.428400 00 | 0.515000-01 | 0.428400 00 |
| 154 | 0.00 | 0.428400 00 | 0.412000 00 | 0.374800 00 | 0.360500 00 | 0.374800 00 |
| 157 | 0.309000 00 | 0.374800 00 | 0.257500 00 | 0.374800 00 | 0.206000 00 | 0.374800 00 |
| 160 | 0.103000 00 | 0.374800 00 | 0.103000 00 | 0.374800 00 | 0.515000-01 | 0.374800 00 |
| 163 | 0.00 | 0.374800 00 | 0.412000 00 | 0.321300 00 | 0.360500 00 | 0.321300 00 |
| 166 | 0.309000 00 | 0.321300 00 | 0.257500 00 | 0.321300 00 | 0.206000 00 | 0.321300 00 |
| 169 | 0.103000 00 | 0.321300 00 | 0.103000 00 | 0.321300 00 | 0.515000-01 | 0.321300 00 |
| 172 | 0.00 | 0.321300 00 | 0.412000 00 | 0.267700 00 | 0.360500 00 | 0.267700 00 |
| 175 | 0.309000 00 | 0.267700 00 | 0.257500 00 | 0.267700 00 | 0.206000 00 | 0.267700 00 |
| 178 | 0.103000 00 | 0.267700 00 | 0.103000 00 | 0.267700 00 | 0.515000-01 | 0.267700 00 |
| 181 | 0.00 | 0.267700 00 | 0.412000 00 | 0.214200 00 | 0.360500 00 | 0.214200 00 |
| 184 | 0.309000 00 | 0.214200 00 | 0.257500 00 | 0.214200 00 | 0.206000 00 | 0.214200 00 |
| 187 | 0.103000 00 | 0.214200 00 | 0.103000 00 | 0.214200 00 | 0.515000-01 | 0.214200 00 |
| 190 | 0.00 | 0.214200 00 | 0.412000 00 | 0.160600 00 | 0.360500 00 | 0.160600 00 |
| 193 | 0.309000 00 | 0.160600 00 | 0.257500 00 | 0.160600 00 | 0.206000 00 | 0.160600 00 |
| 196 | 0.103000 00 | 0.160600 00 | 0.103000 00 | 0.160600 00 | 0.515000-01 | 0.160600 00 |
| 199 | 0.00 | 0.160600 00 | 0.412000 00 | 0.107100 00 | 0.360500 00 | 0.107100 00 |
| 202 | 0.309000 00 | 0.107100 00 | 0.257500 00 | 0.107100 00 | 0.206000 00 | 0.107100 00 |
| 205 | 0.103000 00 | 0.107100 00 | 0.103000 00 | 0.107100 00 | 0.515000-01 | 0.107100 00 |
| 208 | 0.00 | 0.107100 00 | 0.412000 00 | 0.535000-01 | 0.360500 00 | 0.535000-01 |
| 211 | 0.309000 00 | 0.535000-01 | 0.257500 00 | 0.535000-01 | 0.206000 00 | 0.535000-01 |
| 214 | 0.103000 00 | 0.535000-01 | 0.103000 00 | 0.535000-01 | 0.515000-01 | 0.535000-01 |
| 217 | 0.00 | 0.535000-01 | 0.412000 00 | 0.00 | 0.360500 00 | 0.00 |
| 220 | 0.309000 00 | 0.00 | 0.257500 00 | 0.00 | 0.206000 00 | 0.00 |
| 223 | 0.103000 00 | 0.00 | 0.103000 00 | 0.00 | 0.515000-01 | 0.00 |
| 226 | 0.00 | 0.00 | 0.00 | 0.00 | 0.00 | 0.00 |

THE NUMBER OF ELEMENTS IS 375

ELEMENT CONNECTIVITY

| ELEM | MODEL | NODE2 | NODE3 | ELEM | MODEL | NODE2 | NODE3 | ELEM | MODEL | NODE2 | NODE3 | ELEM | MODEL | NODE2 | NODE3 |
|------|-------|-------|-------|------|-------|-------|-------|------|-------|-------|-------|------|-------|-------|-------|
| 1 | 1 | 3 | 2 | 2 | 1 | 4 | 3 | 3 | 1 | 5 | 4 | 3 | 1 | 5 | 4 |
| 4 | 1 | 6 | 5 | 5 | 1 | 7 | 6 | 6 | 1 | 8 | 7 | 6 | 1 | 8 | 7 |
| 7 | 2 | 3 | 13 | 8 | 3 | 4 | 14 | 9 | 4 | 5 | 15 | 12 | 10 | 11 | 19 |
| 10 | 5 | 21 | 22 | 11 | 9 | 10 | 18 | 12 | 10 | 11 | 15 | 15 | 4 | 15 | 14 |
| 13 | 2 | 13 | 12 | 14 | 3 | 14 | 13 | 15 | 4 | 15 | 14 | 16 | 9 | 18 | 17 |
| 16 | 5 | 16 | 15 | 17 | 5 | 22 | 16 | 18 | 9 | 18 | 17 | 21 | 12 | 29 | 28 |
| 19 | 10 | 19 | 18 | 20 | 11 | 20 | 19 | 21 | 12 | 29 | 28 | 24 | 14 | 30 | 29 |
| 22 | 12 | 13 | 29 | 23 | 13 | 14 | 29 | 24 | 14 | 30 | 29 | 27 | 15 | 16 | 31 |
| 25 | 14 | 31 | 30 | 26 | 14 | 15 | 31 | 27 | 15 | 16 | 31 | 30 | 16 | 17 | 26 |
| 28 | 16 | 32 | 31 | 29 | 16 | 26 | 32 | 30 | 16 | 17 | 26 | 33 | 18 | 24 | 34 |
| 31 | 17 | 18 | 27 | 32 | 18 | 34 | 27 | 33 | 18 | 24 | 34 | 36 | 20 | 36 | 23 |
| 34 | 18 | 19 | 24 | 35 | 19 | 20 | 23 | 36 | 20 | 36 | 23 | 39 | 29 | 30 | 38 |
| 37 | 28 | 38 | 37 | 38 | 28 | 29 | 38 | 42 | 30 | 31 | 40 | 42 | 30 | 31 | 40 |
| 40 | 30 | 39 | 38 | 41 | 30 | 40 | 39 | 45 | 52 | 42 | 61 | 45 | 52 | 42 | 61 |
| 43 | 31 | 51 | 40 | 44 | 32 | 41 | 51 | 51 | 51 | 51 | 51 | 51 | 51 | 51 | 51 |
| 46 | 52 | 33 | 42 | 47 | 33 | 53 | 42 | 51 | 42 | 43 | 50 | 51 | 42 | 43 | 50 |
| 49 | 38 | 39 | 49 | 50 | 39 | 40 | 49 | 51 | 42 | 43 | 50 | 54 | 34 | 35 | 44 |
| 52 | 43 | 58 | 50 | 53 | 34 | 44 | 43 | 54 | 34 | 35 | 44 | 57 | 35 | 47 | 48 |
| 55 | 35 | 45 | 44 | 56 | 35 | 46 | 45 | 57 | 35 | 47 | 48 | 60 | 64 | 58 | 63 |
| 58 | 25 | 36 | 47 | 59 | 36 | 48 | 47 | 60 | 64 | 58 | 63 | 63 | 60 | 45 | 46 |
| 61 | 60 | 63 | 44 | 62 | 60 | 44 | 45 | 63 | 60 | 45 | 46 | 66 | 54 | 46 | 47 |
| 64 | 60 | 46 | 65 | 65 | 54 | 62 | 46 | 66 | 54 | 46 | 47 | 69 | 56 | 47 | 48 |
| 67 | 54 | 47 | 55 | 66 | 56 | 55 | 47 | 72 | 65 | 69 | 60 | 72 | 65 | 69 | 60 |
| 70 | 56 | 48 | 57 | 71 | 66 | 68 | 60 | 72 | 65 | 69 | 60 | 75 | 85 | 72 | 75 |
| 73 | 69 | 66 | 60 | 74 | 71 | 66 | 70 | 75 | 85 | 72 | 75 | 78 | 76 | 75 | 54 |
| 76 | 74 | 67 | 73 | 77 | 75 | 62 | 54 | 78 | 76 | 75 | 54 | 81 | 81 | 80 | 86 |
| 79 | 77 | 76 | 54 | 80 | 77 | 54 | 55 | 81 | 81 | 80 | 86 | 84 | 82 | 81 | 77 |
| 82 | 81 | 86 | 76 | 83 | 81 | 76 | 77 | 84 | 82 | 81 | 77 | 87 | 79 | 78 | 56 |
| 85 | 77 | 55 | 56 | 86 | 78 | 77 | 56 | 87 | 79 | 78 | 56 | 90 | 83 | 77 | 78 |
| 88 | 79 | 56 | 57 | 89 | 83 | 82 | 77 | 90 | 83 | 77 | 78 | 93 | 88 | 80 | 81 |
| 91 | 83 | 78 | 79 | 92 | 84 | 83 | 79 | 93 | 88 | 80 | 81 | 96 | 97 | 91 | 82 |
| 94 | 96 | 100 | 88 | 95 | 97 | 96 | 91 | 96 | 97 | 91 | 82 | 99 | 93 | 96 | 97 |
| 97 | 104 | 94 | 102 | 98 | 92 | 102 | 96 | 102 | 96 | 97 | 91 | 102 | 98 | 97 | 83 |
| 100 | 105 | 93 | 97 | 101 | 97 | 82 | 83 | 102 | 98 | 97 | 83 | 105 | 106 | 105 | 97 |
| 103 | 99 | 98 | 83 | 104 | 99 | 83 | 84 | 105 | 106 | 105 | 97 | 108 | 107 | 106 | 99 |
| 106 | 106 | 97 | 98 | 107 | 106 | 98 | 99 | 108 | 107 | 106 | 99 | 111 | 110 | 109 | 104 |
| 109 | 108 | 103 | 95 | 110 | 109 | 108 | 95 | 111 | 110 | 109 | 104 | 114 | 114 | 108 | 109 |
| 112 | 110 | 104 | 105 | 113 | 114 | 113 | 108 | 114 | 114 | 108 | 109 | 117 | 110 | 105 | 106 |
| 115 | 114 | 109 | 110 | 116 | 115 | 114 | 110 | 117 | 110 | 105 | 106 | 120 | 112 | 106 | 107 |
| 118 | 111 | 110 | 106 | 119 | 112 | 111 | 106 | 120 | 112 | 106 | 107 | 123 | 116 | 111 | 112 |
| 121 | 116 | 115 | 110 | 122 | 116 | 110 | 111 | 123 | 116 | 111 | 112 | 126 | 119 | 118 | 114 |
| 124 | 117 | 116 | 112 | 125 | 118 | 113 | 114 | 126 | 119 | 118 | 114 | 129 | 124 | 123 | 118 |
| 127 | 120 | 119 | 114 | 128 | 120 | 114 | 115 | 129 | 124 | 123 | 118 | 132 | 125 | 124 | 120 |
| 130 | 124 | 118 | 119 | 131 | 124 | 119 | 120 | 132 | 125 | 124 | 120 | | | | |

| | | | | | | | | | | | |
|-----|-----|-----|-----|-----|-----|-----|-----|-----|-----|-----|-----|
| 133 | 120 | 115 | 116 | 134 | 121 | 120 | 116 | 135 | 122 | 121 | 116 |
| 136 | 122 | 116 | 117 | 137 | 126 | 125 | 120 | 138 | 126 | 120 | 121 |
| 139 | 126 | 121 | 122 | 140 | 127 | 126 | 122 | 141 | 129 | 126 | 123 |
| 142 | 129 | 123 | 124 | 143 | 130 | 129 | 124 | 144 | 131 | 130 | 124 |
| 145 | 131 | 124 | 125 | 146 | 132 | 131 | 125 | 147 | 133 | 132 | 125 |
| 148 | 133 | 125 | 126 | 149 | 134 | 133 | 126 | 150 | 135 | 134 | 126 |
| 151 | 135 | 126 | 127 | 152 | 136 | 135 | 127 | 153 | 138 | 137 | 128 |
| 154 | 138 | 128 | 129 | 155 | 138 | 136 | 130 | 156 | 139 | 138 | 130 |
| 157 | 140 | 139 | 130 | 158 | 140 | 139 | 131 | 159 | 140 | 131 | 132 |
| 160 | 141 | 140 | 132 | 161 | 142 | 141 | 132 | 162 | 142 | 132 | 133 |
| 163 | 142 | 133 | 134 | 164 | 143 | 142 | 134 | 165 | 144 | 133 | 134 |
| 166 | 144 | 134 | 135 | 167 | 144 | 143 | 135 | 168 | 145 | 144 | 136 |
| 169 | 147 | 146 | 137 | 170 | 147 | 147 | 138 | 171 | 147 | 138 | 139 |
| 172 | 148 | 147 | 139 | 173 | 149 | 148 | 139 | 174 | 149 | 139 | 140 |
| 175 | 149 | 149 | 141 | 176 | 150 | 149 | 141 | 177 | 151 | 150 | 141 |
| 178 | 151 | 151 | 142 | 179 | 151 | 151 | 142 | 180 | 152 | 151 | 143 |
| 181 | 153 | 152 | 143 | 182 | 153 | 153 | 144 | 183 | 153 | 144 | 145 |
| 184 | 154 | 153 | 145 | 185 | 156 | 155 | 146 | 186 | 156 | 146 | 147 |
| 187 | 156 | 157 | 148 | 188 | 157 | 156 | 148 | 189 | 158 | 157 | 148 |
| 190 | 158 | 158 | 149 | 191 | 158 | 159 | 150 | 192 | 159 | 158 | 150 |
| 193 | 160 | 159 | 150 | 194 | 160 | 160 | 151 | 195 | 160 | 151 | 152 |
| 196 | 161 | 160 | 152 | 197 | 162 | 161 | 152 | 198 | 162 | 152 | 153 |
| 199 | 162 | 163 | 154 | 200 | 163 | 162 | 154 | 201 | 165 | 164 | 155 |
| 202 | 165 | 165 | 156 | 203 | 165 | 166 | 157 | 204 | 166 | 165 | 157 |
| 205 | 167 | 166 | 157 | 206 | 167 | 167 | 158 | 207 | 167 | 168 | 159 |
| 208 | 168 | 167 | 159 | 209 | 169 | 168 | 159 | 210 | 169 | 169 | 160 |
| 211 | 169 | 169 | 161 | 212 | 170 | 169 | 161 | 213 | 171 | 170 | 161 |
| 214 | 171 | 161 | 162 | 215 | 171 | 162 | 163 | 216 | 172 | 171 | 163 |
| 217 | 174 | 173 | 164 | 218 | 174 | 164 | 165 | 219 | 174 | 165 | 166 |
| 220 | 175 | 174 | 166 | 221 | 176 | 175 | 166 | 222 | 176 | 166 | 167 |
| 223 | 176 | 177 | 168 | 224 | 177 | 176 | 168 | 225 | 178 | 177 | 168 |
| 226 | 178 | 178 | 169 | 227 | 178 | 169 | 170 | 228 | 179 | 178 | 170 |
| 229 | 180 | 179 | 170 | 230 | 180 | 179 | 171 | 231 | 180 | 171 | 172 |
| 232 | 181 | 180 | 172 | 233 | 183 | 182 | 173 | 234 | 183 | 173 | 174 |
| 235 | 183 | 174 | 175 | 236 | 184 | 183 | 175 | 237 | 185 | 184 | 175 |
| 238 | 185 | 175 | 176 | 239 | 185 | 176 | 177 | 240 | 186 | 185 | 177 |
| 241 | 187 | 186 | 177 | 242 | 187 | 177 | 178 | 243 | 187 | 178 | 179 |
| 244 | 188 | 187 | 179 | 245 | 189 | 188 | 179 | 246 | 189 | 179 | 180 |
| 247 | 189 | 189 | 181 | 248 | 190 | 189 | 181 | 249 | 192 | 191 | 182 |
| 250 | 192 | 182 | 183 | 251 | 192 | 183 | 184 | 252 | 193 | 192 | 184 |
| 253 | 194 | 193 | 184 | 254 | 194 | 184 | 185 | 255 | 194 | 185 | 186 |
| 256 | 195 | 194 | 186 | 257 | 196 | 195 | 186 | 258 | 196 | 186 | 187 |
| 259 | 196 | 196 | 188 | 260 | 197 | 196 | 188 | 261 | 198 | 197 | 188 |
| 262 | 198 | 186 | 189 | 263 | 198 | 189 | 190 | 264 | 199 | 198 | 190 |
| 265 | 201 | 200 | 191 | 266 | 201 | 191 | 192 | 267 | 201 | 192 | 193 |
| 268 | 202 | 201 | 193 | 269 | 203 | 202 | 193 | 270 | 203 | 193 | 194 |
| 271 | 203 | 194 | 195 | 272 | 204 | 203 | 195 | 273 | 205 | 204 | 195 |
| 274 | 205 | 195 | 196 | 275 | 205 | 196 | 197 | 276 | 206 | 205 | 197 |
| 277 | 207 | 206 | 197 | 278 | 207 | 197 | 198 | 279 | 207 | 198 | 199 |
| 280 | 208 | 207 | 199 | 281 | 210 | 209 | 200 | 282 | 210 | 200 | 201 |

THE NUMBER OF CONSTRAINTS IS 39

| MODE | DIRECTION | VALUE |
|------|-----------|-------|
| 1 | 1 | 0.0 |
| 2 | 1 | 0.0 |
| 8 | 1 | 0.0 |
| 11 | 1 | 0.0 |
| 12 | 1 | 0.0 |
| 20 | 1 | 0.0 |
| 28 | 1 | 0.0 |

| | | |
|-----|---|-----|
| 36 | 1 | 0.0 |
| 37 | 1 | 0.0 |
| 46 | 1 | 0.0 |
| 57 | 1 | 0.0 |
| 79 | 1 | 0.0 |
| 84 | 1 | 0.0 |
| 99 | 1 | 0.0 |
| 107 | 1 | 0.0 |
| 112 | 1 | 0.0 |
| 117 | 1 | 0.0 |
| 122 | 1 | 0.0 |
| 127 | 1 | 0.0 |
| 136 | 1 | 0.0 |
| 145 | 1 | 0.0 |
| 154 | 1 | 0.0 |
| 163 | 1 | 0.0 |
| 172 | 1 | 0.0 |
| 181 | 1 | 0.0 |
| 190 | 1 | 0.0 |
| 199 | 1 | 0.0 |
| 208 | 1 | 0.0 |
| 217 | 1 | 0.0 |
| 225 | 1 | 0.0 |
| 218 | 2 | 0.0 |
| 219 | 2 | 0.0 |
| 220 | 2 | 0.0 |
| 221 | 2 | 0.0 |
| 222 | 2 | 0.0 |
| 223 | 2 | 0.0 |
| 224 | 2 | 0.0 |
| 225 | 2 | 0.0 |
| 226 | 2 | 0.0 |

LOAD DEFLECTION HISTORY

FAILURE (INITIAL YIELD) OCCURRED AT A LOAD OF 3774.23 WITH A DEFLECTION AT THE PIN OF 0.11349D-01
ELEMENT 76 YIELDED FOR THE 1 TIME

LOAD INCREMENT = 0.17341D 02
1 ELEMENTS FAILED DURING THIS LOAD STEP
FAILURE (YIELD OR FRACTURE) OCCURRED AT A LOAD OF 3808.91 WITH A DEFLECTION AT THE PIN OF 0.11454D-01
ELEMENT 356 YIELDED FOR THE 1 TIME

LOAD INCREMENT = 0.90004D 02
1 ELEMENTS FAILED DURING THIS LOAD STEP
FAILURE (YIELD OR FRACTURE) OCCURRED AT A LOAD OF 4006.92 WITH A DEFLECTION AT THE PIN OF 0.12054D-01
ELEMENT 353 YIELDED FOR THE 1 TIME

LOAD INCREMENT = 0.83544D 02
5 ELEMENTS FAILED DURING THIS LOAD STEP
FAILURE (YIELD OR FRACTURE) OCCURRED AT A LOAD OF 4341.10 WITH A DEFLECTION AT THE PIN OF 0.13066D-01
ELEMENT 350 YIELDED FOR THE 1 TIME
ELEMENT 351 YIELDED FOR THE 1 TIME
ELEMENT 354 YIELDED FOR THE 1 TIME
ELEMENT 355 YIELDED FOR THE 1 TIME
ELEMENT 357 YIELDED FOR THE 1 TIME

LOAD INCREMENT = 0.47180D 02
1 ELEMENTS FAILED DURING THIS LOAD STEP
FAILURE (YIELD OR FRACTURE) OCCURRED AT A LOAD OF 4435.46 WITH A DEFLECTION AT THE PIN OF 0.13357D-01
ELEMENT 358 YIELDED FOR THE 1 TIME

LOAD INCREMENT = 0.523110 02
 2 ELEMENTS FAILED DURING THIS LOAD STEP
 FAILURE (YIELD OR FRACTURE) OCCURRED AT A LOAD OF
 ELEMENT 97 YIELDED FOR THE 1 TIME
 ELEMENT 315 YIELDED FOR THE 1 TIME
 4540.08 WITH A DEFLECTION AT THE PIN OF 0.136830-01

 LOAD INCREMENT = 0.933060 01
 1 ELEMENTS FAILED DURING THIS LOAD STEP
 FAILURE (YIELD OR FRACTURE) OCCURRED AT A LOAD OF
 ELEMENT 345 YIELDED FOR THE 1 TIME
 4568.74 WITH A DEFLECTION AT THE PIN OF 0.137420-01

 LOAD INCREMENT = 0.101240 02
 1 ELEMENTS FAILED DURING THIS LOAD STEP
 FAILURE (YIELD OR FRACTURE) OCCURRED AT A LOAD OF
 ELEMENT 365 YIELDED FOR THE 1 TIME
 4578.99 WITH A DEFLECTION AT THE PIN OF 0.138070-01

 LOAD INCREMENT = 0.468730 02
 1 ELEMENTS FAILED DURING THIS LOAD STEP
 FAILURE (YIELD OR FRACTURE) OCCURRED AT A LOAD OF
 ELEMENT 328 YIELDED FOR THE 1 TIME
 4672.73 WITH A DEFLECTION AT THE PIN OF 0.141080-01

 LOAD INCREMENT = 0.518820 02
 1 ELEMENTS FAILED DURING THIS LOAD STEP
 FAILURE (YIELD OR FRACTURE) OCCURRED AT A LOAD OF
 ELEMENT 94 YIELDED FOR THE 1 TIME
 4776.50 WITH A DEFLECTION AT THE PIN OF 0.144410-01

 LOAD INCREMENT = 0.102890 02
 1 ELEMENTS FAILED DURING THIS LOAD STEP
 FAILURE (YIELD OR FRACTURE) OCCURRED AT A LOAD OF
 ELEMENT 346 YIELDED FOR THE 1 TIME
 4797.07 WITH A DEFLECTION AT THE PIN OF 0.145080-01

23 LOAD INCREMENTS OMITTED FOR BREVITY

• • •
v

LOAD INCREMENT = 0.664300 01
 2 ELEMENTS FAILED DURING THIS LOAD STEP
 FAILURE (YIELD OR FRACTURE) OCCURRED AT A LOAD OF
 ELEMENT 117 YIELDED FOR THE 1 TIME
 ELEMENT 355 YIELDED FOR THE 2 TIME
 S290.54 WITH A DEFLECTION AT THE PIN OF 0.167960-01

LOAD INCREMENT = 0.835180 01
 1 ELEMENTS FAILED DURING THIS LOAD STEP
 FAILURE (YIELD OR FRACTURE) OCCURRED AT A LOAD OF
 ELEMENT 112 YIELDED FOR THE 1 TIME
 S307.25 WITH A DEFLECTION AT THE PIN OF 0.169600-01

LOAD INCREMENT = 0.724320 01
 0 ELEMENTS FAILED DURING THIS LOAD STEP
 FAILURE (YIELD OR FRACTURE) OCCURRED AT A LOAD OF
 ELEMENT 113 YIELDED FOR THE 1 TIME
 ELEMENT 122 YIELDED FOR THE 1 TIME
 ELEMENT 123 YIELDED FOR THE 1 TIME
 ELEMENT 125 YIELDED FOR THE 1 TIME
 S321.73 WITH A DEFLECTION AT THE PIN OF 0.171040-01

LOAD INCREMENT = 0.120740 02
 3 ELEMENTS FAILED DURING THIS LOAD STEP
 FAILURE (YIELD OR FRACTURE) OCCURRED AT A LOAD OF
 ELEMENT 109 YIELDED FOR THE 1 TIME
 ELEMENT 118 YIELDED FOR THE 1 TIME
 ELEMENT 119 YIELDED FOR THE 1 TIME
 S345.98 WITH A DEFLECTION AT THE PIN OF 0.173560-01

LOAD INCREMENT = 0.502150 01
 1 ELEMENTS FAILED DURING THIS LOAD STEP
 FAILURE (YIELD OR FRACTURE) OCCURRED AT A LOAD OF
 ELEMENT 357 YIELDED FOR THE 2 TIME
 S355.92 WITH A DEFLECTION AT THE PIN OF 0.174640-01

```

*****
LOAD INCREMENT = 0.168600 02
2 ELEMENTS FAILED DURING THIS LOAD STEP
FAILURE (YIELD OR FRACTURE) OCCURRED AT A LOAD OF
ELEMENT 105 YIELDED FOR THE 1 TIME
ELEMENT 358 YIELDED FOR THE 2 TIME
5389.64 WITH A DEFLECTION AT THE PIN OF 0.178280-01
*****

*****
LOAD INCREMENT = 0.130080 02
1 ELEMENTS FAILED DURING THIS LOAD STEP
FAILURE (YIELD OR FRACTURE) OCCURRED AT A LOAD OF
ELEMENT 353 YIELDED FOR THE 2 TIME
5415.66 WITH A DEFLECTION AT THE PIN OF 0.181150-01
*****

*****
LOAD INCREMENT = 0.538890 01
2 ELEMENTS FAILED DURING THIS LOAD STEP
FAILURE (YIELD OR FRACTURE) OCCURRED AT A LOAD OF
ELEMENT 97 YIELDED FOR THE 2 TIME
ELEMENT 365 YIELDED FOR THE 2 TIME
5426.44 WITH A DEFLECTION AT THE PIN OF 0.182340-01
*****

*****
LOAD INCREMENT = 0.119950 02
1 ELEMENTS FAILED DURING THIS LOAD STEP
FAILURE (YIELD OR FRACTURE) OCCURRED AT A LOAD OF
ELEMENT 341 YIELDED FOR THE 1 TIME
5450.43 WITH A DEFLECTION AT THE PIN OF 0.185000-01
*****

*****
LOAD INCREMENT = 0.697750 01
3 ELEMENTS FAILED DURING THIS LOAD STEP
FAILURE (YIELD OR FRACTURE) OCCURRED AT A LOAD OF
ELEMENT 95 YIELDED FOR THE 1 TIME
ELEMENT 140 YIELDED FOR THE 2 TIME
ELEMENT 349 YIELDED FOR THE 1 TIME
5464.38 WITH A DEFLECTION AT THE PIN OF 0.186540-01
*****

```

124 LOAD INCREMENTS OMITTED FOR BREVITY

• • •
▼

ELEMENT 141 YIELDED FOR THE 5 TIME

LOAD INCREMENT = 0.93744D 01
 4 ELEMENTS FAILED DURING THIS LOAD STEP
 FAILURE (YIELD OR FRACTURE) OCCURRED AT A LOAD OF 7316.34 WITH A DEFLECTION AT THE PIN OF 0.12144D 00
 ELEMENT 93 YIELDED FOR THE 4 TIME
 ELEMENT 97 YIELDED FOR THE 5 TIME
 ELEMENT 129 YIELDED FOR THE 5 TIME
 ELEMENT 365 YIELDED FOR THE 5 TIME

LOAD INCREMENT = 0.99726D 01
 5 ELEMENTS FAILED DURING THIS LOAD STEP
 FAILURE (YIELD OR FRACTURE) OCCURRED AT A LOAD OF 7336.29 WITH A DEFLECTION AT THE PIN OF 0.12455D 00
 ELEMENT 80 YIELDED FOR THE 1 TIME
 ELEMENT 111 YIELDED FOR THE 5 TIME
 ELEMENT 115 YIELDED FOR THE 5 TIME
 ELEMENT 337 YIELDED FOR THE 2 TIME
 ELEMENT 371 YIELDED FOR THE 5 TIME

LOAD INCREMENT = 0.51797D 01
 4 ELEMENTS FAILED DURING THIS LOAD STEP
 FAILURE (YIELD OR FRACTURE) OCCURRED AT A LOAD OF 7346.65 WITH A DEFLECTION AT THE PIN OF 0.12618D 00
 ELEMENT 109 YIELDED FOR THE 5 TIME
 ELEMENT 110 YIELDED FOR THE 5 TIME
 ELEMENT 114 YIELDED FOR THE 5 TIME
 ELEMENT 360 YIELDED FOR THE 4 TIME

LOAD INCREMENT = 0.52621D 01
 3 ELEMENTS FAILED DURING THIS LOAD STEP
 FAILURE (YIELD OR FRACTURE) OCCURRED AT A LOAD OF 7357.17 WITH A DEFLECTION AT THE PIN OF 0.12787D 00
 ELEMENT 79 YIELDED FOR THE 1 TIME
 ELEMENT 369 YIELDED FOR THE 5 TIME
 ELEMENT 370 YIELDED FOR THE 5 TIME

```

*****
LOAD INCREMENT = 0.146300 02
2 ELEMENTS FAILED DURING THIS LOAD STEP
FAILURE (YIELD OR FRACTURE) OCCURRED AT A LOAD OF
ELEMENT 104 YIELDED FOR THE 3 TIME
ELEMENT 361 YIELDED FOR THE 4 TIME
7386.43 WITH A DEFLECTION AT THE PIN OF 0.132590 00
*****

*****
LOAD INCREMENT = 0.138290 02
2 ELEMENTS FAILED DURING THIS LOAD STEP
FAILURE (YIELD OR FRACTURE) OCCURRED AT A LOAD OF
ELEMENT 64 YIELDED FOR THE 1 TIME
ELEMENT 81 YIELDED FOR THE 3 TIME
7414.09 WITH A DEFLECTION AT THE PIN OF 0.137060 00
*****

*****
LOAD INCREMENT = 0.102380 02
4 ELEMENTS FAILED DURING THIS LOAD STEP
FAILURE (YIELD OR FRACTURE) OCCURRED AT A LOAD OF
ELEMENT 112 YIELDED FOR THE 5 TIME
ELEMENT 117 YIELDED FOR THE 5 TIME
ELEMENT 125 YIELDED FOR THE 5 TIME
ELEMENT 357 YIELDED FOR THE 5 TIME
7434.57 WITH A DEFLECTION AT THE PIN OF 0.140360 00
*****

*****
LOAD INCREMENT = 0.155070 02
2 ELEMENTS FAILED DURING THIS LOAD STEP
FAILURE (YIELD OR FRACTURE) OCCURRED AT A LOAD OF
ELEMENT 90 YIELDED FOR THE 2 TIME
ELEMENT 113 YIELDED FOR THE 5 TIME
7465.58 WITH A DEFLECTION AT THE PIN OF 0.145490 00
*****

*****
LOAD INCREMENT = 0.537130 01
3 ELEMENTS FAILED DURING THIS LOAD STEP
FAILURE (YIELD OR FRACTURE) OCCURRED AT A LOAD OF
ELEMENT 92 YIELDED FOR THE 2 TIME
7476.32 WITH A DEFLECTION AT THE PIN OF 0.147270 00
*****

```

ELEMENT 358 YIELDED FOR THE 5 TIME
ELEMENT 366 YIELDED FOR THE 5 TIME

LOAD INCREMENT = 0.671500 01

3 ELEMENTS FAILED DURING THIS LOAD STEP
FAILURE (YIELD OR FRACTURE) OCCURRED AT A LOAD OF
ELEMENT 91 YIELDED FOR THE 2 TIME
ELEMENT 367 YIELDED FOR THE 5 TIME
ELEMENT 368 YIELDED FOR THE 5 TIME

7489.75 WITH A DEFLECTION AT THE PIN OF 0.149520 00

LOAD INCREMENT = 0.248850 02

4 ELEMENTS FAILED DURING THIS LOAD STEP
FAILURE (YIELD OR FRACTURE) OCCURRED AT A LOAD OF
ELEMENT 75 YIELDED FOR THE 3 TIME
ELEMENT 120 YIELDED FOR THE 5 TIME
ELEMENT 140 FRACTURED
ELEMENT 362 YIELDED FOR THE 4 TIME

7539.52 WITH A DEFLECTION AT THE PIN OF 0.157910 00

LOAD INCREMENT = 0.135210 04

2 ELEMENTS FAILED DURING THIS LOAD STEP
FAILURE (YIELD OR FRACTURE) OCCURRED AT A LOAD OF
ELEMENT 149 FRACTURED
ELEMENT 150 FRACTURED

5408.24 WITH A DEFLECTION AT THE PIN OF 0.129320 00

***** CRACK INSTABILITY OCCURRED AT A LOAD OF

7539.52 *****

LOAD INCREMENT = 0.166200 04

1 ELEMENTS FAILED DURING THIS LOAD STEP
FAILURE (YIELD OR FRACTURE) OCCURRED AT A LOAD OF
ELEMENT 148 FRACTURED

4653.60 WITH A DEFLECTION AT THE PIN OF 0.110210 00

5408.24 *****

***** CRACK INSTABILITY OCCURRED AT A LOAD OF

LOAD INCREMENT = 0.13860D 04

3 ELEMENTS FAILED DURING THIS LOAD STEP

FAILURE (YIELD OR FRACTURE) OCCURRED AT A LOAD OF

3880.91 WITH A DEFLECTION AT THE PIN OF 0.93687D-01

ELEMENT 146 FRACTURED

ELEMENT 147 FRACTURED

ELEMENT 151 FRACTURED

4653.60 *****

***** CRACK INSTABILITY OCCURRED AT A LOAD OF

LOAD INCREMENT = 0.93025D 03

1 ELEMENTS FAILED DURING THIS LOAD STEP

FAILURE (YIELD OR FRACTURE) OCCURRED AT A LOAD OF

2232.61 WITH A DEFLECTION AT THE PIN OF 0.77012D-01

ELEMENT 145 FRACTURED

3880.91 *****

***** CRACK INSTABILITY OCCURRED AT A LOAD OF

LOAD INCREMENT = 0.72705D 03

2 ELEMENTS FAILED DURING THIS LOAD STEP

FAILURE (YIELD OR FRACTURE) OCCURRED AT A LOAD OF

1744.92 WITH A DEFLECTION AT THE PIN OF 0.68134D-01

ELEMENT 143 FRACTURED

ELEMENT 144 FRACTURED

***** CRACK INSTABILITY OCCURRED AT A LOAD OF 2232.61 *****

LOAD INCREMENT = 0.526720 03

1 ELEMENTS FAILED DURING THIS LOAD STEP

FAILURE (YIELD OR FRACTURE) OCCURRED AT A LOAD OF

1264.14 WITH A DEFLECTION AT THE PIN OF 0.602110-01

ELEMENT 142 FRACTURED

***** CRACK INSTABILITY OCCURRED AT A LOAD OF 1744.92 *****

LOAD INCREMENT = 0.243670 03

1 ELEMENTS FAILED DURING THIS LOAD STEP

FAILURE (YIELD OR FRACTURE) OCCURRED AT A LOAD OF

504.80 WITH A DEFLECTION AT THE PIN OF 0.524900-01

ELEMENT 141 FRACTURED

***** CRACK INSTABILITY OCCURRED AT A LOAD OF 1264.14 *****

IMC2091 IBCOM - PROGRAM INTERRUPT (P) - DIVIDE CHECK OLD PSW IS 071D000FA24378DE - REGISTER CONTAINED 3F1C13332601E810

TRACEBACK ROUTINE CALLED FROM ISN REG. 14 REG. 15 REG. 0 REG. 1

FAIL 0017 4242D04E 00430700 000001C5 003A0EEC

MAIN 0J008C72 013A0D18 008EF870 0043EFF8

ENTRY POINT= 013A0D18

STANDARD FIXUP TAKEN . EXECUTION CONTINUING

IMC2091 IBCOM - PROGRAM INTERRUPT (P) - DIVIDE CHECK OLD PSW IS 071D000FA2A37BDE . REGISTER CONTAINED 3F1BA9C69C8FDF30

TRACEBACK ROUTINE CALLED FROM ISN REG. 14 REG. 15 REG. 0 REG. 1

FAIL 0017 4242004E 004307D0 000001C5 003A0EEC

MAIN 00008C72 013A0018 008EFB70 0043EFF8

ENTRY POINT= 013A0018

STANDARD FIXUP TAKEN . EXECUTION CONTINUING

IMC2091 IBCOM - PROGRAM INTERRUPT (P) - DIVIDE CHECK OLD PSW IS 071D000FA2A37BDE . REGISTER CONTAINED 3F18CAB961000AE0

TRACEBACK ROUTINE CALLED FROM ISN REG. 14 REG. 15 REG. 0 REG. 1

FAIL 0017 4242004E 004307D0 000001C5 003A0EEC

MAIN 00008C72 013A0018 008EFB70 0043EFF8

ENTRY POINT= 013A0018

STANDARD FIXUP TAKEN . EXECUTION CONTINUING

IMC2091 IBCOM - PROGRAM INTERRUPT (P) - DIVIDE CHECK OLD PSW IS 071D000FA2A37BDE . REGISTER CONTAINED 3F18DAE5880FF160

TRACEBACK ROUTINE CALLED FROM ISN REG. 14 REG. 15 REG. 0 REG. 1

FAIL 0017 4242004E 004307D0 000001C5 003A0EEC

MAIN 00008C72 013A0018 008EFB70 0043EFF8

ENTRY POINT= 013A0018

STANDARD FIXUP TAKEN . EXECUTION CONTINUING

IMC2091 IBCOM - PROGRAM INTERRUPT (P) - DIVIDE CHECK OLD PSW IS 071D000FA2A37BDE . REGISTER CONTAINED 3F1C0A2BE7098470

TRACEBACK ROUTINE CALLED FROM ISN REG. 14 REG. 15 REG. 0 REG. 1

FAIL 0017 4242004E 004307D0 000001C5 003A0EEC

MAIN 00008C72 013A0018 008EFB70 0043EFF8

ENTRY POINT= 013A0018

STANDARD FIXUP TAKEN . EXECUTION CONTINUING

IME0001 EXECUTION TERMINATING DUE TO ENHOC COUNT FOR ERROR NUMBER 209
 IMC2001 ISCOM - PROGRAM INTERRUPT (P) - DIVIDE CHECK OLD PSW IS 071D000FA2A378DE - REGISTER CONTAINED 3F1C285E701C23F0

TRACEBACK ROUTINE CALLED FROM ISN REG. 14 REG. 15 REG. 0 REG. 1
 FAIL 0017 4242004E 004307D0 000001C5 003A0EEC
 MAIN 0300BC72 013A0D18 008EF870 0043EFF8

ENTRY POINT= 013A0D18